Genetic and molecular approaches for increasing the isoprenoid pathway flux in *Saccharomyces cerevisiae*

A THESIS

SUBMITTED

FOR THE AWARD OF THE DEGREE OF

DOCTOR OF PHILOSOPHY

IN THE FACULTY OF SCIENCE

2018

BY

MANISHA WADHWA

Department of Biological Sciences

Indian Institute of Science Education and Research (IISER)
Mohali-140306

June 2018

INDIAN INSTITUTE OF SCIENCE EDUCATION AND RESEARCH

MOHALI

Sector 81, SAS Nagar, Mohali

PO Manauli, Punjab, 140306, India

DECLARATION

The work presented in this thesis entitled "Genetic and molecular approaches for increasing the isoprenoid pathway flux in *Saccharomyces cerevisiae*'' has been carried out by me under the supervision of Prof. Anand Kumar Bachhawat at the Department of Biological Sciences, Indian Institute of Science Education and Research (IISER) Mohali.

This work has not been submitted in part or full for a degree, a diploma, or a fellowship to any other university or institute. Whenever contributions of others are involved, every effort is made to indicate this clearly, with due acknowledgment of collaborative research and discussions. This thesis is a bonafide record of original work done by me and all sources listed within have been detailed in the bibliography.

(Manisha Wadhwa)

Date:

Place:

In my capacity as supervisor of the candidate's doctoral thesis work, I certify that above statements by the candidate are true to the best of my knowledge.

(Prof. Anand Kumar Bachhawat)

Department of Biological Sciences

Indian Institute of Science Education and Research Mohali

Dedicated

To My Mother

Table of Contents

Acknowledgement	i-iii
List of Publication and Filed Patents	iv
Abbreviations	v-vi
Synopsis	vii-xiii
Chapter 1. Review of Literature	**1-32**
GENERAL INTRODUCTION	1
PART I: Terpenoid and Terpenoid Biosynthetic pathways	2
1.1 Terpenoids and their function	2
1.2 Classification of terpenoids and their commercial importance	3
1.3 Biosynthetic pathways: The Mevalonate pathway and Methyl-D-erythritol- phosphate pathway	3
1.3.1 Methyl-D-erythritol- phosphate (MEP) pathway	3
1.3.2 MVA pathway	5
1.4 Metabolic engineering of microorganisms for the production of commercially important terpenoids	5
PART II: Metabolic engineering strategies for enhancing the isoprenoid pathway flux	9
1.5 Metabolic engineering strategies for increasing the yield from MVA pathway in *Saccharomyces cerevisiae*	9
1.5.1 Increasing the precursor supply	9
a. Overexpression of all genes of MVA pathway	9
b. Overexpression of truncated *HMG1* (*tHMG1*)	9
c. Overexpression of farnesyl pyrophosphate synthase (*ERG20*)	11
d. Overexpression of geranylgeranyl diphosphate synthase (*BTS1*)	11
e. Overexpression of isopentenyl diphosphate: dimethylallyl diphosphate synthase (*IDI1*)	11
f. Down regulation of squalene synthase (*ERG9*)	11
g. Down regulation of Lipid phosphate phosphatase (*LPP1*) and diacylglycerol pyrophosphate phosphatase (*DPP1*)	12

h. Transcription factor, *UPC2* 12
i. Increasing acetyl-CoA pools: 12
i.1 Pyruvate dehydrogenase (PDH) bypass 13
i.2 Phosphoketolase (PK) pathway 15
i.3 Other heterologous enzymes with special features 15
1.5.2 Cofactor Engineering 17
1.5.3 Balancing of Pathways 17
1.5.4 Spatial Optimization of metabolism 17
PART III: Screening strategies for increased isoprenoid pathway activity in *S. cerevisiae* 19
1.6 Different Screening strategies for increased mevalonate pathway activity 19
1.6.1 Screening by Fluorescence 19
1.6.2 Screening for colored products and by-products using analogues and coupled assays 20
1.6.3 Screening based on selective growth 22
1.6.4 Screening using a specific biosensor 22
1.6.5 Screening for carotenoid pigmentation 23
PART IV: Carotenoids and their biosynthesis 23
1.7 Carotenoids 23
1.7.1 Sources of carotenoids and their biosynthesis 23
1.7.2 Biological role 24
1.7.3 Applications 24
1.7.4 Commercially important carotenoids 25
1.8 Microbial production of important carotenoids 26
1.9 Screening of enhanced isoprenoid flux by carotenoid based assays 27
1.10 Objectives of the present study 32
CHAPTER 2: MATERIALS AND METHODS 33-54
SECTION A: MATERIALS 33
2.1 CHEMICALS AND REAGENTS 34
2.2 STRAINS AND PLASMIDS 34

2.3 OLIGONUCLEOTIDES 34

2.4 MEDIA 40

2.4.1 LB 40

2.4.2 YPD 40

2.4.3 SD 40

2.5 BUFFERS AND STOCK SOLUTIONS 41

2.5.1 Ampicillin Stock Solution (50mg/mL) 41

2.5.2 50% Glycerol 41

2.5.3 Solutions for Plasmid Extraction 41

2.5.4 Agarose Gel Extraction Reagents 42

2.5.5 Solutions for preparation of chemical competent *E. coli* cells 42

2.5.6 Yeast Transformation Solutions 43

2.5.7 STES lysis mixture 43

2.5.8 Solutions for Hydroxylamine mutagenesis 43

2.5.9 Solutions for *A. tumefaciens* mediated transformation of *R. toruloides* 43

SECTION B: METHODS 44

2.6 Growth and maintenance of bacteria and yeast strains 44

2.7 Growth Curve analysis 45

2.8 Growth assay by dilution spotting 45

2.9 Recombinant DNA methodology (restriction digestion, transformation of *E. coli*, amplification etc.) 45

2.10 Custom synthesis of codon optimized genes 45

2.11 Random mutagenesis: Hydoxylamine based mutagenesis 46

2.12 Random mutagenesis: Ethylmethane sulfate (EMS) based mutagenesis 46

2.13 Transformation of *E. coli* 46

2.14 Transformation of yeast: *S. cerevisiae* 46

2.15 Transformation of yeast: *R. toruloides* by *Agrobacterium* (ATMT) 47

2.16 Isolation of plasmid from yeast 48

2.17 Isolation of genomic DNA from yeast 50

2.18 RNA isolation from yeast cells 50
2.19 Real Time qPCR 50
2.20 Microarray Analysis 50
2.21 Sequence analysis 51
2.22 Sequence accession numbers 51
2.23 Dry cell weight Determination 51
2.24 Extraction of carotenoids from *S. cerevisiae* and their analysis by HPLC 51
2.25 Extraction of carotenoids from *R. toruloides* and their analysis by HPLC 52
2.26 Identification and quantification of α-Farnesene 52
2.27 Measurement of extracellular metabolites by HPLC 53
2.28 Simulation studies for Flux balance analysis 53
2.29 Whole genome sequencing analysis 54
CHAPTER 3: Development of a carotenoid based visual genetic assay for evaluating metabolic flux in the isoprenoid pathway of *Saccharomyces cerevisiae* 55-74
3.1 Introduction 56
3.2 Results 57
3.2.1 Reconstruction of carotenoid biosynthetic pathway in *Saccharomyces cerevisiae* using enzymes from *R. toruloides* reveals β-carotene as the majorly produced carotenoid 57
3.2.2 Combinatorial approach of strong and weak promoters for obtaining a low-color strain compatible for screening the isoprenoid flux 63
3.2.3 Rate limiting phytoene dehydrogenase (*Rt*CRTI) hinders the successful development of carotenoid based genetic screen 65
3.2.4 Addressing the metabolic bottleneck phytoene dehydrogenase (*Rt*CRTI) by directed evolution strategy yields catalytically more efficient mutants of enzyme 65
3.2.5 The catalytically efficient mutant of *Rt*CRTI (*Rt*CRTI_A393T) also fails to yield the desired carotenoid based visual screen 68
3.2.6 Decreasing the levels of geranyl geranyl diphosphate (GGPP), the 72

metabolic precursor to phytoene yields successful development of a colored based visual screen
3.3 Discussion 74
CHAPTER 4: To isolate mutants for increasing flux in the isoprenoid pathway by using carotenoid based genetic screen **76-84**
4.1 Introduction 77
4.2 Results 77
4.2.1 *SPT15* mutagenesis and selection for mutants using the phenotypic pigmentation screen: Identification of *spt15_R98H*, *spt15_A100T*, *spt15_A101T* 77
4.2.2 The isolated *spt15* mutants increase the overall general isoprenoid pathway flux 80
4.2.3 Mutagenesis of *S. cerevisiae* using Ethylmethane sulfate (EMS) for isolating mutant strains with increased isoprenoid pathway flux 80
4.3 Discussion 84
CHAPTER 5: To investigate the mechanism of increased isoprenoid flux in the *spt15_A101T* mutant that was isolated in the screen **85-109**
5.1 Introduction 86
5.2 Results 86
5.2.1 The spt15_A101T mutant bearing cells display a decreased growth rate in comparison to the SPT15 WT strain in minimal medium 86
5.2.2 Metabolic flux balance analysis of *SPT15* WT and *spt15_A101T* strains with whole genome scale metabolic model reveals carbon rerouting in *spt15_A101T* strain for increasing the isoprenoid flux 87
5.2.3 Role of Phosphate and NADPH on the isoprenoid flux 97
5.2.4 Transcriptome profile analysis of *spt15_A101T* indicates up-regulation of phosphate signaling and response (PHO) pathway and pyruvate decarboxylase 99
5.2.5 Transcriptomic constraints and other transport/diffusion constraints for simulating the flux balance distribution of *spt15_A101T* 101
5.2.6 Flux Balance distribution of *spt15_A101T* strain along with transcriptional and transport/diffusion constraints reveals truncation of the TCA cycle and an 101

increased demand of phosphate in the mitochondria
5.2.7 Flux balance distribution of *spt15_A101T* under increased extracellular phosphate pushes the flux to biomass rather than the isoprenoid pathway 103
5.2.8 Evaluation of the role of pyruvate decarboxylase (*PDC6*) in increasing the isoprenoid pathway flux 105
5.3 Discussion 106
BIBLIOGRAPHY **110-124**
APPENDIX 1: Development of tools and techniques for *Rhodosporidium toruloides*: Attempts to decipher the gene encoding Torularhodin synthase **125-137**
A1.1 Background 126
A1.2 Construction of modified vectors for transformation and disruption in *R. toruloides* 126
A1.3 Construction of knockout (disruption) vector for disruption/gene deletion of putative torularhodin synthase (RHTO_06383) 130
A1.4 Efforts at cloning and expressing the putative Cytochrome P450 and the reductase in *S. cerevisiae* 135
A1.5 Standardization of carotenoid profile of *R. toruloides* 135
A1.6 Conclusions 137
A1.7 References 137

Acknowledgement

During the course of my Ph.D. journey, I associated with many persons, who have influenced my professional as well as personal life profoundly. They made this journey a memorable part of my life. Completion of this doctoral dissertation was possible with the support of several people. I would like to take this opportunity to express my immense gratitude and regards from the core of my heart to all those people.

Foremost, I owe my greatest debt and heartfelt gratitude to my Ph.D. supervisor Prof. Anand K. Bachhawat. A person with an amicable and positive disposition. I would especially like to thank him as he provided me the opportunity to work in his lab but also showed a sense of faith in me. His valuable guidance, scholarly inputs and consistent encouragement I received throughout the research work. This feat was possible only because of the unconditional support given by him. His extraordinary patience, understanding, optimism and confidence in me have shaped my personality to a large extent. I admire and respect him for the amount of freedom he give to his students. It was my great fortune that I came under his guidance during the early period of my scientific career, whereby I learnt the alphabets & morals of science. He guided me with his explicit writing skills for writing papers, grants and this thesis. I have to say that I'm extremely fortunate to have a mentor like him.

I would like to thank to IISER Mohali director, Prof. Debi P. Sarkar for providing excellent amicable academic environment and state of art modular lab facilities with cutting edge instrument. Thanks for allowing round the clock access to all these facilities.

I express my immense gratitude to my doctoral committee members, Dr. Shravan Kumar Mishra and Dr. Rachna Chaba for their helpful suggestions and timely review of the progress of my work.

I express my immense gratitude to Dr. Shashi Bhushan Pandit for helping me to carry out bioinformatic analysis and valuable scientific inputs and discussions during early phase of Ph.D. I am also thankful to lab members of Dr. Shravan Kumar Mishra for helping me in carrying out RNA related work and scientific discussions. I am also thankful to Dr. Kavita Babu and her lab members especially Pallavi, Ashwani, Dr. Pratima, Dr. Yogesh and Nagesh for helping me in carrying out real time PCR and fluorescence microscope images. I am also thankful to Dr. Manjari Jain and Dr. Ranjana Jaiswara for helping me to learn ecology and working with them was an immense pleasure.

I would also like to put on record a special word of thanks for Dr. R. Vijaya Anand and Dr. Asim Kumar Chowdhury for allowing me to work in his lab for carrying out chemistry related work and valuable suggestions for standardization of extraction and HPLC. This work formed a crucial part of my study. I am also thankful to Dr. Sripada S. V Rama Sastry forvaluable

scientific discussions regarding chemistry related work. I am also thankful to Dr. K. P. Singh and Dr. Vinayak Sinha for initial experiments with fematosecond laser and PTRMS in their labs respectively.

I am grateful to Dr. Manishankar Bhattacharya, IMTECH, Chd for helping me in designing and suggestions to carry out dry cell weight experiment in his lab.

I would like extend my thanks to Dr. K. P. Venkatesh IIT Bombay for collaborating with us and allowed me to work his lab. His scientific acumen helped us to decide the course to be taken for spt15 mutant work. I would also like to thank Dr. Sumana Srinivasan, IIT Bombay for helping me with the metabolic flux analysis and scientific discussions. I am also thankful to Dr. P.J. Bhat, IIT Bombay for allowing me to carry out experiments in the lab and valuable scientific discussions. I am also thankful to lab members of Dr. P.J. Bhat, Mahesh, Asha, Vijendra, Archana and Nandinee for helping me to carry out experiments smoothly, their help for peaceful and enjoyable stay at IIT Bombay. I am also thankful to Dr. Santosh Norhona, IIT Bombay for providing HPLC facility.

I can't find the word to express my gratitude to Dr. Nandita mam to whom I shared all my personal and professional issues. She understands my problems and guides me to right path. Her calmness and guidance aids me to maintain balance in professional and personal life.

I would like to convey my sincere appreciation and heart-felt gratitude to my B. Sc and M. Sc teacher Dr. Jasveen Dua, Dr. Smriti Dhawan and Dr. Jagdeep Kaur for being a constant source of inspiration.

Thanks are due to the entire IISER family, administration, library, instrumentation, store and purchase sections, mess staffs, canteen staff, hostel caretakers for their cooperation in the smooth running of my Ph.D.

I am extremely grateful to have incredible lab members. Due to the wonderful seniors and cordial environment in the lab, I considered myself lucky to learn from my seniors both academically and non-academically. Thanks to my seniors Dr. Anil Thakur and Dr. Shailesh Kumar, Dr. Anup Deshpande, Dr. M. Zulkifli, Dr. Aman, Dr. Avinash, Dr. Banani for their great help and support in and out of the lab. Anil sir, Shailesh Sir, Anup Sir and Zulfi taught me the basic yeast genetics and molecular biology and give me the training of different lab techniques. I am also thankful to my lovable juniors Muskan, Anuj, Shambhu, Sriharsha, Prarthna and Shradha for their help and co-operation when needed. I am also thankful to Dr. Banani and Sriharsha for scientific discussions and useful suggestions. Special thanks to Dr. Bannai and Dr. Anup with whom I can share my personal and professional issues. They are co-operative lab mates who very patiently, extended their help whenever I asked for. Thanks to all of you for giving me a great working environment in our lab. Also I would like to acknowledge Thoithoi Lourembam and Kristina for helping in my research project. I and Thoithoi worked together for one year during

her final year in MS. She not only contributed to carotenoid- based screening project, but also became a good friend. Thanks to Vidya who works hard to maintain the lab and arrange things on time.

Stay at IISER probably, would not have been as memorable as it is, in the absence of many people. They have been like rock-solid support to me as and when required. There is a whole bunch Bhupinder, Devashish, Prashant, Shivani, Pallavi, Krishna, Shoumitro, Rohan, Shiv, Rivi, Prince, Aastha… my batch mates who made life at IISER a lot soothing. I would also like to thank all my friends like Harshita, Pranay Rungta, Krishna, Jithin, Kuldeep, Prashant Billa, Pallavi, Ashwani.

The prominent place of acknowledgement goes to Harshita and Krishna who are good friends and like younger sisters who very patiently, extended their help whenever I asked for. Harshita is the one with whom I argued, and discussed both personal and professional issues.

Banani Mam and Manishankar Sir always treated me like their own family member and were always very caring & supportive.

It is difficult to describe the gratitude one feels towards their family. This Ph.D and any and all of my achievements in life till date and in the future, have been and will always be because of their love, support, encouragement, sacrifices for me and the values instilled in me. Without them, this thesis would never have been written. My family (Mummy, Papa, Shruti, kanu)'s immense unwavering faith in me and my abilities, greater than my own has always driven me to aim higher. I am also thankful to my grandfather and grandmother who always stand as pillar of strength and support for me. I am dedicated this thesis to my mother whose unconditional support and love drives me to do highest degree in this premiere institute. I cannot imagine myself at this place without her.

I owe my earnest gratitude towards my friend and my husband "Suranand" for his support and understanding of my goals and aspirations. He was with me during the last year of Ph.D and and had been strong pillar of strength. He listened to me and take care of me when I was low and depressed. He always motivated me to achieve my goals. I am thankful to my in-laws (Aathma, Mamayya, Praveena Bujji, Triveni Bujji, Umesh anna, Srinivas anna, ishanvi and virat) for their love and support.

At last I must acknowledge and thank The Almighty GOD for blessing, protecting and guiding me throughout my educational journey and brining me at the door step of Ph.D.

Manisha Wadhwa

List of Publications and patents filed

1) A genetic screen for increasing metabolic flux in the isoprenoid pathway of *Saccharomyces cerevisiae*: Isolation of SPT15 mutants using the screen
   Manisha Wadhwa, Anand K Bachhawat* Metabolic Engineering Communications, 3(2016): 164-172.

2) Role of phosphate limitation and pyruvate decarboxylase in rewiring of the metabolic network for increasing flux towards isoprenoid pathway in a TATA binding protein mutant of *Saccharomyces cerevisiae*
   Manisha Wadhwa[1], Sumana Srinivasan[2], Anand K Bachhawat[1*], K. V. Venkatesh[2*]
   Microbial cell factories 2018; 17:152

3) US patent granted "Increased production of isoprenoid in *Saccharomyces cerevisiae* by carotenoid optimization and screening", Indian patent filed application no. 2016 (642/DEL/2015) dated March 10, 2015, US patent grant application no. 15/066296, dated August 9, 2018.

ABBREVIATIONS

Weights and measures

%	Percent
µmol, nmoles, mmoles,	micromole, nanomoles, millimoles,
°C	Degree centigrade
bp, kb	Base pair, kilobase
kDa	Kilodalton
mA	Milliampere
O.D.	Optical density
Psi	Pounds per square inch
rpm	Revolutions per minute
RT	Room temperature
Sec, min, h	Second, minute, hour,
V , KV	Volt, kilovolt,
µCi, Ci	Microcurie, curie
µg, mg, g	microgram, milligram, gram
µl, ml, L	Microliter, milliliter, liter,
µM, mM, M,	micromolar, millimolar, molar

Symbols

~	Approximately
=	Equal to
α	Alpha
β	Beta
γ	Gamma
Δ	Delta

Techniques

PCR	Polymerase Chain Reaction
HPLC	High pressure liquid chromatography
GC	Gas chromatography

Chemicals

Amp	Ampicillin
Spec	Spectionomycin
ATP	Adenosine Triphosphate
ADP	Adenosine diphosphate
BSA	Bovine Serum Albumin
dNTPs	2'-deoxyadenosine 5'-triphosphate
EDTA	Ethylenediamine-tetra-acetic acid
HCl	Hydrogen Chorid

PCI	Phenol-chloroform-isoamyl alcohol
PEG	Poly Ethylene Glycol
EMS	Ethyl methanesulfonate

Miscellaneous

BLAST	Basic Local Alignment Search Tool
EUROSCARF	European *S. cerevisiae* archive for functional Analysis
GFP	Green Fluorescent Protein
LB	Luria Bertani
NCBI	National Center for Biotechnology Information
ORF	Open Reading Frame
PBS	Phosphate Buffer Saline
TE	Tris chloride and EDTA
WT	Wild Type

SYNOPSIS

Introduction and Background

Isoprenoids or terpenoids belongs to the largest class of natural products that include many commercially valuable compounds. Terpenoids have found use as flavor & fragrances, nutraceuticals, pharmaceuticals, colourants and biofuels. Owing to limitations in their production from natural sources, difficult extraction procedures, seasonal variations and difficult chemical synthesis, increasing efforts are targeting their production from recombinant microbes e.g. *Escherichia coli* and *Saccharomyces cerevisiae.* The yeast, *S. cerevisiae* has emerged as one of the preferred host organisms for the production of isoprenoids due to the relatively high native isoprenoid/mevalonate pathway flux, ease of genetic manipulation, GRAS (generally regarded as safe), knowledge of its genetic and physiological characteristics and availability of engineering tools (Vickers et al., 2017). The first aspect to the production of terpenoids in microbes is the deciphering of biosynthetic pathway. While in case of many simpler terpenoids this is known, in many cases the pathways need to be deciphered. However where the pathway is known, different synthetic biology approaches can be used to reconstruct the metabolic pathways and re-engineer the native pathways and networks to increase the yield of terpenoids. Most synthetic biology approaches for increasing the yield of terpenoids have focused on increasing precursors of mevalonate pathway, cofactor engineering and balancing of pathways. Some strategies that have been employed include overexpression of truncated HMG-CoA reductase (*tHMG1)* (that lacks feedback regulation) (Ro et al., 2006b; Westfall et al., 2012a; Zhou et al., 2012b), a hyperactive transcription factor *upc2-1* (that increases expression of the mevalonate pathway)(Ro et al., 2006b; Westfall et al., 2012a), reducing expression of squalene synthase (*ERG9)* (that prevents isoprenoids from branching off excessively into sterol biosynthesis) (Asadollahi et al., 2010; Babiskin and Smolke, 2011), increasing the precursor acetyl-CoA by engineering pyruvate dehydrogenase (PDH) bypass (Shiba et al., 2007), over expression of alcohol dehydrogenase (*ADH2*) (Lv et al., 2014), decreasing competition for acetyl-CoA in the glyoxylate cycle by deleting malate synthase (*MLS1)* and citrate synthase (*CIT2)* (Chen et al., 2013). Using these above mentioned strategies, increased flux has been demonstrated and the yield of isoprenoids further increases when these different mutations and strategies are combined. However, in the cell, metabolic pathways are interconnected and tightly regulated (Szappanos et al., 2011) and it

is possible that besides the mevalonate pathway genes, there may be other genes which affect directly or indirectly isoprenoid pathway flux. To identify these mutants and genes from a pool of million requires a genetic screen that would ideally be robust, sensitive, rapid and applicable to all isoprenoids. However, such a screen has been lacking.

Carotenoids which are tetratepenoids and colored compounds have the potential to be used in such a screening assay, as they can provide visual, fast, colorimetric readouts for altered isoprenoid pathway flux. A few groups have attempted to increase the metabolic flux in the isoprenoid pathway using this carotenoid based visual screen using the carotenogenic enzymes from *Xanthophyllomyces dendrorhous* (Ozaydin et al., 2013; Verwaal et al., 2007b; Yuan and Ching, 2014). However these studies have met with limited success due to a lack of correlation being observed between pigmentation and increased isoprenoid flux. Thus they were unable to pick up desired genes or mutations.

With this background, the following objectives were framed

1. To develop and validate a carotenoid-based visual genetic screen for increasing the metabolic flux in the isoprenoid pathway of *S. cerevisiae*
2. To isolate mutants for increasing flux in the isoprenoid pathway by using a carotenoid-based genetic screen
3. To investigate the mechanism of increased isoprenoid flux in the spt15_A101T mutant that was isolated in the screen.

Results and conclusions

1. To develop and validate a carotenoid-based genetic screen for increasing the metabolic flux in the isoprenoid pathway of *S. cerevisiae*

Despite the extensive progress in metabolic engineering strategies for *S. cerevisiae* to increase the yield of commercially valuable isoprenoids, an unbiased screen for identifying genes/mutations increasing the isoprenoid flux has been lacking. In this chapter, we addressed this lacuna and described the efforts towards the development of a carotenoid-based visual genetic screen. Previous efforts working with carotenogenic enzymes from *Xanthophyllomyces dendrorhous* revealed a rate limiting block of phytoene dehydrogenase,

that appeared as a hindrance for the development of this screen. We therefore chose carotenogenic enzymes from the red yeast *Rhodosporidium toruloides* which was reported to be the highest producer of β-carotene (Mata-Gomez et al., 2014). The core carotenogeneic genes namely GGPP synthase (*Rt*GGPPS), phytoene synthase (*Rt*PSY1) and phytoene dehydrogenase (*Rt*CRTI) were identified from the genome of *R. toruloides* through bioinformatics approaches, codon optimized, custom synthesized and expressed in *S. cerevisiae.*

Expression of the above genes from the strong TEF promoter and in a single copy centromeric vector led to significant levels of β-carotene levels, higher than the previous reports (Verwaal et al., 2007b). However, despite the expectation that the higher capacity of the *R. toruloides* carotenogenic enzymes would pull the isoprenoid flux into carotenoids without metabolic bottlenecks, a metabolic block resulting from a rate limiting phytoene dehydrogenase (*Rt*CRTI) was encountered. To overcome this block, we employed a directed evolution strategy to isolate mutants of phytoene dehydrogenase (*Rt*CRTI) from *R. toruloides* with increased activity. More efficient phytoene dehydrogenase mutants were isolated (*Rt*CRTI_A393T, *Rt*CRTI_A394G), but we still were unable to successfully develop the visual screen that responded phenotypically to expression of *tHMG1*, a known flux enhancer. This was due to the accumulation of the intermediate metabolite phytoene. We therefore limited the phytoene pools by employing a less efficient version of GGPP synthase from *S. cerevisiae* (*Sc*BTS1). At each developmental stage, the screen was validated with the known isoprenoid flux increaser, *tHMG1*. Combining these different strategies which includes varying promoter strength of carotenogenic enzymes, directed evolution of phytoene dehydrogenase and using catalytically less efficient version of GGPP synthase (*Sc*BTS1), a carotenoid-based genetic screen was developed. This screen was also validated with *tHMG1* where we observed increased pigmentation with increased isoprenoid pathway flux.

2. To isolate mutants for increasing flux in the isoprenoid pathway by using a carotenoid- based genetic screen

To identify the genes/mutants with increased isoprenoid pathway flux using the visual genetic screen that we developed, we took two approaches. In the first we used a candidate gene approach, in which a global regulator was targeted for mutagenesis. In the second

approach, a random mutagenesis of the yeast genome was carried out. In the candidate gene approach, we employed a method referred to as global transcription machinery engineering (gTME) for isolating mutants of a global TATA binding protein, *SPT15* for improved isoprenoid pathway flux. gTME has been successfully applied previously for isolation of *spt15* variants for conferring ethanol tolerance and oxidative stress tolerance (Alper et al., 2006b). In the present study, dominant gain of function mutants of a plasmid borne *SPT15* were isolated using the carotenoid-based screen in *S. cerevisiae* containing a native wild type *SPT15* gene. The mutant residues were found to be located at the positions R98H, A100V or A101T. These mutants were not previously reported for ethanol or oxidative stress tolerance but had the ability to increase the yield of carotenoids.

These mutants were also examined for their ability to increase overall flux in the isoprenoid pathway using an alternate isoprenoid, α- farnesene. For production of α- farnesene, farnesene synthase cDNA of *Arabidopsis thialiana* was obtained and overexpressed in *S. cerevisiae.* It was observed that the spt15 mutants increased the carotenoid as well as α-farnesene levels, suggesting that they were able to increase the overall isoprenoid pathway flux in *S. cerevisiae* and were not specific for carotenoids. Multiple sequence alignment of SPT15 protein revealed that the mutated residues were conserved in fungi.

In a second approach, we isolated mutants with increased isoprenoid pathway flux through whole genome mutagenesis using ethylmethane sulfonate (EMS). Mutants were screened on basis of increased pigmentation. Interestingly, we were able to isolate two mutants (M1 and M2) with increased pigmentation and lycopene (carotenoid) levels. These mutants were further analyzed for identification of mutations through whole genome sequencing (WGS) approach. WGS data revealed that the mutant residues were different in both strains and present in different genes. However, the role of individual mutations on the isoprenoid pathway flux still needs to be investigated.

What we were able to establish however was that novel mutants affecting isoprenoid pathway flux can be isolated. These novel mutants will help in understanding hitherto unknown factors critical for the isoprenoid pathway & its flux. It will also help in understanding of integration of the isoprenoid pathway to the larger metabolic and regulatory networks

3. To investigate the mechanism of increased isoprenoid flux in the spt15_A101 mutant

Among the three *spt15* variants isolated through the global transcription machinery engineering (gTME), the spt15_A101T mutant showed highest increase in the isoprenoid pathway flux. To understand the metabolic basis for increased isoprenoid flux in the spt15_A101T mutant strain, we employed a combination of metabolic flux analysis (MFA) and transcriptomics. The predictions were validated using the phenotypic assays.

Growth comparison of SPT15WT and spt15_A101T mutant strain were carried out in order to evaluate the fluxes. The mutant strain had slower growth rate as compared to the wild type strain, despite showing an increased isoprenoid pathway flux. The growth rate, glucose consumption rate and secretion rate of three extracellular metabolites- acetate, glycerol and ethanol were determined during the exponential phase of growth of SPT15WT and the spt15_A101T strains. Using the above mentioned parameters, constraint based metabolic flux analysis of wild type and mutant strains were carried out using the whole genome scale model of *S. cerevisiae*, iMM904. In the metabolic flux analysis, the phenotypic state characterized by the fluxes in the metabolic network was used to postulate the mechanism for increased isoprenoid pathway flux. The MFA of the mutant strain showed rerouting of carbon, increased NADPH pools, increased ATP and phosphate demand in the cell for increased isoprenoid pathway flux.

The mutant strain showed an increased flux in the reaction catalyzed by pyruvate decarboxylase (*PDC*) as seen from MFA. This led to new route of production of acetyl CoA from acetate resulting in an increased ATP demand in the cell. The increased pool of acetyl-CoA was channeled to HMG-CoA which increased the flux towards the isoprenoid pathway. The remaining carbon was routed towards the TCA cycle which was truncated as the cycle cycle was completed via the glyoxylate shunt as opposed to via succinyl-CoA since this requires additional phosphate for ATP generation. The glyoxylate shunt balances the CoA pool without the need for additional phosphate and hence is the preferred pathway to complete the TCA cycle, especially under phosphate limitation.

To refine the flux balance analysis, transcriptomic analysis of wild type and mutant strain were carried out. The differential expression of genes observed in mutant strain suggested the

up-regulation of phosphate signaling and phosphate regulation (PHO) pathway and pyruvate decarboxylase (*PDC6*). The role of pyruvate decarboxylase (*PDC6*) and phosphate limitation on the isoprenoid pathway in the mutant strain were validated through over expression and deletion studies of *PDC6*. The results suggested that the mutant strain essentially requires *PDC6* for growth and increased flux through the isoprenoid pathway under phosphate limitation conditions. Therefore, up-regulation of *PDC6* was exploited by the mutant strain for increased acetaldehyde, acetate and acetyl-CoA pools (both in cytosol and mitochondria) which were essential for the increased flux through the isoprenoid pathway.

References:

Alper, H., Moxley, J., Nevoigt, E., Fink, G. R., Stephanopoulos, G., 2006. Engineering yeast transcription machinery for improved ethanol tolerance and production. Science. 314**,** 1565-8.

Asadollahi, M. A., Maury, J. r. m., Schalk, M., Clark, A., Nielsen, J., 2010. Enhancement of farnesyl diphosphate pool as direct precursor of sesquiterpenes through metabolic engineering of the mevalonate pathway in Saccharomyces cerevisiae. Biotechnology and bioengineering. 106**,** 86-96.

Babiskin, A. H., Smolke, C. D. C., 2011. A synthetic library of RNA control modules for predictable tuning of gene expression in yeast. Molecular systems biology. 7**,** 471.

Chen, Y., Daviet, L., Schalk, M., Siewers, V., Nielsen, J., 2013. Establishing a platform cell factory through engineering of yeast acetyl-CoA metabolism. Metab Eng. 15**,** 48-54.

Lv, X., Xie, W., Lu, W., Guo, F., Gu, J., Yu, H., Ye, L., 2014. Enhanced isoprene biosynthesis in Saccharomyces cerevisiae by engineering of the native acetyl-CoA and mevalonic acid pathways with a push-pull-restrain strategy. J Biotechnol. 186**,** 128-36.

Mata-Gomez, L. C., MontaÃ±ez, J. C., MÃ©ndez-Zavala, A., Aguilar, C. b. N. C., 2014. Biotechnological production of carotenoids by yeasts: an overview. Microbial cell factories. 13**,** 12.

Ozaydin, B., Burd, H., Lee, T. S., Keasling, J. D., 2013. Carotenoid-based phenotypic screen of the yeast deletion collection reveals new genes with roles in isoprenoid production. Metabolic engineering. 15**,** 174-183.

Ro, D. K., Paradise, E. M., Ouellet, M., Fisher, K. J., Newman, K. L., Ndungu, J. M., Ho, K. A., Eachus, R. A., Ham, T. S., Kirby, J., Chang, M. C., Withers, S. T., Shiba, Y., Sarpong, R., Keasling, J. D., 2006. Production of the antimalarial drug precursor artemisinic acid in engineered yeast. Nature. 440**,** 940-3.

Shiba, Y., Paradise, E. M., Kirby, J., Ro, D. K., Keasling, J. D., 2007. Engineering of the pyruvate dehydrogenase bypass in Saccharomyces cerevisiae for high-level production of isoprenoids. Metab Eng. 9**,** 160-8.

Szappanos, B. z., KovÃ¡cs, K. r., Szamecz, B. l., Honti, F., Costanzo, M., Baryshnikova, A., Gelius-Dietrich, G., Lercher, M. J., Jelasity, M. r., Myers, C. L., Andrews, B. J., Boone, C., Oliver, S. G., PÃ¡l, C., Papp, B. z. C., 2011. An integrated approach to characterize genetic interaction networks in yeast metabolism. Nature genetics. 43**,** 656-662.

Verwaal, R., Wang, J., Meijnen, J. P., Visser, H., Sandmann, G., van den Berg, J. A., van Ooyen, A. J., 2007. High-level production of beta-carotene in Saccharomyces cerevisiae by successive transformation with carotenogenic genes from Xanthophyllomyces dendrorhous. Appl Environ Microbiol. 73**,** 4342-50.

Vickers, C. E., Williams, T. C., Peng, B., Cherry, J., 2017. Recent advances in synthetic biology for engineering isoprenoid production in yeast. Curr Opin Chem Biol. 40**,** 47-56.

Westfall, P. J., Pitera, D. J., Lenihan, J. R., Eng, D., Woolard, F. X., Regentin, R., Horning, T., Tsuruta, H., Melis, D. J., Owens, A., Fickes, S., Diola, D., Benjamin, K. R., Keasling, J. D., Leavell, M. D., McPhee, D. J., Renninger, N. S., Newman, J. D., Paddon, C. J., 2012. Production of amorphadiene in yeast, and its conversion to dihydroartemisinic acid, precursor to the antimalarial agent artemisinin. Proc Natl Acad Sci U S A. 109**,** E111-8.

Yuan, J., Ching, C. B., 2014. Combinatorial engineering of mevalonate pathway for improved amorpha-4,11-diene production in budding yeast. Biotechnology and bioengineering. 111**,** 608-617.

Zhou, Y. J., Gao, W., Rong, Q., Jin, G., Chu, H., Liu, W., Yang, W., Zhu, Z., Li, G., Zhu, G., Huang, L., Zhao, Z. K., 2012. Modular pathway engineering of diterpenoid synthases and the mevalonic acid pathway for miltiradiene production. Journal of the American Chemical Society. 134**,** 3234-3241.

CHAPTER 1:

Review of Literature

Review of Literature

GENERAL INTRODUCTION

The major focus of this thesis has been to try and devise strategies that would allow one to identify new genes or mutants from pools of millions that can increase the flux in the isoprenoid pathway. To provide some background to this work, the general introduction has been divided into four parts, Part I: Terpenoid and terpenoid biosynthetic pathways Part II: Metabolic engineering strategies for increasing the isoprenoid pathway flux in *S. cerevisiae* Part III: Screening strategies for increased isoprenoid pathway activity in *S. cerevisiae* Part IV: Carotenoid and their biosynthesis

Part I: Terpenoid and terpenoid biosynthetic pathways

1.1 Terpenoids and their function

Isoprenoids (terpenes and terpenoids) are the largest class of natural products. The term isoprenoids is derived from five- carbon isoprene units. All terpenoids are derived from the universal five-carbon building blocks, isopentenyl diphosphate (IPP) and its isomer dimethylallyl diphosphate (DMAPP) and thus is often referred to as the isoprene rule (KH, 2010). Terpenoids are produced by all kingdoms of life including archaebacteria bacteria, fungi, plants and humans. In prokaryotes, terpenoids play a key role in biological processes that are essential for their growth and survival, e.g. cell wall and membrane biosynthesis (bactoprenol, hopanoids), electron transport (ubiquinone, menaquinone) and conversion of light into chemical energy (bacteriochlorophylls, rhodopsin, carotenoids). In addition to the terpenoids involved in biological processes, prokaryotes also produce some terpenoids as secondary metabolites e.g. as odor constituents, antibiotics and pigments. For example geosmin, a sesquiterpene derivative is responsible for characteristic odor of moist soil and some antibiotics are produced by Actinomycetes (Dairi, 2005). Higher fungi (Ascomycota and Basidiomycota) also produce an array of terpenoid natural products, including mycotoxins, antibiotics, antitumor compounds and phytohormones. The secondary metabolome of Ascomycota is dominated by polyketides and non-ribosomal peptides (NRPSs) (Boettger and Hertweck, 2013; Chooi and Tang, 2012; Evans et al., 2011), whereas basidiomycota are known for the production of terpenoids such as sesquiterpenoids and tritepenoids. In plants which are the largest source, terpenoids have

functions in growth, metabolism and specialized functions such as chemical interactions and protection in abiotic and biotic environment.

1.2 Classification of terpenoids and their commercial importance

Terpenoids can be classified on the basis of the number and structural organization of five carbon isoprene unit as shown in table 1.1.

1.3 Biosynthetic pathways: The mevalonate pathway (MVA) and The methyl-D-erythritol 4-phosphate (MEP) pathway

There are two major pathways that produce the precursors of all terpenoids- the mevalonate pathway (MVA) and the methyl-D-erythritol 4-phosphate (MEP) pathway.

1.3.1 The methyl-D-erythritol 4-phosphate (MEP) pathway

The MEP pathway occurs in most eubacteria and in all photosynthetic eukaryotes, cyanobacteria, apicomplexan protozoa and plant plastids (Boucher and Doolittle, 2000; Lange et al., 2000; Rohmer, 1999). The MEP pathway in plants is used for the biosynthesis of hemiterpenoids, monoterpenoids, diterpenoids, tetraterpenoids such as carotenoids and their breakdown products, cholorophyll, tocopherols, cytokinins, gibberellins and plastoquinones. This pathway is absent in animals, fungi and archaeabacteria. As shown in detailed pathway in figure 1A, the MEP pathway consists of seven enzymatic steps. The first step is the synthesis of 1-deoxy-D-xylulose-5-phosphate by an enzyme DXP synthase. Several studies have reported that DXP synthase is the important regulatory and rate limiting step in the biosynthesis of plastidial terpenes in plants (Estevez et al., 2001; Fraser et al., 1994). The last step is a branching step where HMBPP (4-hydroxy-3-methylbut-2-enyl diphosphate) is converted to mixture of IPP and DMAPP with a ratio of 5 to 6:1 by an enzyme 4-hydroxy-3-methylbut-2-enyl diphosphate reductase (HDR, IspH).

Terpenoids	Number of C atoms/ isoprene units	Precursor	Example	Commercial importance
Hemiterpenoids (C_5)	05/01	IPP/DMAPP	Isoprene	Potential Biofuel Used for production of synthetic version of natural rubber
Monoterpenoids (C_{10})	10/02	GPP	Myrecene, Geraniol Linalool, Citroellol, Menthol, Thymol, Eucalyptol, Camphor	Component of essential oils, used for flavor and aroma.
Sesquiterpenoids (C_{15})	15/03	FPP	β-Farnesene, Amorha-4, 11-diene, α-humulene, Nootkatone Zinglberene, Artemisinin, Caryophyllene, Bisabolene	Antimicrobial, anti-inflammatory and antitumor, Flavor and Fragrance, Fuel
Diterpenoids (C_{20})	20/04	GGPP	Taxa-4(5),11(12)-diene, Taxol, Ginkgolides	Pharmaceutical-Treatment and management of cancer, treatment of cerebrovascular diseases
Sesterterpenoids (C_{25})	25/05	FGPP	Ophiobolin A, Bilosespene A	Antibacterial, antifungal and antinematode
Triterpenoids (C_{30})	30/06	FPP	Squalene, Cholesterol, Hopane	Antioxidants, cosmetics, nutrition, vaccines
Tetraterpenoids (C_{40})	40/08	GGPP	Carotenoids-Lycopene, β-carotene, Astaxanthin, Torularhodin	Antioxidants, Colorants

Table 1.1 Classification of terpenoids and their commercial importance

1.3.2 The mevalonate (MVA) pathway

The MVA pathway is the only pathway producing terpenoid precursors in fungi and animals including humans. It also occurs in the cytosol of plants and provides the precursors for cytosolic biosynthesis of sesquiterpenoids, triterpenoids, polyprenols, phytosterols and for terpenoid biosynthesis in mitochondria (e.g. ubiquinone, polyrenols). Plants thus have two pathways, the MEP pathway which occurs in plastids and the MVA pathway which occurs in the cytosol. As shown in figure 1B, the MVA pathway consists of six steps. The first step is condensation of two molecules of acetyl-CoA to form acetoacetyl CoA catalyzed by acetoacetyl CoA thiolase (*AACT*). The acetoacetyl CoA is combined with acetyl CoA to form S-3-hydroxy-3-methylglutaryl-CoA (HMG-CoA) catalyzed by an enzyme HMG-CoA synthase (*HMGS*). This is followed by a rate-limiting step catalyzed by a NADPH dependent HMG-CoA reductase (*HMGR*) to produce *R*-mevalonate (MVA) from *S*-HMG-CoA. The MVA is sequentially phosphorylated to mevalonate-5-phosphate and mevalonate-diphosphate catalyzed by the ATP-dependent mevalonate kinase (*MK*) and the ATP- dependent phosphomevalonate kinase (*PMK*) respectively. This is followed by an ATP-driven decarboxylative elimination catalyzed by mevalonate diphosphate decarboxylase (*MVD* or *MPDC*) to produce isopentenyl diphosphate (IPP). IPP can be converted into its allylic isomer dimethyl allyl pyrophosphate (DMAPP) by an enzyme IPP/DMAPP isomerase (*IDI1*).

1.4 Metabolic engineering of microorganisms for production of commercially important terpenoids

All terpenoids/isoprenoids are derived from the universal C5 monomers, IPP and DMAPP which are produced from both the pathways, MVA and MEP. These precursors IPP and DMAPP are condensed to first form geranylphosphate (GPP). This is then converted to farnesyl diphosphate (FPP) and subsequently geranylgeranyl diphosphate (GGPP). As shown in figure 2, GPP acts as a precursor for the synthesis of monoterpenoids, and FPP acts as a precursor for the synthesis of triterpenoids and sesquiterpenoids. GGPP acts as a precursor for the synthesis of tetraterpenoids. Most of these commercially important terpenoids are produced by plants and hence are extracted from the plants through laborious and expensive procedures. This is made more difficult because of seasonal variation and accumulation in minute quantities, laborious extraction procedures. The chemical synthesis of most of these terpenoids is complex.

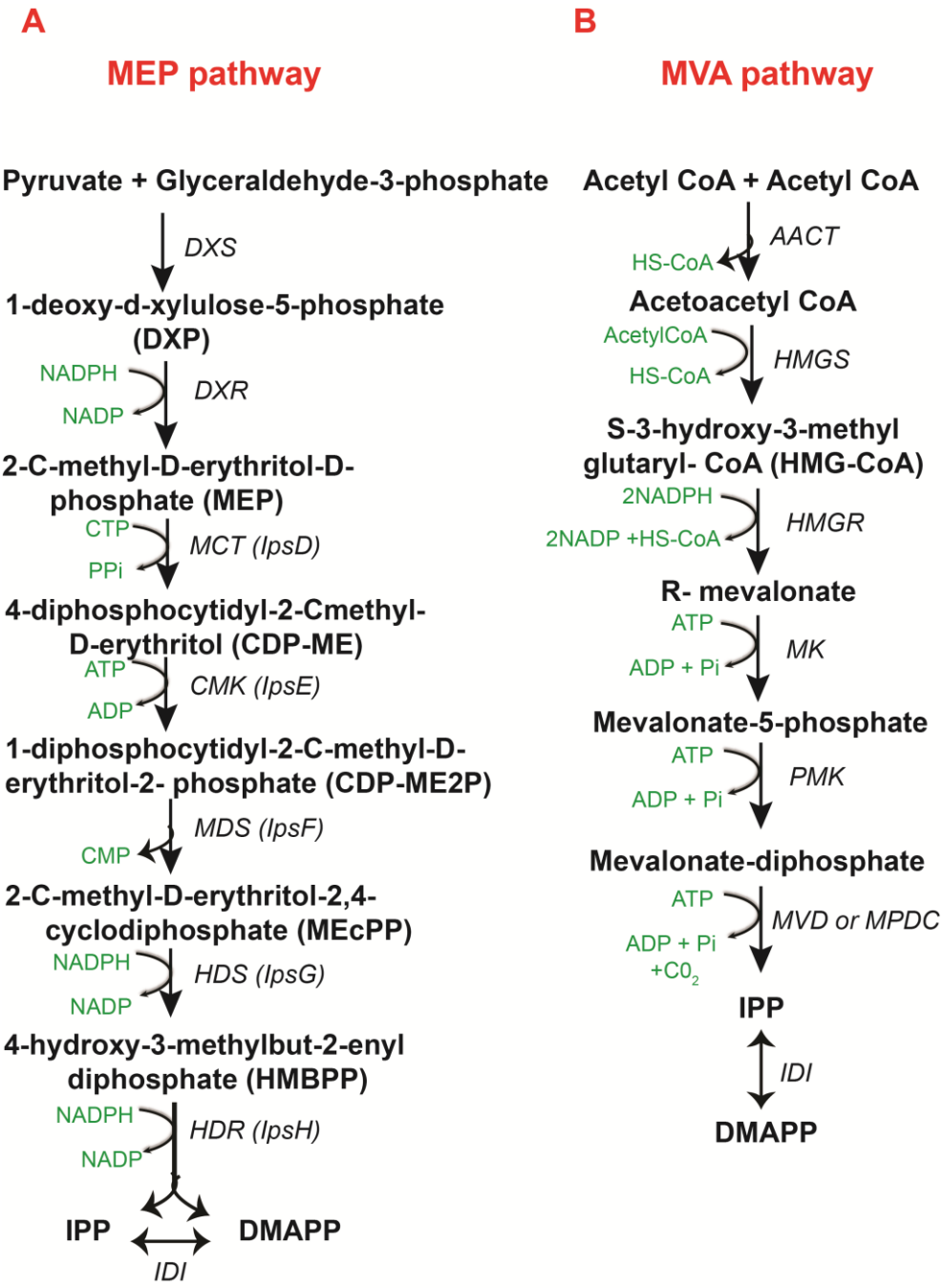

Figure 1. Schematic representation of terpenoid pathways (A) MEP pathway (B) MVA pathway *DXS*- 1-deoxy-D-xylulose 5-phosphate (DXP) synthase, *DXR*- DXP reductoisomerase, *MCT*- 2-*C*-methyl-D-erythritol (MEP) cytidylyltransferase, *CMK*- 4-(cytidine 5'-diphospho)-2-*C*-methyl-D-erythritol kinase, *MDS*- 2-*C*-methyl-D-erythritol 2,4-cyclodiphosphate (MEcPP) synthase, *HDS*- 4-hydroxy-3-methylbut-2-enyl diphosphate (HMBPP) synthase, *HDR*- HMBPP reductase, *IDI1*- Isopentenyl diphosphate isomerase, *AACT*- acetoacetyl-CoA thiolase, *HMGS*- 3-hydroxy-3-methyl-glutaryl-CoA (HMG-CoA) synthase, *HMGR*- HMG-CoA reductase, *MK*- Mevalonate kinase, *PMK*- Phosphomevalonate kinase, *MVD*- mevalonate diphosphate decarboxylase. IPP- isopentenyl pyrophosphate, DMAPP- dimethylallyl pyrophosphate

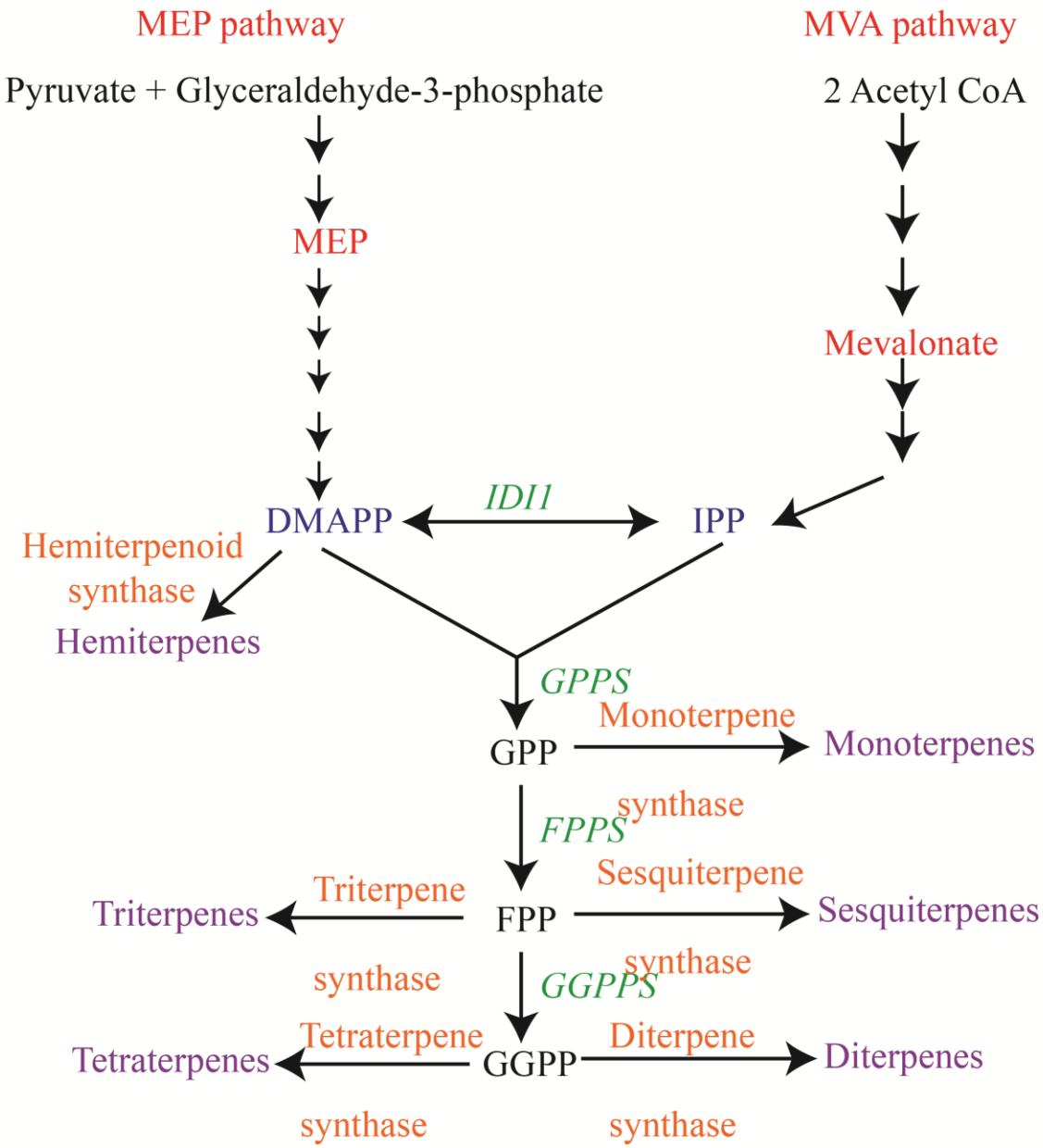

Figure 2. Schematic representation of production of different terpenoids from different precursors of terpenoid pathway.

IPP- isopentenyl pyrophosphate, DMAPP- dimethylallyl pyrophosphate, GPP- geranyl pyrophosphate, FPP- farnesyl pyrophosphate, GGPP- geranylgeranyl pyrophosphate, *IDI*- Isopentenyl diphosphate isomerase, *GPPS*- geranyl pyrophosphate synthase, *FPPS*- farnesyl pyrophosphate synthase, *GGPPS*- geranylgeranyl pyrophosphate synthase

Thus, efforts have focused on the heterologous production of these valuable compounds. If the biosynthetic pathways are known, the metabolic engineering of microorganisms for the production of terpenoids provides a relatively fast and inexpensive route, and can also result in purer products and higher yields (Farhi et al., 2011; Herrero et al., 2008; Keasling, 2010). *Saccharomyces cerevisiae* and *Escherchia coli* are preferred hosts for terpenoid production due to the available molecular tools with these organisms and well characterized genetic information. However, the biosynthesis of many terpenoids involves complex membrane bound enzymes belonging to the cytochrome P450 family which are difficult to express in *E. coli* due to differences in membrane structure. Therefore, for the production of terpenoids involving these specialized cytochrome P450 enzymes, *S. cerevisiae* is a better choice as a host organism. To date, *S. cerevisiae* has been successfully exploited for the production of valuable terpenoids ginsenosides (Dai et al., 2013) and artemisinic acid in high titer (Paddon et al., 2013) among other terpenoids. Besides these microorganisms, other prokaryotic organisms such as *Corynebacterium glutamicum* (Heider et al., 2012) and *Bacillus subtilis* (Zhou et al., 2013) have also been engineered for the production of isoprenoids. Recently, the red yeast *Rhodosporidium toruloides* has received lots of attention as a host organism for the production of valuable terpenoids due to the highly efficient lipid biosynthesis (Zhu et al., 2012). The table 1.2 provides the list of commercially important terpenoids produced in different host organisms.

Class of terpenoid	Terpenoid/Product	Production Host	Commercial application
Monoterpenoid	Linalool	*S. cerevisiae*	Flavour
	Geraniol	*S. cerevisiae, A. thaliana*	Flavour
	Citranellol	*S. cerevisiae*	Flavour
Diterpenoid	Taxa-diene	*S. cerevisiae, E. coli*	Pharmaceutical
Sesquiterpenoid	Amorha-4,11-diene	*S. cerevisiae, E. coli*	Pharmaceutical
	Nootkatone	*S. cerevisiae*	Flavour
	8-epi-cedrol	*S. cerevisiae, E. coli*	Fragrance
	8-cadinene	*E. coli*	Flavour, Cosmetics
Tetraterpenoids (Carotenoids)	Lycopene	*S. cerevisiae, E. coli*	Colourants, Nutraceutical
	β-carotene	*S. cerevisiae, E. coli*	Colourants
	Astaxanthin	*S. cerevisiae, E. coli*	Colourants

Table 1.2 Classification of terpenoids and their commercial importance

Part II: Metabolic engineering strategies

1.5 Metabolic engineering strategies for increasing the yield from MVA pathway in *S. cerevisiae*

The yeast MVA pathway has been extensively manipulated to increase the yield of commercially important terpenoids. The MVA pathway is connected to central carbon metabolism via acetyl coenzyme A (acetyl-CoA), ATP (energy) and NADPH (reducing power) (Vickers et al., 2017). Different metabolic engineering strategies have been utilized to manipulate the metabolic flux and regulation of native MVA pathway in *S. cerevisiae* so as to increase the yield of terpenoids and shown in figure 3. These are explained below:

1.5.1 Increasing the precursor supply

The approach is to increase the supply of universal precursors- IPP/DMAPP, FPP, GGPP of MVA pathway. This has been achieved by several approaches:

a. Overexpression of all genes of MVA pathway

In this approach all the MVA pathway genes were over expressed by integration of an additional copy of all MVA pathway genes into the genome of *S. cerevisiae* (Keasling J, 2010). In an alternate approach, the promoters of all relevant MVA pathway genes have been replaced to increase the yield of the terpenoid, amorphadiene in *S. cerevisiae* (Westfall et al., 2012b).

b. Overexpression of truncated *HMG1* (*tHMG1)*

Hydroxymethylglutaryl Coenzyme A reductase (HMG-CoA) is a rate limiting enzyme for MVA pathway. It is under feedback regulation and has an N-terminal regulatory region. The deregulated version of *HMG1, tHMG1,* has a truncated N-terminal and contains only the soluble catalytic domain. This was first overexpressed to produce a sterol over-producing strain (Polakowski et al., 1998). The overexpression of *tHMG1*either episomally or in chromosomal integration has subsequently been utilized in many metabolic engineering strategies so as to increase the yield of terpenoids (Westfall et al., 2012b). Expression of *HMG2 (K6R)* had also been reported to enhance monoterepne and sesquiterpene production by stabilizing HMG2(K6R) protein from degradation (Ignea et al., 2011).

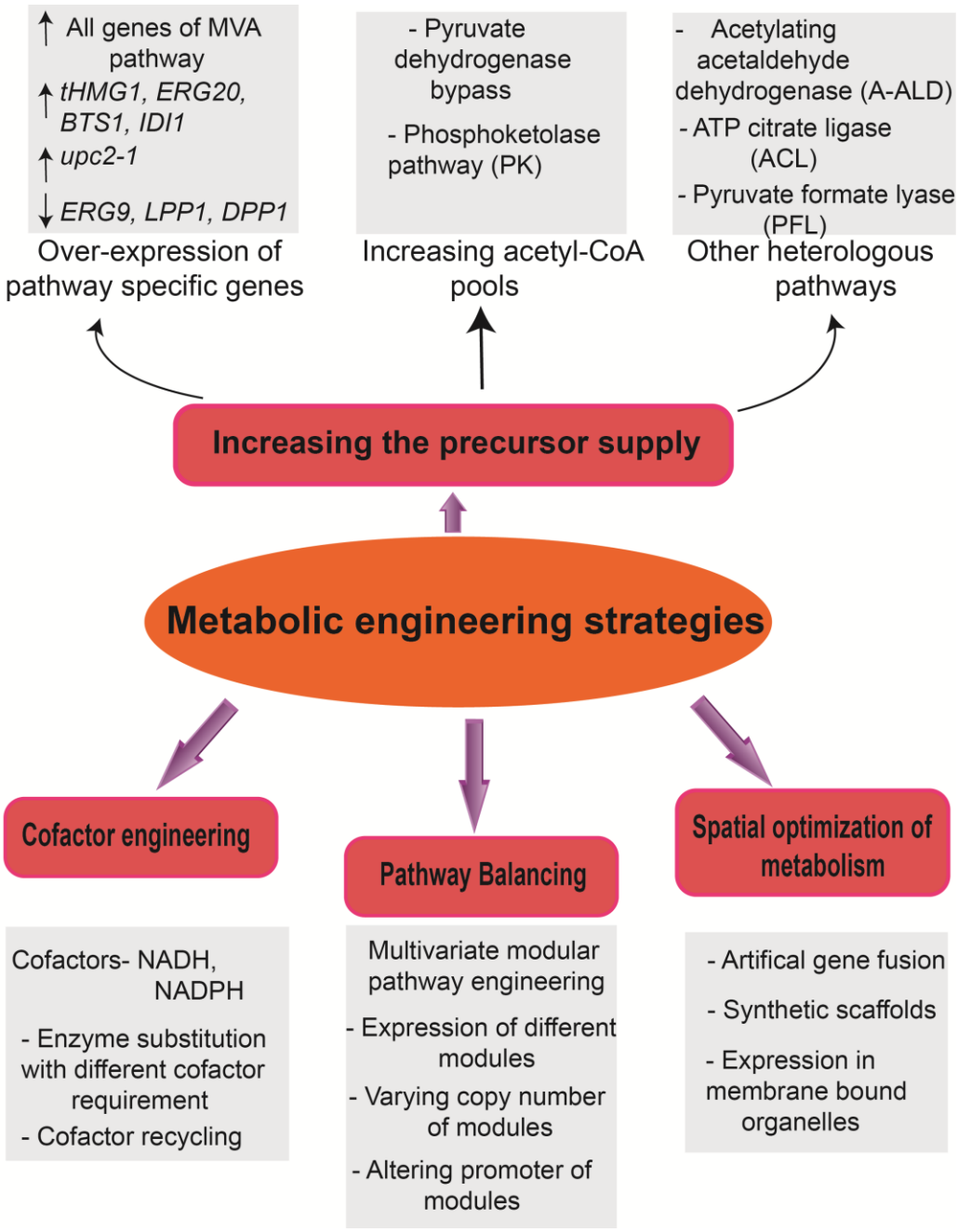

Figure 3. Schematic representation of different currently employed metabolic engineering strategies for increasing the mevalonate pathway flux in *S. cerevisiae*

tHMG1- truncated hydroxymethyl glutaryl coenzyme A reductase 1, *ERG20*- Farnesyl pyrophosphate synthase, *BTS1*- geranylgeranyl diphosphate synthase, *IDI1*- Isopentenyl diphosphate isomerase, *upc2-1*- mevalonate pathway specific transcription factor mutant (G888D), *ERG9*- squalene synthase , *LPP1*- Lipid phosphate phosphatase, *DPP1*- Diacylgycerol pyrophosphate phosphatase

c. Overexpression of farnesyl pyrophosphate synthase (*ERG20)*

Wild type farnesyl pyrophosphate synthase, *ERG20* produces precursors GPP and FPP in ratio of 25:75. Overexpression of *ERG20* has also been used as an approach to increase the yield of artemisinin (Paddon et al., 2013). A mutant *ERG20 (K197E)* was reported to produce GPP:FPP in the ratio of 70:30, and has been utilized to enhance the production of monoterpene, geraniol (Fischer et al., 2011).

d. Overexpression of geranylgeranyl diphosphate synthase (*BTS1)*

The *BTS1* gene of *S. cerevisiae* encodes the enzyme called geranylgeranyl diphosphate synthase which catalyzes the production of GGPP. It acts as a precursor for synthesis of ubiquinone and geranylgeranylation of proteins for membrane attachment. It is also a substrate for the synthesis of diterpenoids and tetraterpenoids. Overexpression of native *BTS1* and GGPP synthase (*GGPPS*) from other carotenoid producing organisms e.g. red yeast *X. dendrorhous* has been utilized to enhance the production of carotenoids such as, astaxanthin (Ukibe et al., 2009; Verwaal et al., 2007a).

e. Overexpression of isopentenyl diphosphate:dimethylallyl diphosphate isomerase (*IDI1)*

IDI1 catalyzes the conversion of DMAPP to IPP. Overexpression of *IDI1* has been reported to increase the production of monoterpenes (Ignea et al., 2011).

f. Down-regulation of squalene synthase (*ERG9)*

ERG9 encodes for squalene synthase that directs the flux from FPP to the ergosterol pathway in *S. cerevisiae*. Therefore, to increase flux towards the synthesis of the desired terpenoid products, downregulation of *ERG9* reduces the flux to the ergosterol pathway. Complete knockout of *ERG9* is not feasible as deletion of this gene is lethal. Therefore, to reduce the activity of *ERG9*, promoter replacement has been used as a successful strategy. Downregulation of *ERG9* through the use of promoters that could be repressed in presence of methionine (P_{MET3}), or copper (P_{CRT3}) or glucose limiting conditions (P_{HTX1}) promoter have been used for enhancing the production of the sesquiterpenes (Asadollahi et al., 2008; Paddon et al., 2013; Scalcinati et al., 2012a). Native ERG promoters of genes *ERG11*, *ERG3* and *ERG2* which were downregulated by high

ergosterol levels have been used to control *ERG9* expression and enhance the expression of amorphadiene by 2-5 fold (Yuan and Ching, 2015). Deactivated Cas9 have also been targeted to the promoters of MVA pathway genes, which causes repression of *ERG9* to control fluxes (Jensen et al., 2017). There have also been efforts to control levels of *ERG9* proteins by attaching protein degradation tags to the C-terminal of ERG9 protein (Peng et al., 2017b). A modified diauxic-inducible GAL expression system was also used to control the expression of genes by coupling flux to different growth phases (Peng et al., 2017a).

g. Down-regulation of Lipid phosphate phosphatase (*LPP1)* and diacylgycerol pyrophosphate phosphatase *(DPP1)*

LPP1 encodes for lipid phosphate phosphatase and *DPP1* encodes for diacylglycerol pyrophosphate phosphatase. Both these phosphatidic acid hydrolases catalyze the dephosphorylation of FPP and GPP which was reported as a mechanism to alleviate the potentially toxic effects of accumulation of these substrates (Faulkner et al., 1999). Deletion of *DPP1* was also reported to result in a modest increase of the sesquiterpene α-santalene (Scalcinati et al., 2012a).

h. Transcription factor, *UPC2*

Upc2p belongs to a family of zinc cluster transcription factor. *UPC2* regulates a number of ergosterol (*ERG*) biosynthetic pathway genes in yeast. It binds to the sterol response elements (SRE) in the promoters of target genes and positively regulating their transcription. The *upc2-1* mutant contains a single amino acid change (G888D) within the activation domain of the protein (Crowley et al., 1998; MacPherson et al., 2006) and overexpression of *upc2-1* had been reported as a strategy to increase the production of amorphadiene alone or in combination with *tHMG1* and P_{MET3}-ERG9 (Peralta-Yahya et al., 2011; Ro et al., 2006a; Westfall et al., 2012b).

i. Increasing acetyl-CoA pools

In *S. cerevisiae*, acetyl CoA is an intermediate metabolite. Its metabolism is compartmentalized in the cytosol, mitochondria, peroxisome and nucleus (Figure 4). Engineering of acetyl CoA is a complex process due to its compartmentalization and non-transport across the compartments. Acetyl-CoA is a substrate for TCA cycle in the mitochondria, fatty acid synthesis and protein

acetylation which is important for the regulation of enzyme function and DNA transcription. It is also a precursor for mevalonate pathway and is the end product of fatty acid degradation. As shown in figure 4, mitochondrial acetyl CoA is synthesized through pyruvate dehydrogenase complex (*PDHC*) from pyruvate while cytosolic acetyl CoA is synthesized from the pyruvate dehydrogenase (PDH) bypass via acetaldehyde dehydrogenase (*ALD6*) and acetyl CoA synthase (*ACS1* and *ACS2*). Acetyl CoA pools is also utilized in the glyoxylate cycle, where acetyl CoA combines with oxaloacetate to form citrate by citrate synthase (Cit2p). In this cycle, acetyl CoA condenses with glyoxylate to form malate by malate synthase (MS). Different strategies have been utilized so far to enhance cytosolic acetyl-CoA pools to increase yield of terpenoids. These strategies includes (1) Overexpression of PDH bypass enzymes (2) Overexpression of acetylation resistant acetyl CoA synthase mutant (ACS_{SE}^{L641P}) (3) Overexpression of alcohol dehydrogenase 2 (*ADH2*), (4) deletion of one of two glyoxylate cycle genes, peroxisomal citrate synthase (*CIT2*) and malate synthase (*MLS1*) (5) deletion of glycerol and ethanol biosynthesis pathway genes (6) heterologous expression of pyruvate dehydrogenase complex (PDHC) from *Enterococcus faecalis*) (7) Overexpression of heterologous acetyl CoA producing enzymes, pyruvate formate lyase (*PFL*) and ATP citrate ligase (*ACL*), (8) Overexpression of phosphoketolase pathway, xylulose-5-phosphate phosphoketolase (*xPK*) from *Aspergillus nidulans* and phosphate acetyltransferase (*PTA*). All of these strategies are shown in figure 5.

i.1 Pyruvate dehydrogenase (PDH) bypass

To increase cytosolic acetyl-CoA pools, traditional strategies include over expression of the PDH bypass enzymes acetylaldehyde dehydrogenase (*ALD6*) and acetyl-CoA synthase (*ACS1* and *ACS2*) along with native pyruvate decarboxylase (*PDC*). In a separate study, PDH bypass was further enhanced by over expression of acetylation resistant acetyl CoA synthase (L641P) (ACS_{SE}^{L641P}) of *Salmonella enterica* for increasing the amorphadiene production by (Shiba et al., 2007). In addition to over expressing *ALD6* and ACS_{SE}^{L641P} , overexpression of endogeneous alcohol dehydrogenase 2 (*ADH2*) which catalyzes the conversion of ethanol to acetylaldehyde was also used for isoprene synthesis (Lv et al., 2014). Deletion of one of two glyoxylate cycle genes, namely peroxisomal citrate synthase (*CIT2*) and cytosolic malate synthase (*MLS1*) along with over expression of native thiolase gene *ERG10* has been utilized in addition to

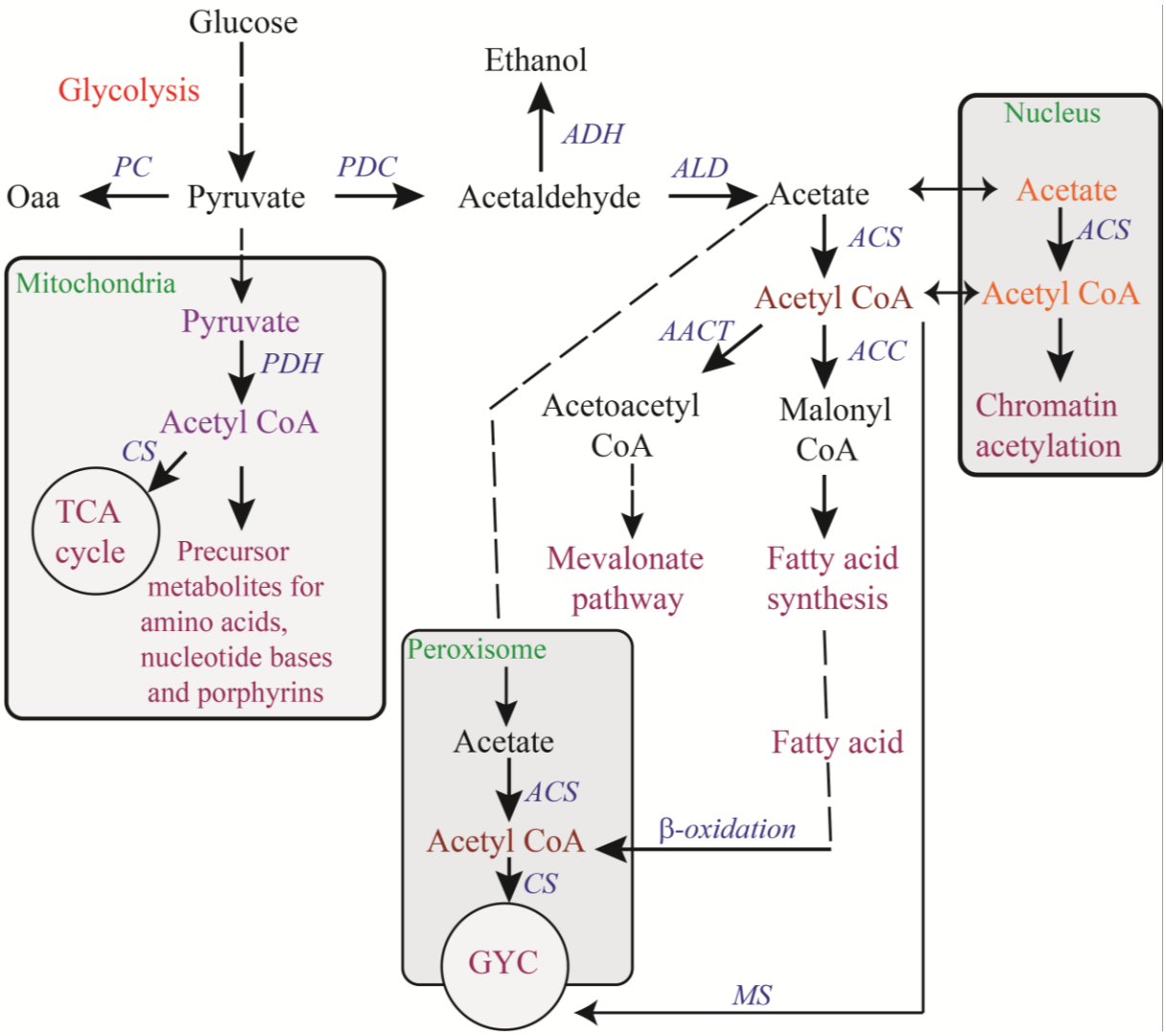

Figure 4. Overview of acetyl CoA metabolism in *Saccharomyces cerevisiae.*

In yeast, Acetyl CoA is compartmentalized in nucleus, cytosol, peroxisome and mitochondria. Cytosolic acetyl-CoA is generated from pyruvate via acetylaldehyde and acetate by action of pyruvate decarboxylase (*PDC*), acetaldehyde dehydrogenase (*ALD*), acetyl CoA synthase (*ACS*). Cytosolic acetyl CoA is utilized in fatty acids synthesis and mevalonate pathway and glyoxylate cycle in peroxisomes by action of acetyl CoA carboxylase (*ACC*), acetoacetyl-CoA thiolase (*AACT*) and malate synthase (*MS*) respectively. Mitochondrial acetyl CoA is synthesized from pyruvate via pyruvate dehydrogenase complex (*PDH*) and utilized in TCA cycle and providing precursors for amino acids, nucleotide bases and porphyrins, in peroxisomes, acetyl CoA is synthesized from acetate by acetyl CoA synthase and from β- oxidation of fatty acids and utilized for glyoxylate cycle. In nucleus, acetyl CoA is synthesized from acetate by acetyl CoA synthase and used for chromatin acetylation.

overexpression of *ALD6*, ACS_{SE}^{L641P} and *ADH2* for enhancing the production of α-santelene (Chen et al., 2013). However, the deletion of *CIT2* or *MLS1* had also been reported to have deleterious/ negative effects on the production of polyhydroxybutyrate (PHB) (Kocharin et al., 2012). Decreasing the ethanol and glycerol production by deletion of genes encoding for alcohol dehydrogenases (*ADH1* and *ADH4*) and glycerol-3-phosphate dehydrogenases (*GPD1* and *GPD2*) was also reported to increase the acetyl-CoA levels by 2 fold (Lian et al., 2014).This deletion strategy was combined with ACS_{SE}^{L641P} to increase the production of 1-butanol. In another approach, bacterial pyruvate dehydrogenase (PDH) was evaluated for generation of cytosolic acetyl CoA in yeast (Kozak et al., 2014b). In this study, pyruvate dehydrogenase (PDH) complex from *Enterococcus faecalis* was expressed in *S. cerevisiae* and showen to be functional under both aerobic and anaerobic conditions where it was able to replace the ACS-dependent pathway for the production of acetyl-CoA.

i.2 Phosphoketolase (PK) pathway

The expression of fungal phosphoketolase (PK) pathway in *S. cerevisiae* has been reported to increase the production of polyhydroxybutyrate (PHB) (Kocharin et al., 2013) and fatty acid ethyl esters (FAEEs) (de Jong et al., 2014). Expression of PK pathway involves expression of xylulose-5-phosphate phosphoketolase (XpkA) and acetate kinase (Ack) from *Aspergillus nidulans.* In addition to these two enzymes, cytosolic transhydrogenase gene *sth* was expressed to increase the drain for NADPH so as to increase the pathway flux. Phosphate acetyl transferase (PTA) alongwith XpkA was also reported to enhance yield of FAEEs. In another study, over expression of PK pathway was combined with over expression of acylating acetaldehyde dehydrogenase (ADA) to reduce ATP requirements which led to the increased yield of farnesene (Meadows et al., 2016).

i.3 Other heterologous enzymes with special features

In *S. cerevisiae,* acetyl CoA synthase requires ATP for synthesis of acetyl CoA from acetate. To reduce ATP demand by acetyl CoA synthase, acetylating acetaldehyde dehydrogenase (A-ALD) which catalyzes ATP-independent conversion of acetaldehyde to acetyl CoA also used as a strategy to reduce ATP requirements of cell. *E. coli eutE* and *Listeria innocua lin1129* were reported to be best A-ALD (Kozak et al., 2014a).

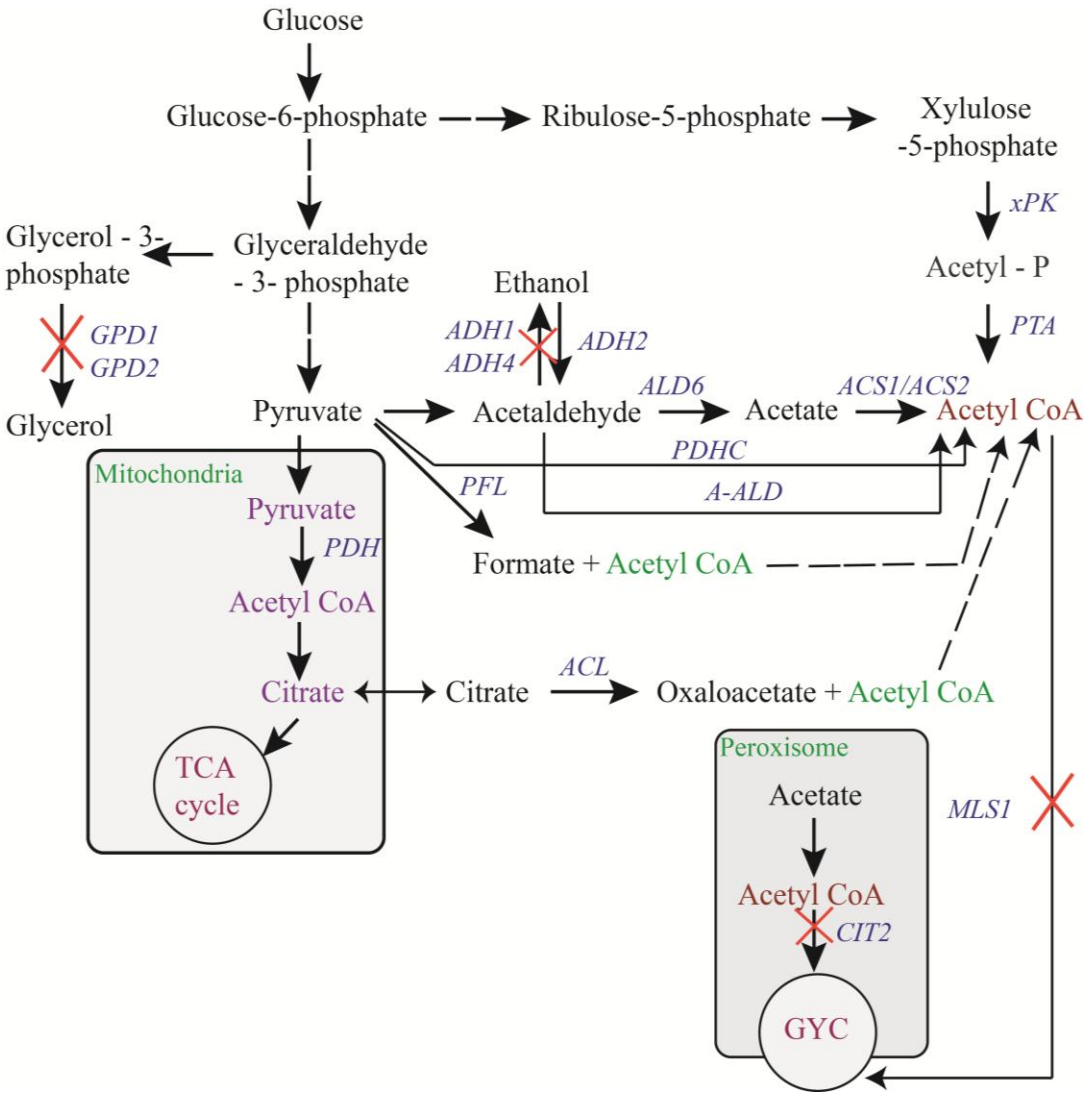

Figure 5. Overview of metabolic engineering strategies employed for increasing acetyl CoA pools in *S. cerevisiae*. (1) Overexpression of PDH bypass enzymes, acetaldehyde dehydrogenase (*ALD6*), acetyl CoA synthase (*ACS1, ACS2*) (2) Overexpression of acetylation resistant acetyl CoA synthase mutant (ACS_{SE}^{L641P}) from *Salmonella enterica* (3) Overexpression of alcohol dehydrogenase 2 (*ADH2*), (4) Decreasing cytosolic acetyl CoA utilization by knockout of one of two glyoxylate cycle genes, peroxisomal citrate synthase (*CIT2*) and malate synthase (*MLS1*) (5) deletion of glycerol and ethanol biosynthesis pathway genes (6) Production of acetyl CoA by from pyruvate by overexpression of pyruvate dehydrogenase complex (PDHC) from *Enterococcus faecalis* and pyruvate formate lyase (PFL) from *E. coli* and *Lactobacillus plantarum* (7) production of acetyl CoA from citrate by overexpression of ATP citrate ligase (ACL) from oleaginous yeast, *Yarrowia lipolytica* (8) production of acetyl CoA froom acetaldehyde by overexpression of acetylating acetaldehyde dehydrogenase (A-ALD) (9) By reducing ethanol and glycerol production by knockout of alcohol dehydrogenase and glycerol-3-phosphate dehydrogenase (*GPD1, GPD2*) (10) production of acetyl CoA from xylulose-5-phosphate by overexpression of phosphoketolase pathway, xylulose-5-phosphate phosphoketolase (*xPK*) from *Aspergillus nidulans* and phosphate acetyltransferase (PTA)

ATP citrate lyase (ACL) acts on citrate and converts it into acetyl CoA and oxaloacetate at the cost of one ATP. ACL are ubiquitous and present in fungi, plants and animals. ACL enzymes are absent in non-oleaginous yeast such as *S. cerevisiae* and play a crucial role in acetyl CoA generation during the lipid accumulation phase in oleaginous yeasts. ACL from the oleaginous yeast, *Yarrowia lipolytica* was reported to increase by 2 fold the production of 1-butanol in the *adh1Δadh4Δgpd1Δgpd2Δ* strain (Lian et al., 2014).

Pyruvate formate lyase (PFL) is widespread in facultative and obligate anaerobic eubacteria as well as archaeabacteria. It catalyzes the production of acetyl CoA from pyruvate. PFL as a potential source of acetyl-CoA was investigated in yeast and it was reported that strains expressing PFL from *E. coli* and *Lactobacillus plantarum* were able to grow anaerobically on glucose plates, and expression of either PFL or A-ALD could restore growth in *acs1Δacs2Δ* mutants (Kozak et al., 2014a).

1.5.2 Cofactor Engineering

NADH and NADPH are required by enzymes as cofactors for oxidoreductive reactions. NADH is a major redox product of catabolism and NADPH is used as a reducing agent in anabolic reactions. In the MVA pathway of *S. cerevisiae*, HMG-CoA reductase is a key enzyme and requires NADPH as cofactor therefore it has to compete with the NADPH requirements of other anabolic pathways. To address this increased cofactor requirement, one approach is enzyme substitution with different cofactor requirement. Thus, NADPH-dependent HMG-CoA reductase was substituted by NADH-dependent HMG-CoA from *Delftia acidovorans* and resulted in 50% enhancement in production of sesquiterpene, amorphadiene (Ma et al., 2011). The yield was further enhanced by increasing the intracellular NADH availability using a NAD^+ dependent formate dehydrogenase from *Candida boidinii* and with formate supplementation.

Another approach is cofactor recycling, in which deletion of a NADPH consuming reaction, glutamate dehydrogenase (*GDH1*) and simultaneously over expressing the NAD^+-dependent glutamate dehydrogenase encoded by *GDH2* restored the impaired NADH/NADPH balance due to heterologous production of santelene in *S. cerevisiae* (Scalcinati et al., 2012b).

1.5.3 Balancing of Pathways

In multienzyme pathways, it is also important to balance the relative expression levels of enzymes so as to prevent accumulation of metabolic intermediates which might be toxic to the host cell. One approach called Multivariate modular pathway engineering has been adopted by different groups for production of different terpenoids such as taxadiene (Ajikumar et al., 2010), miltiradiene (Zhou et al., 2012a), fatty acids (Xu et al., 2013) and pinocembrin (Wu et al., 2013). In this approach, the different enzymes of pathway are present in different modules, and the metabolic network is redefined by the collection of distinct modules. For expression of the fatty acid biosynthetic pathway in *E. coli*, the authors decompose the pathway into three modules (Xu et al., 2013). The first module was the GLY module: upstream glycolysis module which encodes for five genes. The second is the ACA module for acetyl CoA activation and also encodes for five genes. The third module is the FAS module which is a fatty acid biosynthetic module and encodes for five genes of fatty acid biosynthesis pathway. The first module provides acetyl CoA pools for fatty acid production, and the third module provides sink for fatty acids production. Both these modules are linked through the intermediary ACA module. Expression of these different modules is sequentially and systematically tuned by varying plasmid copy number so as to minimize the accumulation of toxic intermediates and selection of optimal strain with higher fatty acid productivity. Tuning of translation rates is also performed by altering promoter strength of different modules and selecting for optimized strain with high productivity (Xu et al., 2013).

1.5.4 Spatial Optimization of metabolism

In addition to modular optimization, spatial coupling of complex metabolic reactions has also been adopted as a strategy for improving the pathway function so as to ensure that the cell does not waste metabolic resources by producing unnecessary enzymes and channel flux through the appropriate metabolic route. Therefore for spatial optimization of metabolic reactions, diferent approaches include artificial gene fusion, use of synthetic scaffolds and organization of metabolic pathways in specific membrane bound organelles. Fusion of FPP synthase with patchoulol synthase in *S. cerevisiae* led to 2-fold increase in the production of patchoulol (Albertsen et al., 2011).

Synthetic scaffolds of protein, DNA and RNA have also been developed to colocalize the multiple enzymes in a designable manner so as to increase the production of MVA pathway function. Protein and DNA scaffolds have been reported to increase the production of mevalonate in *E. coli* (Conrado et al., 2012; Dueber et al., 2009).

Transport of enzymes, substrates and cofactors across different compartments also results in less yield of product. To reduce the loss of intermediates to competing pathways and to remove the need for transport of molecules, one strategy is to target the pathway into the membrane bound organelle. By targeting two enzymes, heterologous FPP synthase and amorphadiene synthase to the mitochondria of *S. cerevisiae,* 20-fold increase in the production of amorphadiene was reported (Farhi et al., 2011) .

Part III: Screening strategies

1.6 Different screening strategies for increased mevalonate pathway activity

Most metabolic engineering strategies mentioned in section 1.4, focused on the precursors, enzymes and their cofactor requirements of the isoprenoid pathway. However, apart from the core mevalonate pathway genes, genes from different connecting pathways that directly or indirectly affecting the mevalonate/isoprenoid pathway flux may have an important influence. Therefore, for identification of novel genes/mutants affecting the mevalonate pathway flux and to improve the isoprenoid pathway activity through directed evolution of different isoprenoid synthases, there is a need for efficient and high throughput screening assays. Most isoprenoid compounds are highly water-insoluble, volatile and toxic to the production host. Therefore, the development of screening strategies for enhanced production of isoprenoid compounds is quite challenging (Emmerstorfer-Augustin et al., 2016). Nevertheless, several groups came up with excellent strategies for enhanced isoprenoid pathway activity which are described below and shown in figure 6.

1.6.1 Screening by fluorescence

In this approach, fluorescent dyes such as Nile Red and BODIPY were used for screening isoprenoid synthases for improved performance. Nile red (9-diethylamino-5H-benzo[a] phenoxazine-5-one) is the most commonly used lipophilic stain. It is a hydrophobic and

metachromatic dye with poor solubility and fluorescence in water, with color emission varying from deep red to strong yellow gold in hydrophobic environments. Depending on excitation and emission wavelength, the dye can be used to stain different hydrophobic molecules. BODIPY 505/515 (4,4-difluoro-1,3,5,7-tetramethyl-4-bora-3a,4a-diaza-s-indacene) is a green lipophilic fluorescent dye recently used as an alternative to Nile red staining. It is insensitive to pH and the polarity of the environment.

Therefore, it is possible to fine tune its fluorescence characteristics by making small modifications to its structure and resulting in a variety of dyes with different excitation and emission maxima. Nile red was used for improving farnesene production in recombinant *S. cerevisiae* (L.Frenz, 2012). The authors optimized the spectral conditions so as fluorescence from Nile Red bound to farnesene was uninfluenced by background fluorescence of biomass. The advantage of the Nile Red assay is that it has a broad substrate range that can be used in medium to high throughput screens, but the disadvantage is low product specificity and the expensive nature of fluorescent dyes.

Another screening approach was based on the fluorescence of the isoprenoid product. Recombinant cells were screened by fluorescence-activated cell sorting by flow cytometry and magnetic cell sorting (FCM). FCM was used to screen for high level production of this carotenoid astaxanthin in *Xanthophyllomyces dendrorhous* (Brehm-Stecher and Johnson, 2012; Ukibe et al., 2008). Astaxanthin is also fluorescent. This approach was high throughput but it was limited to only fluorescent isoprenoids.

1.6.2 Screening for colored products and by-products using analogues and coupled assays

This screening method was developed based on colorimetric detection of colored products or by-products. (Lauchli et al., 2013) A specially synthesized vinyl methyl ether substrate called substrate which was structurally similar to FPP, was utilized as a substrate by sesequiterpene synthases resulting in the production of methanol. This methanol was converted by an alcohol oxidase to formaldehyde. This resulting formaldehyde further reacted with Purpald® to form a purple colored product. This approach had been used to improve thermostability of sesquiterpene synthase *Bc*BOT2 from *Botrytis cinerea* and stabilization of SSCG_02150 enzymes for the production of (-)-δ-cadinene (Lauchli et al., 2013).

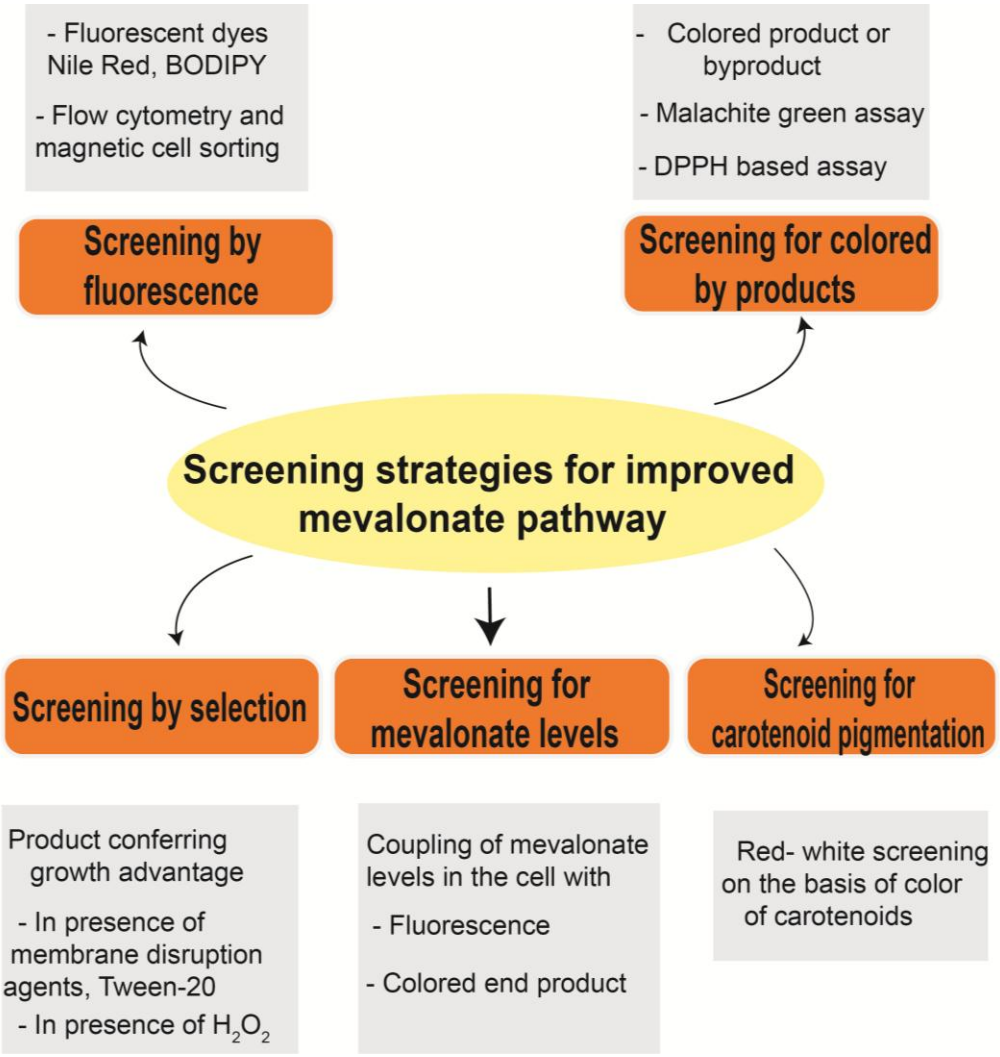

Figure 3. Schematic representation of different currently employed metabolic engineering strategies for increasing the mevalonate pathway flux in *S. cerevisiae* *tHMG1*- truncated hydroxymethyl glutaryl coenzyme A reductase 1, *ERG20*- Farnesyl pyrophosphate synthase, *BTS1*- geranylgeranyl diphosphate synthase, *IDI*- Isopentenyl diphosphate isomerase, *upc2-1*- mevalonate pathway specific transcription factor mutant (G888D), *ERG9*- squalene synthase , *LPP1*- Lipid phosphate phosphatase, *DPP1*- Diacylgycerol pyrophosphate phosphatase

Another colorimetric assay was based on the malachite green assay (Vardakou et al., 2014). The principle of this assay was that when isoprenoid synthase acted on the substrate, FPP to produce the product, there was also release of inorganic diphosphate (PPi) as a by-product. This was acted on by diphosphatases to release monophosphates which reacted with molybdate and malachite green to form a turquoise complex which could be quantified spectrophotometrically. This method has been utilized for testing β-farnesene synthase (*Aa*FS) from *Artemisia annua*.

DPPH (2,2-diphenyl-1-picrylhydrazyl) has been used for screening of the monoterpenoid product, limonene using n-dodecane as an extractant (Behrendorff et al., 2013). When electrons were transferred from DPPH to monoterpenoid limonene, DPPH changed its color from purple to green. The drawback of these approaches is the requirement of cell disruption for measurement of activity. Hence these methods were not applicable for high throughput assays.

1.6.3 Screening based on selective growth

Screening methods are based on distinct growth advantages or disadvantages. As isoprenoid molecules are not essential for cell growth, these methods are difficult to establish for improving isoprenoid pathway activity. A mutant with 30% higher α-bisabolene production levels was isolated by screening a mutant library in presence of Tween 20 (Kirby et al., 2014). The principle behind this strategy was that when α-bisabolene was produced in *S. cerevisae* cells without dodecane (extractant), it remain bound to the cell membrane resulting in the alteration of membrane composition and hence cell protective properties against the membrane disruption agent, Tween 20.

Carotenoids (tetra terpenoids) are antioxidants in nature and it is possible that greater production of carotenoids would also lead to increased resistance to oxidative stress. This property was utilized to select highest producers of carotenoids by using a periodic hydrogen peroxide treatment strategy (Reyes et al., 2014).

1.6.4 Screening using a specific biosensor

In this screening method, biosensors were developed for sensing mevalonate levels in the cell. This approach employed a sensor *E. coli* strain which was auxotrophic for mevalonate and also engineered to produce green fluorescent protein constitutively. Secretion of mevalonate allowed

the cells to grow, and growth was correlated with GFP expression. Using this strain, a seven-fold improvement in the production of mevalonate was reported (Pfleger et al., 2006).

In an another study, an *E. coli* strain was engineered to express AraC protein (arabinose operon) under the transcriptional repressor of P_{BAD} promoter which was engineered to be regulated by mevalonate instead of arabinose (Tang and Cirino, 2011). The strain also contained a chromosomal lacZ (β-galactosidase activity) under the control of P_{BAD} promoter and hence was used to screen colonies based on dark blue color of 5-bromo-4-chloro-3-indolyl-β-D-galactopyranoside correlating with increased mevalonate levels.

1.6.5 Screening for carotenoid pigmentation

Carotenoids are colored terpenoids. Therefore, in carotenoid based screening strategies, enhanced isoprenoid activity can be visualized by the naked eye as well as colorimetrically. These are described in the next section after discussing the carotenoids.

Part IV: Carotenoids and their biosynthesis

1.7 Carotenoids

Carotenoids are tetraterpenoids and consists of eight isoprenoid rings. Carotenoids primarily produce yellow, red and orange colors and are the most widely distributed pigments which are useful for industrial applications (Delgado-Vargas et al., 2000; Gomez-Garcia Mdel and Ochoa-Alejo, 2013). The carotenoids can be further divide into two major groups: (a) Carotenes (B) Oxycarotenoids. Carotenes are carotenoids with carbon and hydrogen additions e.g. α-carotene, β-carotene, Lycopene, while Oxycarotenoids (commonly known as "xanthophylls") have carbon, hydrogen, and oxygen additions e.g. lutein, bixin (Delgado-Vargas et al., 2000).

1.7.1 Sources of carotenoids and their biosynthesis

Carotenoids are mainly produced in nature by plants and many microorganisms that includes bacteria, fungi and algae. Animals cannot synthesize carotenoids but they can metabolize them. The biosynthesis of carotenoids differs in organisms. However, almost all carotenoid producing organisms share the common primary metabolic pathway. All pathways initiate from the same C5 building block, isopentenyl pyrophosphate (IPP) or its isomer, dimethylallyl diphosphate

(DMAPP), produced from either Acetyl-CoA (the cytosolic mevalonic acid pathway (MVA) pathway) or pyruvate and G3P (the plastidic methylerythritol 4-phosphate (MEP) pathway) described in section 1.3.1 and 1.3.2. IPP is further converted to geranyl-geranyl diphosphate (GGPP) which upon dimerisation leads to phytoene and the stepwise dehydrogenation gives lycopene. Subsequent cyclisation, dehydrogenations, and oxidation reactions, lead to the other naturally occurring carotenoids.

1.7.2 Biological Role

Among the diverse number of the known carotenoids so far, about 30 carotenoids play important roles in photosynthesis (Varela et al., 2015). Most of carotenoids are bound with the Light Harvesting Complexes (LHCs) and are located in the thylakoid membranes of chloroplast where they absorb light and participate in photosynthesis (Nisar et al., 2015). Secondary carotenoids like astaxanthin and canthaxanthin play a role in cell protective mechanisms. Unlike primary carotenoids, the secondary carotenoids are produced to high levels and are dispensed in oily droplets. They form a protective layer when the cells are exposed to stressed conditions, and provide the characteristic pink/red color of some stressed algae (Begum et al., 2016; Wang et al., 2015). Due to their anti-oxidant nature, they can protect cells from reactive radicals, prevent lipid peroxidation, and promote the stability and functionality of the photosynthetic apparatus (Grossman et al., 2004). Carotenoids also promote the integrity of membranes which is essential for cell survival. In particular, they improve the cell membrane fluidity under high temperature or high light conditions. Similar stabilization effects were reported for low temperature as well when the lipids became more unsaturated (Ramel et al., 2012).

1.7.3 Applications

Carotenoids are used as colorants to many manufactured foods, drinks, and animal feeds, either in the forms of natural extracts (e.g annatto, paprika or marigold extracts) or as pure compounds manufactured by chemical synthesis. Carotenoids also have provitamin A activity, as this particular vitamin is a product of carotenoid metabolism. They also have widespread applications in cosmetics and feed additives (Ye et al., 2008). Carotenoids also provide a protective role for humans. Many studies have reviewed the health benefits of carotenoids, which are usually related to their anti-oxidant activities (Britton, 1995; Chuyen and Eun, 2017; Fiedor and Burda,

2014; Manayi et al., 2016; Zhang et al., 2014). The anti-oxidant property in general mediates the harmful effects of free radicals, and hence can potentially protect humans from compromised immune response, premature aging, certain cancers, cardiovascular diseases, and/or arthritis. Anti-oxidant pigments are also frequently reported to reduce the risks of AIDS, diabetes, cataract, macular degeneration, and neurodegeneration (Varela et al., 2015). Deficiency in these pigments may result in exophthalmia, night blindness, and in severe case keratinization of the conjunctiva and cornea (Britton, 1995).

1.7.4 Commercially important carotenoids

Astaxanthin and β-carotene are the two most recognized carotenoids in the global market, and make-up almost half of the carotenoid market. Astaxanthin is mainly used as feed which gives the pinkish color to aquatic fish and shrimps. It is a stronger antioxidant than vitamin E and β-carotene. It has been reported to enhance antibody production, anti-aging, sun-proofing. It also demonstrates anti-inflammatory effects when administered with aspirin (Li et al., 2011). Another carotenoid, β-carotene also help in improving the immune system, and may have a preventative role in eye diseases like night blindness and cataract.

Other carotenoids which are also of market interest are lutein (with zeaxanthin), lycopene, and canthaxanthin, fucoxanthin. Fucoxanthin is not a major market sharer but it has been marketed as an anti-obesity functional food, and for anti-cancer and potential anti-inflammatory activities (Heo et al., 2010; Nanba et al., 2008). It is reported that it did not exhibit toxicity and mutagenicity at low dosages (Beppu et al., 2009; Peng et al., 2011) and this was considered a safe compound for human health.

Lycopene is marketed as an anti-oxidant and has been proposed for help in the treatment of cardiovascular diseases and prostate cancer. Canthaxanthin was also reported to prevent blood disorder diseases. However, it was also reported to potentially cause blindness or aplastic anemia when consumed in large quantities for the purpose of creating skin tan color (Clinton, 1998; Zhang et al., 2014).

Lutein and zeaxanthin are two pigments which play a significant role in eye health (Manayi et al., 2016), hence are important in the nutraceutical market. Lutein is a predominant pigments in the macula and is clinically proven to prevent cataract and macular degeneration. These

compounds also may function as strong anti-oxidants to decrease around 60 chronic disease risks (Ye et al., 2008). These are also not considered toxic and are relatively safe for human consumption.

1.8 Microbial production of commercially important carotenoids

As mentioned in section 1.6, carotenoids are commercially important coumpounds. Commercial production of natural carotenoids from microorganisms is more eco-friendly than synthetic manufacture by chemical procedures and extraction from their natural sources. Due to its increasing importance, industrial biotechnological methods of carotenoids production have been developed with the algae *Dunaliella salina* and *Haematococcus pluvialis*, the fungus *Blakeslea trispora*, and the heterobasidiomycetous yeast *Xanthophyllomyces dendrorhous.*

There is also an interest in production of carotenoids from the heterologous host, *S. cerevisiae,* by over-expression of carotenogenic genes. The heterologous production of β-carotene in *S. cerevisiae* was observed by expressing carotenogenic genes from carotenoid producing red yeast, *Xanthophyllomyces dendrorhous* (Verwaal et al., 2007a). *X. dendrorhous* is known to produce the carotenoid, astaxanthin. After identification of the enzyme encoding astaxanthin synthase from *X. dendrorhous,* heterologous expression of astaxanthin synthase (*crtS*) which belongs to cytochrome P450 oxidase family of enzymes along with cytochrome P450 reductase (*CrtR*) resulted in the production of small amounts of astaxanthin (Ukibe et al., 2009). Both these reports suggested that *S. cervisiae* can be used as a cell factory for the production of commercially important carotenoids.

Yeasts belonging to *Rhodotorula* spp. are widely distributed in nature. Genus belonging to *Rhodotorula* spp. that includes *Rhodotorula glutinis*, *Rhodotorula minuta*, *Rhodotorula mucilaginosa*, *Rhodotorula acheniorum* and *Rhodotorula graminis* are individually important yeasts as they make high levels of carotenoids. The amount of carotenoids by these yeasts is reported to be high (>500 µg/g) (Mata-Gomez et al., 2014). These yeasts are reported as the highest producers of β-carotene (Mata-Gomez et al., 2014). Apart from β-carotene, they also produce other carotenoids such as Torulene, Torularhodin and γ-carotene.

General carotenoid biosynthesis pathway in yeast was first proposed by (Simpson et al., 1964) in 1961 and later was revised by (Goodwin, 1980). Carotenoid biosynthetic pathway is linked to

central carbon metabolism through MVA (isoprenoid) pathway. Acetyl CoA acts as a precursor for MVA and hence carotenoid biosynthetic pathway. The proposed carotenoid biosynthetic pathway in *Rhodotorula* spp. is shown in figure 7 and is briefly described below:

Glucose is first converted to pyruvate through glycolysis. Then, pyruvate is subsequently utilized for the synthesis of acetyl CoA. Acetyl CoA is converted to 3-hydroxy-3-methyl glutaryl-CoA (HMG-CoA) by HMG-CoA synthase. HMG-CoA is then converted to mevalonic acid (MVA). MVA is subsequently converted by phosphorylation and decarboxylation reaction to isopentenyl pyrophosphate (IPP). IPP is isomerized to dimethyllayl pyrophosphate (DMAPP). Three molecules of IPP and one molecule of DMAPP are then added by geranyl geranyl diphosphate synthase (GGPP synthase) to form geranyl geranyl pyrophosphate (GGPP). Then, two molecules of GGPP are condensed to form phytoene by phytoene synthase. Subsequently, phytoene is desaturated by phytoene desaturase (dehydrogenase) to form Lycopene. Lycopene undergoes a number of metabolic reactions to produce a number of cyclic compounds such as γ-carotene, β-carotene, Torulene and Torularhodin. γ-carotene act as a branch point for synthesis of β-carotene and Torulene. Hydroxylation and oxidation of torulene by mixed function oxidase leads to the formation of Torularhodin (Frengova and Beshkova, 2009). The mixed function oxidase for torularhodin synthesis is still unknown.

Schematic representation of heterologous expression of carotenogenic enzymes of *Rhodosporidium toruloides* for the production of carotenoids from mevalonate pathway of *Saccharomyces cerevisiae* is shown in figure 8.

1.9 Screening of isoprenoid flux by carotenoid-based assays

The utilization of carotenoids as a screening strategy dates back to 1994, where a carotenoid based screening method was called 'red-white screening'. The red-white screening method employed an *E. coli* strain which was engineered with heterologous carotenogenic genes phytoene synthase (*crtB*) and phytoene desaturase (*crtI*) from *Erwinia uredovora* for the production of carotenoids. This strain did not produce colored carotenoids, hence the strain was white in color. The strain would form red colored colonies only when functional GGPP synthase was expressed which led to the production of lycopene (colored carotenoid).

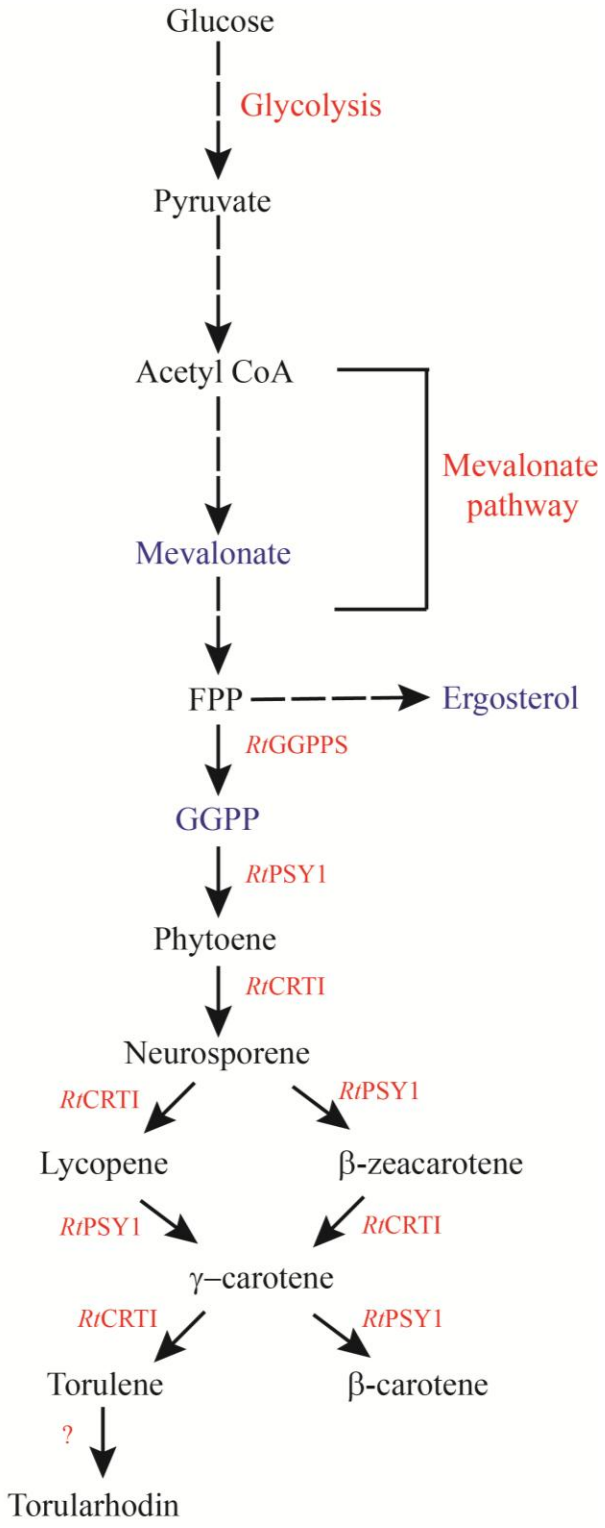

Figure 7. Schematic representation of carotenoid pathway in *Rhodosporidium toruloides*. *Rt*GGPPS- geranylgeranyl diphosphate synthase, *Rt*PSY1- Phytoene synthase, *Rt*CRTI- Phytoene dehydrogenase

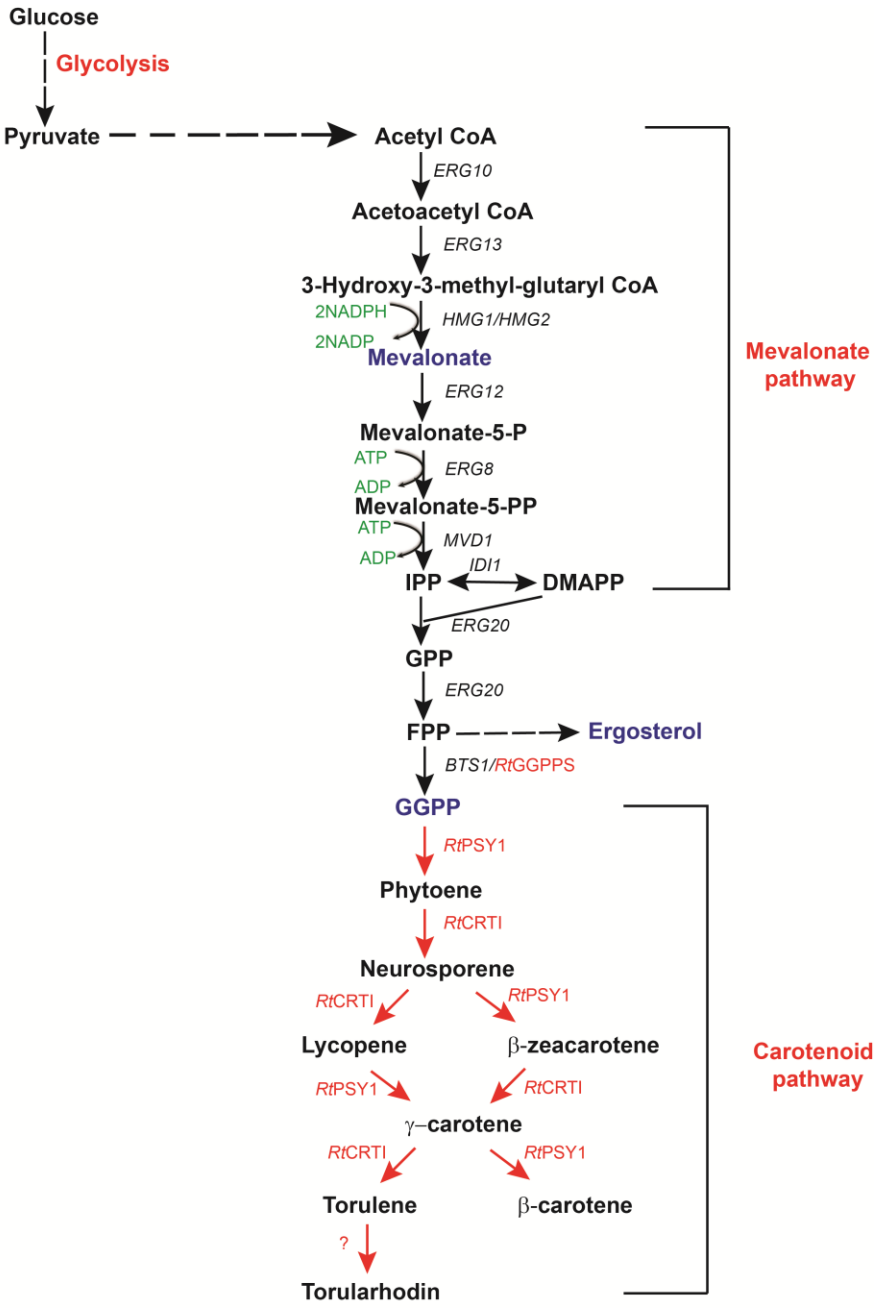

Figure 8. Schematic representation of expression of carotenogenic genes of *Rhodosporidium toruloides* in *Saccharomyces cerevisiae*. Carotenoid pathway is linked to Mevalonate and glycolysis pathways. Enzymes from *S. cerevisiae* and *R. toruloides* are shown in black and red color respectively. *ERG10*- acetoacetyl CoA thiolase, *ERG13*- 3-hydroxy-3-methylglutaryl coenzyme A synthase, *HMG1/HMG2*- 3-hydroxy-3-methyl-glutaryl CoA reductase, *ERG12*- Mevalonate Kinase, *ERG8*- Phosphomevalonate Kinase, *MVD1*- Mevalonatepyrophosphate decarboxylase, *IDI1*-isopentenyl diphosphate dimethylallyl diphosphate isomerase, *ERG20*- Farnesyl pyrophosphate synthase, *BTS1*- geranylgeranyl diphosphate synthase, *R. toruloides* carotenogenic genes, *Rt*GGPPS- geranylgeranyl diphosphate synthase, *Rt*PSY1- Phytoene synthase, *Rt*CRTI- Phytoene dehydrogenase

This red-white screening had been utilized by many research groups, e.g screening of genomic library from *Sulfolobus acidocaldarius* for isolation of GGPP synthase (Ohnuma et al., 1994), evolution of *E. coli* geranyl diphosphate synthase for GGPP production (Lee et al., 2005) and to isolate improved variants of GGPP synthase from *Taxus canadensis* (Leonard et al., 2010).

Thus carotenoid based visual screens were not only utilized for improving GGPP synthase activity but also utilized for the screening of mutant libraries of carotene synthases and carotenoid pathway genes for the production of unusual and new carotenoids (Schmidt-Dannert et al., 2000; Umeno and Arnold, 2004; Umeno et al., 2002).

This colored based screening approaches were brought to the next level when they were used in synthetic biology approaches for improving the heterologous production of terpenoids. In one study, a carotenoid based screen was used for selection of yeast Erg20p variants which catalyzes all the steps for production of GGPP from IPP in *S. cerevisiae* (Ignea et al., 2015). This Erg20p variant had also been reported to increase the levels of other terpenoid products, such as sclareol, cis-abienol and abietadiene.

Carotenoid producing strains have also been utilized for screening recombinant strains with high level production of isoprenoids and diverse isoprene synthases. The hypothesis of this strategy was that isoprene synthases would compete with carotenoid pathway genes for precursor molecule, FPP. Hence higher the activity of isoprene synthases, less would be the availability of the substrate for the production of carotenoids, hence resulting in decreased pigmentation of host cells. This strategy had been utilized for improving the performance of taxadiene synthase (TXS), geraniol synthase (GES) and tobacco 5-epi-aristolochene synthase (TEAS) (Furubayashi et al., 2014).

Colored carotenoid producing microrganisms could be used as assay strain for identification of genes/mutants which affect the isoprenoid pathway flux. The hypothesis of this approach is that an increase in the isoprenoid pathway flux would increase the pigmentation of colonies in these carotenoid producing strains. This approach was used to screen the gene knockout library of *S. cerevisiae* to isolate the gene deletions which positively affect the isoprenoid pathway flux (Ozaydin et al., 2013). A plasmid encoding carotenogenic genes was transformed (Verwaal et al., 2007a) into *S. cerevisiae* gene deletion library and screened for the colonies with increased

pigmentation. Twenty four gene deletions were isolated which resulted in increased pigmentation and carotenoid levels. These twenty four gene deletion strains were further checked for improved production of another isoprenoid product, bisabloene by expressing bisabolene synthase (*Ag*BIS) from *Abies grandis.* Surprisingly, none of the deletion strains resulted in increased production of bisabolene, instead the yield of bisabolene decreased in all of twenty four deletion strains. Further, after employing the known metabolic engineering strategies for increasing isoprenoid pathway flux i.e over-expression of *ERG20* and *tHMG1* along with expression of *Ag*BIS, the authors reported the increase in the production of bisabolene in four gene deletion strains (*rox1*, *prb1*, *yjl064w* and *ypl062w*).

In an another study, the carotenoid based screen was used and this created a library of yeast colonies with varying degree of orange colors (Yuan and Ching, 2014). These different colored colonies were checked for improving the production of another terpenoid, amorphadiene. However, they observed that increasing the isoprenoid pathway activity result in decreased in orange pigmentation. Hence, they were able to isolate only one mutant with improved production of amorphadiene.

More recently in another study the authors employed a slightly different strategy than the above two mentioned screens (Trikka et al., 2015). They used a heterozygous deletion screen to identify the gene deletions that improve the carotenoid as well as the production of sclareol. Through iterative application of this approach, they identified six gene deletions that resulted in 12 fold increase in sclareol titre.

The probable reason for the failure of first two carotenoid based screens was that the carotenoid producing strain used in screening the gene deletion library was not validated with known flux increaser of the pathway for increased pigmentation. Therefore, the assay strain probably did not show direct correlation between the pigmentation and isoprenoid pathway flux in the colonies.

The advantage of the carotenoid based approaches is that it allows screening of whole cells. One disadvantage of using these screening methods is the high rate of false positives during the selection of loss-of-function mutations for improving the isoprenoid synthases. Decreased pigmentation in loss of function mutant strains would not be necessarily due to positive effect on the isoprenoid biosynthesis activity, it could be due to factors that reduced cell viability.

1.10 Objectives of the present study

Looking at the need for simple carotenoid based assay for isoprenoid flux, the following objectives were framed.

1. To develop and validate a carotenoid based visual genetic assay for increasing the metabolic flux in the isoprenoid pathway of *S. cerevisiae*
2. To isolate mutants for increasing flux in the isoprenoid pathway by using carotenoid based genetic screen
3. To investigate the mechanism of increased isopreoid flux in the spt15_A101T mutant that was isolated in the screen

CHAPTER 2:

Materials and Methods

SECTION A: MATERIALS

2.1 CHEMICALS AND REAGENTS

All chemicals used were obtained from commercial sources and were of analytical grade. Media components, fine chemicals, reagents and HPLC grade solvents were purchased from Sigma Aldrich, (St. Louis, USA), HiMedia, (Mumbai, India), Merck Millipore India Ltd (Mumbai, India), USB Corporation (Ohio, USA) or Difco, USA. Oligonucleotides (primers) were designed using SnapGene® and were purchased from Integrated DNA technologies (IDT) or Sigma Aldrich (Bangalore, India). Enzymes (restriction enzymes, T4 DNA ligase, Calf Intestinal Phosphatase (CIP), Vent DNA polymerase, Phusion DNA polymerase) and dNTPs, were purchased from New England Biolabs Inc, (Beverly, MA, USA). Sequencing was done through Eurofins (Bangalore, India) or 1st Base (Malaysia). Gel-extraction kits and plasmid miniprep columns were obtained from QIAGEN (Valencia, CA, USA) or Fermentas (Vilnius, Lithuania). The standards of β-carotene, Lycopene, β-Farnesene were obtained from Sigma, Aldrich India. The standards of γ-carotene, phytoene, Torulene and Torularhodin were obtained from CaroteNature GmbH, Switzerland.

2.2 STRAINS AND PLASMIDS

Escherichia coli DH5α cells were used as cloning hosts. The genotype for the *E. coli* strain and the yeast strains used in the study are given in table 2.1. The list of various plasmids used in this study is given in table 2.2.

2.3 OLIGONUCLEOTIDES

The list of various oligonucleotide primers used in this study is given in table 2.3.

Table 2.1 List of strains used in this study

Strain	Genotype	Source
Escherichia coli strain		
ABE 460 (DH5α)	*F⁻ gyrA96*(Nal) *recA1 relA1 endA1 thi-1 hsdR17* ($r_k^- m_k^+$) *glnV44 deoR*Δ *(lacZYA-argF) U169* [ϕ80dΔ *(lacZ) M15*]	Lab strain
***Saccharomyces cerevisiae* strains**		
ABC 276	*MATα,ura3-52, leu2Δ1, his3Δ200,trp 1,lys 2-801*	Lab strain
ABC 733 (BY4741)	*MATa, his3Δ1, leu2Δ0, met15Δ, ura3Δ0*	J. Boeke
ABC 3620 (CEN.PK-1C)	*MATa,ura3-52,trp1-289,leu2-3_112,his3Δ1, MAL2-8^c,SUC2*	Euroscarf
ABC 5449 (*pho13Δ)*	*MAT a, ura3Δ0, his3Δ1,leu2Δ0, met15Δ0, YDL236W::kan MX4*	Euroscarf
ABC 5722 (*pdc6Δ)*	*MAT a, ura3Δ0, his3Δ1,leu2Δ0, met15Δ0, YGR087c::kan MX4*	Euroscarf
ABC 4929 (M2 strain)	EMS mutagenized BY4741, *MATα,ura3-52, leu2Δ1, his3Δ200,trp 1,lys 2-801*	This study
ABC 4930 (M1 strain)	EMS mutagenized BY4741, *MATα,ura3-52, leu2Δ1, his3Δ200,trp 1,lys 2-801*	This study
***Agrobacterium tumefaciens* strain**		
AB 5345 (*A.tumefaciens* AGL1)	EHA101 recA::bla pTiBo542ΔT Mop+ Cb^R	Temasek Limited, Singapore
AB 5396	AGL1-pRH203 (AGL1 strain carrying pRH203 plasmid)	This study
AB 5576/AB 5577	AGL1-pRH203-1 (AGL1 strain carrying pRH203-1 plasmid)	This study
AB 5771	AGL1-pMWR101 (AGL1 strain carrying pMWR101 plasmid)	This study
AB5772	AGL1-pMWR101-1000bp-06383 (AGL1 strain carrying pMWR101-disruption vector plasmid)	This study
***Rhodosporidium toruloides* strain**		
AB 5353/ AB 5354	*R. toruloides* ku70Δe (NCBI accession number – KF850470	Temasek Limited, Singapore

Table 2.2: List of Primers used in this study

Sr. no	Primer name	Sequence (5'-3')
1	p416TEF_F	TTGATATTTAAGTTAATAAACGG
2	p416TEF_R	TTCAGGTTGTCTAACTCCTTC
3	*tHMG1* _F	GATCGCGGATCCATGGACCAATTGGTGAAAACTGAAG
4	*tHMG1* R	CATGCGCCCGGGTTAGGATTTAATGCAGGTGACG
5	*Spt15* F	GATCGCGGATCCATGGCCGATGAGGAACGTTTAAAG
6	*Spt15* R	CATGCGCTCGAGTCACATTTTTCTAAATTCAC
7	At*FS* F	GACGTTCTAGAATGCCTAAACGACAGGCTCAAC
8	At*FS* R	GGCTCGGATCCTTAATTGAGTGGAAGAGGGTGG
9	POS5 FP	GACTGTGGATCCATGTTTGTCAGGGTTAAATTG
10	POS5 RP	GACTCGCTCGAGTTAATCATTATCAGTCTGTCTC
11	PDC6 FP	ATGCGGGATCCATGTCTGAAATTACTCTTGGAAAATAC
12	PDC6 RP	ATGCTCTCGAGTTATTGTTTGGCATTTGTAGCGG
13	PHO5 FP RT	CTCGTGATTTGCCTGAAGGTTG
14	PHO5 RP RT	CCATTTCCAAATCATCGTCAT
15	PHO84 FP RT	GGCAACAAGTTAAGACCATCTC
16	PHO84 RP RT	CAACAATATCAGCTAAAGTACC
17	PHO89 FP RT	CTTCTAGATCTCTAAAATACTG
18	PHO89 RP RT	GCAGTAGCAAATGTTAACCAAC

Table 2.3 List of Plasmids used in the study

Plasmid name	Clone no.	Description
pRS416TEF	ABE 443	The CEN-vector bearing *URA3* marker and TEF promoter-MCS-terminator for yeast expression and Amp^r marker for selection in *E. coli* (Mumberg et al., 1995).
pRS313TEF	ABE 3569	The CEN-vector bearing *HIS3* marker and TEF promoter-MCS-terminator for yeast expression and Amp^r marker for selection in *E. coli.* Vector was constructed by excising TEF promoter and MCS from pRS416TEF using *Sac*I and *Apa*I site and cloned at pRS313 vector at *Sac*I and *Apa*I site.
pRS314TEF	ABE 3498	The CEN-vector bearing *TRP1* marker and TEF promoter-MCS-

		terminator for yeast expression and Amp^r marker for selection in *E. coli.* Vector was constructed by excising TEF promoter and MCS from pRS416TEF using *Sac*I and *Apa*I site and cloned at pRS314 vector at *Sac*I and *Apa*I site.
pRS315TEF	ABE 3488	The CEN-vector bearing *LEU2* marker and TEF promoter-MCS-terminator for yeast expression and Amp^r marker for selection in *E. coli.* Vector was constructed by excising TEF promoter and MCS from pRS416TEF using *Sac*I and *Apa*I site and cloned at pRS315 vector at *Sac*I and *Apa*I site.
pRS315TEF-BTS1	ABE 3499	*BTS1* gene of *S. cerevisiae* was cloned at *Xba*I and *Bam*HI site of pRS315TEF.
pRS313TEF-BTS1	ABE 3571	*BTS1* gene of *S. cerevisiae* was cloned at *Xba*I and *Bam*HI site of pRS313TEF.
pRS314TEF-CRTI	ABE 3500	Codon optimized *Rt*CRTI gene (phytoene dehydrogenase) of *Rhodosporidium toruloides* was cloned at *Bam*HI and *Sal*I site of pRS314TEF.
pRS313TEF-CRTI	ABE 4869	Codon optimized *Rt*CRTI gene (phytoene dehydrogenase) of *Rhodosporidium toruloides* was cloned at *Bam*HI and *Sal*I site of pRS313TEF.
pRS314CYC- CRTI	ABE 3649	TEF promoter (407bp) in pRS314TEF-CRTI (ABE 3500) was excised using *Sac*I and *Bam*HI and replaced by CYC promoter (300 bp) at *Sac*I and *Bam*HI site.
pRS315TEF-GGPPS	ABE 3518	Codon optimized *Rt*GGPPS gene (GGPP synthase) of *R. toruloides* was cloned at *Xba*I and *Bam*HI site of pRS315TEF.
pRS313TEF-GGPPS	ABE 3572	Codon optimized *Rt*GGPPS gene (GGPP synthase) of *R. toruloides* was cloned at *Xba*I and *Bam*HI site of pRS313TEF.
pRS315CYC-GGPPS	ABE3633	TEF promoter (407bp) in pRS315TEF-GGPP (ABE 3572) was excised using *Sac*I and *Xba*I and replaced by CYC promoter (300 bp) at *Sac*I and *Xba*I site.
pRS416TEF-PSY1	ABE 3519	Codon optimized *Rt*PSY1 gene (phytoene synthase) of *R. toruloides* was cloned at *Bam*HI and *Xho*I site of pRS416TEF.
pRS416CYC-PSY1	ABE3650	TEF promoter (407bp) in pRS416TEF-PSY1 (ABE 3519) was excised using *Sac*I and *Bam*HI and replaced by CYC promoter (300 bp) at *Sac*I and *Bam*HI site.
pRS314TEF-CP450 oxidase	ABE 3550	Codon optimized Cytochrome P450 oxidase (RHTO_06383) of *R. toruloides* was cloned at *Bam*HI and *Xho*I site of pRS314TEF.

pRS313TEF-CP450 reductase	ABE 3585	Codon optimized Cytochrome P450 reductase (RHTO_06309) of *R. toruloides* was cloned at *Sal*I and *Xho*I site of pRS313TEF.
pRS313TEF-tHMG1	ABE 3663	*HMG1* gene of *S. cerevisiae* is cloned without N-terminal (1575bp) at *Bam*HI and *Xma*I site of pRS313TEF.
pRS416TEF-tHMG1	ABE 4732	*HMG1* gene of *S. cerevisiae* is cloned without N-terminal (1575bp) at *Bam*HI and *Xho*I site of pRS416TEF.
pRS315TEF-tHMG1	ABE 4740	*HMG1* gene of *S. cerevisiae* is cloned without N-terminal (1575bp) at *Bam*HI and *Xma*I site of pRS315TEF.
pRS313TEF-SPT15	ABE 3750	*SPT15* gene of *S. cerevisiae* is cloned at *Bam*HI and *Xho*I site of pRS313TEF.
pRS314CYC-CRTI_A393T	ABE 3972	*Rt*CRTI (phytoene dehydrogenase) gene of *R. toruloides* with A393T mutation and cloned in pRS314CYC.
pRS314CYC-CRTI_A394V	ABE 4098	*Rt*CRTI (phytoene dehydrogenase) gene of *R. toruloides* with A394V mutation and cloned in pRS314CYC.
pRS314TEF-CRTI_A393T	ABE 4100	*Rt*CRTI (phytoene dehydrogenase) gene of *R. toruloides* with A393T mutation and cloned in pRS314TEF.
pRS314GPD-CRTI_A393T	ABE 4137	*Rt*CRTI (phytoene dehydrogenase) gene of *R. toruloides* with A393T mutation and cloned in pRS314GPD.
pRS313GPD-CRTI_A393T	ABE 4232	*Rt*CRTI (phytoene dehydrogenase) gene of *R. toruloides* with A393T mutation and cloned in pRS313GPD.
pRS315GPD-CRTI_A393T	ABE 5245	*Rt*CRTI (phytoene dehydrogenase) gene of *R. toruloides* with A393T mutation and cloned in pRS315GPD.
pRS416TEF-PS(At)	ABE 4159	*At*PS (phytoene synthase) from *Arabidopsis thaliana* cloned at *Bam*HI and *Xho*I site of pRS416TEF.
pRS313TEF-SPT15_A98H	ABE 4217	*SPT15* gene of *S. cerevisiae* with A98H mutation and cloned in pRS313TEF.
pRS313TEF-SPT15_A100V	ABE 4218	*SPT15* gene of *S. cerevisiae* with A100V mutation and cloned in pRS313TEF.
pRS313TEF-SPT15_A101T	ABE 4219	*SPT15* gene of *S. cerevisiae* with A101T mutation and cloned in pRS313TEF.
pRS313TEF-ZWF1	ABE 5287	*ZWF1* gene of *S. cerevisiae* is cloned at *Bam*HI and *Eco*RI site of pRS313TEF.
pRS314TEF-ZWF1	ABE 5288	*ZWF1* gene of *S. cerevisiae* is cloned at *Bam*HI and *Eco*RI site of pRS314TEF.
pRS313TEF-POS5	ABE 5289	POS5 gene of *S. cerevisiae* is cloned at *Bam*HI and *Xho*I site of pRS313TEF.

pRS314TEF-POS5	ABE 5290	*POS5* gene of *S. cerevisiae* is cloned at *Bam*HI and *Xho*I site of pRS314TEF.
pEX2	ABE 5342	pEX2 plasmid obtained from Temasek Science Laboratory ltd.
pRH203	ABE 5343	pRH203 plasmid obtained from Temasek Science Laboratory ltd.
pEX2-3' 6383	ABE 5363	pEX2 plasmid with 1000 bp of 3' end of RHTO_06383 from *R. toruloides* cloned at *Spe*I and *Bam*HI sites.
pEX2-5'-3' 6383	ABE 5364	pEX2 plasmid with 1000 bp of 3' end of RHTO_06383 from *R. toruloides* cloned at *Spe*I and *Bam*HI sites and 1000 bp of 5' end of RHTO_06383 cloned at *Pme*I and *Hin*dIII sites
pEX2-5' CAR2	ABE 5394	pEX2 plasmid with 1000 bp of 5' end of *CAR2* gene from *R. toruloides* cloned at *Pme*I and *Pst*I sites.
pEX2-3' CAR2	ABE 5395	pEX2 plasmid with 1000 bp of 3' end of *CAR2* gene from *R. toruloides* cloned at *SacI* blunted and *Bam*HI sites.
pRH203-1	ABE 5575	pRH203-1 plasmid obtained from Temasek Science Laboratory ltd.
pMWR101	ABE 5626	Constructed from pRH203-1, contains hygromycin cassette details are given in appendix, Section A1.2
pMWR102	ABE 5627	Constructed from pRH203-1, contains GFP cassette, details are given in appendix, Section A1.2
pMWR103	ABE 5740	Constructed from pRH203-1, contains hygromycin cassette and GFP cassette, details are given in appendix, Section A1.2
pRS313TEF-PDC6	ABE 5696	*PDC6* gene of *S. cerevisiae* is cloned at *Bam*HI and *Xho*I site of pRS313TEF.
pRS313GAL1-PDC6	ABE 5697	TEF promoter in ABE 5696 is replaced by GAL1 promoter (483 bp) in pRS313TEF-PDC6 using *Sac*I and *Bam*HI sites.
pRS314TEF-PDC6	ABE 5737	*PDC6* gene of *S. cerevisiae* is cloned at *Bam*HI and *Xho*I site of pRS314TEF.
pRS315TEF-PDC6	ABE 5738	*PDC6* gene of *S. cerevisiae* is cloned at *Bam*HI and *Xho*I site of pRS315TEF.
pMWR101-1000 bp-06383	ABE5770	1000 bp of 5' end of RHTO_06383 is cloned at *XbaI* and *Kpn*I site and 1000 bp of 5' end of RHTO_06383 is cloned at *SpeI* and *Eco*RI site of pMWR101 vector.

2.4 MEDIA

All the media, buffers and stock solutions were prepared using Millipore elix5 deionized water unless otherwise mentioned. They were sterilized, as recommended, either by autoclaving at 15 lb/inch^2 (psi) pressure at 121ºC for 15 minutes, or by using membrane filters (Advanced Microdevices Pvt. Ltd., India) of pore size 0.2-0.45 µm (for heat labile compounds).

2.4.1 LB (Luria–Bertani) Medium (per 1000ml)	Yeast extract 5 g Tryptone 10 g NaCl 10 g pH of the above medium was adjusted to 7.0 with 1N NaOH and volume was made upto 1000 ml. Agar was added, if required, at a final concentration of 2.2%. Ampicillin was added at a final concentration of 100µg/ml (after autoclaving of the medium) for the selection of recombinant clones and their routine growth.
2.4.2 YPD (Yeast extract-Peptone-Dextrose) Medium (per 1000 ml)	Yeast extract 10 g Peptone 20 g Dextrose 20 g Agar was added, if required, at a final concentration of 2.2%.
2.4.3 SD (Synthetic defined) Medium (per 1000 ml)	YNB 1.7g (Yeast Nitrogen Base without ammonium sulphate) Ammonium Sulphate 5 g Glucose 20 g Amino acids 80 mg

2.5 BUFFERS AND STOCK SOLUTIONS

2.5.1. Ampicillin Stock Solution (50mg/ml)

The required amount of ampicillin (sodium salt) was dissolved in the required volume of deionized water, and it was filter-sterilized using 0.2 μm filter membrane. It was stored at -20 °C in a tight container.

2.5.2 50% Glycerol (used for preparing –80 °C stocks of *E. coli*)

2.5.3 Solutions for Plasmid extraction

a) Solution-I (Re-suspension Solution)	50 mM Glucose 25 mM Tris-HCl (pH 8.0) 10 mM EDTA (pH 8.0) Autoclaved and stored at 4ºC.
b) Solution-II (Lysis Solution) (freshly prepared)	0.2N NaOH (freshly diluted from a 10N stock) 1% SDS (freshly diluted from a 10% stock) Store at room temperature.
c) Solution-III (Neutralization Solution) (100ml)	5 M Potassium acetate 60 ml Glacial acetic acid 11.5 ml Deionized water 28.5ml The resulting solution is 3M with respect to potassium and 5M with respect to acetate. It was stored at 4ºC.
d) TE Buffer (Tris-EDTA) (pH 8.0)	10mM Tris-HCl (pH 8.0). 1mM EDTA (pH 8.0).
e) TE-RNAse (stock prepared at 10mg/ml)	Working stock 20μg/ml in TE Buffer, pH 8.0.

f) PCI (Phenol-chloroform-isoamyl alcohol) Solution (100ml)	Phenol 50 ml [Equilibrated with Tris-HCl (pH 7.6)] Chloroform 48ml Isoamyl alcohol 2ml Stored at 4°C in dark brown bottle.

2.5.4 Agarose Gel Electrophoresis Reagents

a) 1X TAE (Tris-acetate-EDTA) Buffer (per 1000ml) **(prepared from 50X TAE stock)**	40 mM Tris-acetate. 1mM EDTA (pH 8.0). Autoclaved and stored at room temperature.
b) Orange-G dye (Gel loading dye, 6X)	0.25% orange-G 30% glycerol
c) 0.7-1% Agarose gel in 1X TAE	
d) Ethidium Bromide (10mg/ml) Stock	Final working concentration used at 0.5 µg/ml.

2.5.5 Solutions for preparation of Chemical competent *E. coli* cells (Nishimura et al., 1990)

a) SOB	Bactotryptone 20 g Bacto yeast extract 5 g NaCl 0.5 g Above mentioned components were dissolved in 950 ml of water. 10ml of 250 mM KCl was added and pH was adjusted to 7 with 5N NaOH, volume was made up to 995 ml and autoclaved. Just before use, 5 ml of filter sterilized 2M $MgCl_2$ was added.
b) SOC	SOB + 20mM Glucose
c) 1 mM HEPES buffer	
d) 10% glycerol	

2.5.6 Yeast Transformation Solutions (*S. cerevisiae*) (Ito et al., 1983)

a) 0.1M Lithium acetate in TE (pH 7.5)

b) 50% PEG-3350 in 0.1 M Lithium acetate in TE (pH 7.5).

2.5.7 STES lysis mixture (for plasmid / genomic DNA isolation from yeast)

10 mM Tris-HCl (pH 8.0)

1 mM EDTA (pH 8.0)

100 mM NaCl

1% SDS

2% Triton X-100

2.5.8 Solutions for Hydroxlyamine mutagenesis (Rose and Fink, 1987a)

NaOH	90mg
Hydroxylamine HCl	350 mg

Dissolved in 5 ml water and pH adjusted to 6.5. The solution was made fresh just before use.

2.5.9 Solutions for *Agrobacterium* mediated transformation of *R. toruloides* (ATMT)

- **K-salts:** 20.5% K2HPO4, 14.5% KH2PO4 (autoclaved)
- **M-salts:** 3% MgSO4*7H2O, 1.5% NaCl, 2.5% (NH4)2SO4 (autoclaved)
- **$NH4NO_3$**: 20% (autoclaved)
- **$CaCl_2$**: 1% (autoclaved)
- **Z-Salts:** 0.01% each of ZnSO4*7H2O, CuSO4*5H2O, H3BO3, MnSO4*h2O and NaMbO4*2H2O) * (filtered through 0.2 micron membrane into an autoclaved bottle.)
- **FeSO4:** 0.01% (filtered through 0.2 micron membrane into an autoclaved bottle.)
- **Glucose:** 20% (or ~1M) (autoclaved)
- **Glycerol:** 50% (autoclaved)

A. MinAB broth (for each litre)

- 10 ml K-salts

- 20 ml M-salts
- 2.5 ml NH4NO3 (20%)
- 1 ml CaCL2 (1%)
- 5 ml Z-Salts
- 10 ml FeSO4 (0.01%)

This buffer is about pH6.7. It should be filter-sterilized . Just before use, add 1 ml glucose (20%) to each 100 ml MinAB broth prepared above.

B. IM Broth (IMB)

- 500 ml MinAB broth;
- 20 ml 1 M MES (non-adjusted) (final 40 mM);
- 5 ml 50% glycerol (final 0.5% (W/V) glycerol). Adjust pH to 5.5-5.7 with HCl
- Aliquot into 100 ml and autoclaved.

Just before use: add 0.2 ml 0.1M AS (acetosyringon,or 3'5'-dimethoxy-4'-hydroxyl-acetophenone) (final 200 μM) to 100 ml IMB.

C. IM Agar (IMA)

- 200ml IMB (make a few bottles at a time)
- 4g Bacto agar (2%)

Autoclaved. Shake well when it remains hot after the autoclaving. Use directly or store at RT as stock. Add acetosyringone (AS) to 200μM and glucose to 5 mM making plates.

SECTION B: METHODS

2.6 Growth and maintenance of bacteria and yeast strains

The *Escherichia coli* strains DH5α was used as a cloning host for molecular cloning work and grown at 37 °C. *E. coli* transformants were selected and maintained on LB medium supplemented with either ampicillin or spectinomycin.

The *S. cerevisiae* and *R. toruloides* strains were regularly maintained on yeast extract, peptone and dextrose (YPD) medium and grown at 28-30 °C. *S. cerevisiae* transformants were selected

and maintained on synthetic defined minimal medium containing yeast nitrogen base, ammonium sulphate and dextrose supplemented with appropriate amino acids as per requirement.

2.7 Growth Curve analysis

A single colony of yeast strain was used to inoculate 5 mL minimal medium supplemented with appropriate amino acids and grown overnight at 30 ^{o}C with shaking at 250 rpm. Secondary culture was inoculated at 0.05 OD_{600} in 50 mL minimal media in 250 mL shake flask supplemented with appropriate amino acids and grown at 30 ^{o}C with shaking at 250 rpm. For performing growth curve analysis at different concentration of extracellular phosphate, inorganic potassium dihydrogen phosphate (KH_2PO_4) is used as source of extracellular phosphate and added during secondary culture. Cell concentration was determined by measuring the absorbance at OD_{600} using a spectrophotometer (Perkin elmer UV/VIS Spectrophotometer, USA).

2.8 Growth assay by dilution spotting

S. cerevisiae strains carrying different plasmids were grown overnight in minimal media supplemented with appropriate amino acids, re-inoculated in fresh media at 0.1 OD_{600} and grown at 30 ^{o}C till 0.6-0.8 OD_{600}. Cells were then harvested and washed with deionized water and resuspended in water to make dilutions of different OD_{600}: 0.2, 0.02, 0.002, 0.0002. 10µL of different dilutions were spotted on SD plates supplemented with appropriate amino acids.

2.9 Recombinant DNA methodology (restriction digestion, ligation, transformation of *E. coli.* PCR amplification, etc.)

All the molecular techniques used in the study for manipulation of DNA, protein, bacteria and yeast were according to standard protocols (Guthrie and Fink, 1991; Sambrook and Russell, 2001), or as per manufacturers' protocol, unless specifically mentioned.

2.10 Custom synthesis of codon optimized genes

The genes for Geranylgeranyl diphosphate (GGPP) synthase (Rt*GGPPS*), Phytoene synthase (Rt*PSY1*) and Phytoene dehydrogenase (Rt*CRTI*) of *R. toruloides* were codon optimized by using EnCor Biotechnology Inc.(http://www.encorbio.com/protocols/Codon.htm) software and

custom synthesized by GenScript USA. Cytochrome P450 oxidase (RHTO_06383) and cytochrome P450 oxidoreducatse (RHTO_06309) were codon optimized and custom synthesized from Invitrogen GeneArt Gene synthesis, Thermofisher Scientific, USA.

2.11 Random mutagenesis: Hydroxylamine based mutagenesis

The protocol used here was adopted from previous reports (Rose and Fink, 1987b). 10 µg plasmid DNA was dissolved in 0.5 ml of Hydroxylamine solution (90 mg NaOH, 350 mg hydroxylamine HCl in 5 ml water, pH around 6.5. freshly made up before use). This mixture was incubated at 37 °C for 20 hrs and the DNA was purified using Qiagen column. Finally the pool of mutagenized plasmid was directly transformed into the appropriate yeast strain.

2.12 Random mutagenesis: Ethylmethane sulfate (EMS) based mutagenesis

EMS mutagenesis of BY4741 *S. cerevisiae* strain carrying carotenogenic plasmids was carried out. Briefly, 10^8 cells were harvested and followed by washing with autoclaved distilled water and 5mL 0.1M phosphate buffer. Then, the cells were resuspended in 1.8 mL of 0.1M phosphate buffer and 50µL of EMS was added. Cells were incubated with EMS for 20 minutes at 30 °C for >95% killing. Reaction was stopped by adding 8mL of 5% sodium thiosulphate. 1mL aliquot was taken to check killing and the rest sample was centrifuged and washed with autoclaved distilled water and spread on selection plates for selecting mutants.

2.13 Transformation of *E. coli*

E. coli competent cells were prepared using calcium chloride method in accordance with standard protocols (Sambrook, 1989).Transformation was carried out by adding plasmid or ligation mixture to the competent cells, incubated, followed by a thermal shock at 42 ^{o}C for 1 minute. Transformed cells were incubated in LB at 37 ^{o}C for 45 min, and plated on LB medium containing either ampicillin or spectinomycin.

2.14 Transformation of yeast: *S. cerevisiae*

The transformation of *S. cerevisiae* strains was carried out by lithium acetate method (Ito *et al*., 1983). *S. cerevisiae* cultures were grown in YPD at 30 ^{o}C with shaking for 16-24 hrs and then re-inoculated in fresh YPD media to an initial OD_{600} of 0.1, cells were allowed to grow at 30 ^{o}C for

4-5 hrs with shaking. Cells were harvested at 6000 rpm for 5 min, then were washed with sterile water followed by subsequent wash with 0.1 M lithium acetate solution (prepared in TE, pH 7.5) and were finally re-suspended in the same solution. Cells were incubated at 30 ^{o}C for 30 min with shaking. The cells were spun down, suspended in 0.1 M lithium acetate solution to a cell density of 1×10^{9} cells/ml and divided into 100µl aliquots. Approximately 50 µg (5µl of 10 mg/ml stock solution) of heat denatured, salmon sperm carrier DNA, followed by 0.3 µg- 0.7 µg of plasmid/DNA fragment were added to each aliquot and whole cell suspension was incubated at 30 ^{o}C for 30 min. After the incubation, 0.3 ml of 50% PEG 3350 (prepared in 0.1 M lithium acetate, pH 7.5) was added to each tube, mixed well and again kept at 30 ^{o}C for 45 min. The cell suspensions were subjected to heat shock at 42 ^{o}C for 5 min. and the cells were allowed to cool to room temperature. The cells were pelleted down at 7000 rpm for 3 min. The cell pellet was re-suspended in sterile water and appropriate volume of cell suspension was plated on selection plates.

2.15 Transformation of yeast: *R. toruloides* by *Agrobacterium* (ATMT)

The protocol was adopted from previous reports (Liu et al., 2013)

1. Inoculate 10 mL of YPD with *R. toruloides* (from fresh plate) and 10 mL of MinAB supplemented with spectinomycin (50 mg/L) with transformed *Agrobacterium tumefaciens AGL1* cells.(Note that both cells should be freshly prepared, not more than 1 week old)
2. Incubate both the culture at 28 ^{o}C with shaking 280 rpm for overnight (16-18 hours).
3. After overnight culture, inoculate the secondary culture of *R. toruloides* in 10 mL YPD and secondary culture of *A. tumefaciens AGL1* in 10 mL IMB (pH- 5.5- 5.7) with 200 µM acetosynrigone at 0.12 OD600.
4. Incubate both the cultures at 28 ^{o}C with shaking 280 rpm for 6 hours.
5. Take IMA agar plate (with acetosyringone- 200µM), air dry for 30 minutes in a laminar flow and then cover the lids.
6. Place a sheet of Hybond membrane (catalogue no. RPN82B) onto the surface of IMA plates using a pair of forcep (sterilized by heating). Avoid trapping air-bubbles by putting

the membrane disk one side of the plate and slowly lowering the membrane over the surface.

7. After 6 hours of growth, the yeast cell culture reaches to an OD600 - 0.6-0.7 and *Agrobacterium* reaches OD600 0.3-0.4. Mix 100 µL yeast cells with 100 µL *Agrobacterium* cells in an Eppendorf tube.
8. Take 200µL cell mixtures prepared above and spot evenly into about 10 spots over the surface of the membrane. Spread gently by rotating (while floating off the membrane) the L-spreader 1-2 circles. (Do not spread in more than 2 circles, which result in uneven spreading!).
9. Air-dry the IMA plate for 30 minutes and then seal with parafilm.
10. Incubate at 24 ^{o}C for 2-3 days (top-side-up). A good layer of cells is needed for efficient transformation. If not, lengthen the co-culture time.
11. Prepare the YPD plates with appropriate concentration of antibiotics (Hygromycin 150ug/ml and 300ug/ml Ceftoaxime). Dry for 30 min or more in a laminar flow.
12. Transfer the nylon membrane from the co-culture plates to YPD with antibiotics (Cef+, Hyg+). Air dry for 30 min-60 min;
13. Incubate 28-30 ^{o}C for 4-5 days (upside-up). (colonies start appearing from the 3rd day).

2.16 Isolation of plasmid from yeast

Selected yeast transformants were inoculated in 3 ml of selection medium and the cultures were incubated at 30 ^{o}C with shaking for 18-20 hr. After the incubation, the cells were harvested at 8,500 rpm for 5 min at room temperature and the pellets were suspended in 200 µl of STES lysis solution. Equal amounts of sterile, acid-washed glass beads (425 to 600 µm, Cat# G8772, Sigma) were added and the cell suspensions were vortexed vigorously for 1 min at room temperature. The lysed suspensions were then treated with phenol-chloroform adding 200 µl of phenol-chloroform solution and then vortexing for 1-2 min at room temperature. The lysates were spun down at 12,000 rpm for 5 min at RT and the aqueous phase was collected in a fresh microfuge tube. 2 µl of this DNA was electro-transformed in *E. coli* and transformants were selected on LB plates (containing ampicillin). The *E. coli* transformants were then grown to isolate plasmids and verified by re-transformation into yeast.

2.17 Isolation of genomic DNA from yeast

Genomic DNA from *S. cerevisiae* strains was isolated as described previously (C, 1994) using the glass bead lysis method and the STES lysis buffer, described in section 2.5.10.

2.18 RNA isolation from yeast cells

Total RNA was isolated by hot acid phenol method as described previously (Inada and Pleiss, 2010). *S. cerevisiae* transformants constitutively over expressing either *SPT15*WT or *spt15_A101T* were grown in 10 mL SD media supplemented with appropriate amino acids at 30 ^{o}C. When cells reached to an OD_{600} -1.5, cells were harvested and washed with cold sterilized water. Then 2 mL of acid phenol: chloroform solution and 2 mL of AES buffer (50mM sodium acetate, 10 mM EDTA and 1% SDS) was added. The samples were mixed properly and kept in a waterbath at 65 ^{o}C for 5-7 minutes with vortexing of the samples after every one minute. Then the samples were incubated on ice for 5 minutes. The phase lock tubes (PLT) were centrifuged at 3000 rpm for 1 minute. Then ,the sample was added to PLT tubes and centrifuged at 3000 rpm for 5 minutes at 4 ^{o}C. Then 2 mL of phenol: chloroform: isoamyl alcohol solution was added and centrifuged at 3000 rpm for 5 minutes at 4 ^{o}C. Then 2 mL of chloroform was added and followed by centrifugation at 3000 rpm for 5 minutes at 4 ^{o}C. Supernatant from the sample was taken in fresh falcon tube and 2.2 mL of isopropanol and 200 µL of 3M sodium acetate was added and followed by centrifugation at 15000 rpm for 20 minutes at 4 ^{o}C. The RNA pellet was given two washes with 70% ethanol, followed by centrifugation at 15000 rpm for 5 minutes at 4 ^{o}C . The pellet was then dried at 37 ^{o}C for 15 minutes and dissolved in 100 µL of DNAse free sterile water. Total RNA isolation was followed by DNase treatment (cat. no. M6101, Promega) at 30 ^{o}C for 15 minutes. RNA was cleaned up with Zymo Spin II column (Zymo research, cat. no. C1008-250) and stored at -70 ^{o}C until use.

2.19 Real Time qPCR

Total RNA was quantified with spectrophotometer by measurement at OD260/OD280 nm (Nanodrop). 3µg of total RNA was used for cDNA synthesis using reverse transcriptase and random-hexamer primers (GoScript™ Reverse Transcription system (cat. no. A5000) Promega) at 42 ^{o}C for 16 hours. Real Time quantitative PCR (RT-qPCR) was carried out on LightCycler®

480 II System (Roche molecular Diagnostics) by using SYBR green dye-based reagents (Maxima Sybr Green QPCR Master Mix, cat. no. K0251, Thermofisher). In the real-time PCR step, PCR reactions were performed in triplicates with 1 µL of cDNA/25 µL reaction and primers specific for PHO5, PHO84 and PHO89 and SYBR Premix. Thermal cycling was initiated at 94 ^{o}C for 30 sec followed by 40 cycles of PCR (94 ^{o}C for 5 sec and 68 ^{o}C for 30 sec). β-actin was used as an endogenous control. The relative changes in gene expression were calculated using the formula: fold change in gene expression , $2^{-\Delta\Delta Ct}$ where -ΔΔCt = [(Ct G.O.I $_{control}$ –Ct H.K.G$_{control}$) - [(Ct G.O.I $_{experimental}$ –Ct H.K.G$_{experimental}$) and *Ct* represents threshold cycle number, G.O.I and H.K.G represents gene of interest and housekeeping gene respectively.

2.20 Microarray Analysis

S. cerevisiae cells constitutively expressing either *SPT15*WT or *spt15_A101T* were grown overnight in SD media containing appropriate amino acids and then re-inoculated at 0.1 OD_{600} in same medium. At an OD_{600} - 1.5, the cells were harvested, washed and resuspended in RNA*later*® (10^8 cells). Four samples (two for *SPT15*WT (control) and two for *spt15_A101T*) (test)) were used for microarray analysis. Samples were sent for microarray analysis to Genotypic *Co*, Bangalore. For microarray analysis samples were treated as per the following protocol.

Total RNA extraction was done using Trizol, followed by quality check using Agilent Bioanalyser. Total RNA extracted was processed for single color labeling and hybridized to Agilent arrays (8*15K).The hybridized array were scanned using Agilent Microarray Scanner, followed by extraction of raw data by Agilent Feature Extraction software.

In preliminary and advance analysis of the data obtained, Normalization, Quality control, Statistical analysis, fold change analysis, and Clustering, Significant pathway and Gene ontology analysis using Agilent Genespring GX v11.2 was carried out.

With respect to control sets, fold change was calculated (logbase2) and genes showing Fold change of ±0.6 were further considered for analysis**.** In order to identify the genes whose expression was affected by in samples, we used a cut off of log_2 value of 1 which reflects the 2 fold change in expression of genes.

2.21 Sequence analysis

The ORF sequences as well as the corresponding proteins sequences were retrieved from Saccharomyces genome database (SGD) or from NCBI website (http://www.ncbi.nlm.nih.gov/).

For the multiple sequence alignment of the protein sequences was generated using CLUSTAL X program using default parameters (Thompson et al., 1997).

The SNAPGENE software was used for restriction analysis and oligo analysis.

2.22 Sequence accession numbers:

The codon optimized and custom synthesized genes – GGPP synthase (Rt*GGPPS*), Phytoene synthase (Rt*PSY1*) and phytoene dehydrogenase (Rt*CRTI*) were submitted to Genbank database and have the following accession numbers KU041640, KU041641 and KU041642 respectively.

2.23 Dry cell weight Determination

For estimating the dry cell weight, samples were kept at 80 ^{o}C in an oven for 48 hours and their dry weight was determined.

2.24 Extraction of carotenoids from *S. cerevisiae* and their analysis by HPLC

Extraction of carotenoids were carried out as described earlier (Moline et al., 2012) with some modifications. Essentially, yeast cells containing carotenogenic genes were grown in 100 mL SD media supplemented with appropriate amino acids and grown at 30 ^{o}C with shaking (250 rpm). After five days, cells were harvested and washed with deionized water and kept at -20 ^{o}C. To the frozen pellet was added 3 mL of Dimethyl sulphoxide (DMSO), vortexed for 1 min and incubated at 55 ^{o}C in the water bath for 1 hour. 1g 0.50-0.75 mm glass beads were added, and cells were broken using glass bead beater. Cells were centrifuged to remove the cell debris. Acetone was added to the pellet, vortexed and centrifuged and the process repeated till the pellet becomes colourless. The acetone and DMSO fractions were mixed with an equal amount of Hexane. The coloured hexane layer was collected after separation of two layers. The hexane layer was washed with distilled water and then with brine solution twice. The coloured hexane layer was collected. The solvent was evaporated under rotary evaporator to dryness in dim light and was dissolved in 1mL hexane for analysis by high performance liquid chromatography

(HPLC). HPLC separation and quantification was performed on Waters System using C_{18}-5µm intersil ODS-P, 250 x 4.6mm column (LCGC) using solvent acetonitrile:methanol:2-propanol (85:10:5 v/v) with flow rate 1mL/min at 32°C. Separated carotenoids were detected by photodiode array detector. Quantification of carotenoids was done using a standard curve prepared for β-carotene, lycopene and phytoene. Standards for β-carotene and lycopene were obtained from Sigma Aldrich, India and phytoene were obtained from CaroteNature GmbH, Switzerland. Standards of β-carotene, lycopene and phytoene were dissolved in hexane and the concentration of β-carotene, lycopene were calculated using extinction coefficient ($A^{1\%}$) of 2590, 3450 in hexane respectively and the concentration of phytoene was calculated using extinction coefficient ($A^{1\%}$) of 750 in hexane/2% CH_2Cl_2. The concentration of β-carotene, lycopene and phytoene in samples were expressed in microgram per gram dry cell weight (microgram/gram DCW). Data represented in form of standard mean error of at least two independent experiments.

2.25 Extraction of carotenoids from *R. toruloides* and their analysis by HPLC

R. toruloides cells was grown in 100 mL YPD and grown at 30 °C with shaking (250 rpm). After five days, cells were harvested and washed with deionized water and can be stored at -80 °C until use. To the pellet of 2 mL cells, 500 µL of 100mM NaCl solution was added and 1g 0.50-0.75 mm glass beads were added, and cells were broken using glass bead beater for total of eight cycles with 1 minute ON and 1 min OFF on incubation on ice. Then 500 µL of ethyl acetate was added and vortex it on glass bead beater for 1 minute. Centrifuged the samples at 12000 rpm for 5 minutes. Then, collect the organic layer and evaporated under rotary evaporator to dryness. Then dissolve in mobile solvent and quantification of carotenoids was performed in HPLC using C_{18}-5µm intersil ODS-P, 250 x 4.6mm column (LCGC) using solvent Acetonitrile: Propanol: Ethyl acetate (40:40:20 v/v) with flow rate 1mL/min at 32°C. for analysis. . Standards for Torulene and Torularhodin were obtained from CaroteNature GmbH, Switzerland. concentration of Torularhodin was calculated using extinction coefficient ($A^{1\%}$) of 1932 in hexane.

2.26 Identification and quantification of α-Farnesene

S. cerevisiae ABC 276 was transformed with pRS315TEF-At*FS*. Transformants were grown in SD media containing appropriate amino acids. Secondary culture was inoculated at 0.05 O.D and when O.D reaches to 0.6-0.8, culture was overlaid with 10% dodecane. After 48 hrs, the

dodecane phase of the two- phase culture was collected by centrifugation of culture at 6000 rpm for 5 minutes. 1 uL of dodecane phase was subjected to GC-FID analysis. Samples were injected at a split ratio of 1:10. The oven temperature was initially held at 80°C for 1 min and was increased at a rate of 10°C/min to 250°C where it was held for 1 minute. Carrier gas was nitrogen. And the temperature of detector was maintained at 260°C. All the conditions used for GC analysis was followed from (Wang et al., 2011). Standard curve of trans β-Farnesene was prepared using GC- FID. Trans β-Farnesene (Cat. 73492) from Sigma Aldrich, India was used as standard.

2.27 Measurement of extracellular metabolites by HPLC

Concentration of extracellular metabolites such as glucose, ethanol, acetate and glycerol in the media during exponential phase of growth of yeast transformants were measured by JASCO HPLC system using Aminex HPX-87H column (Bio-Rad, Hercules, CA, USA) using a previous protocol (Li et al., 2016). Briefly, 1mL of samples were collected and centrifuged and then supernatant was filtered through 0.2 µm filter before running through the column. The column was kept at 65 °C and 0.01N sulfuric acid was used as a mobile phase with a flow rate of 0.5 mL/min. All the experiments were performed in duplicates and error bars represent the standard error mean of two biological replicates.

2.28 Simulation studies for Flux balance analysis

iMM904 is a genome scale metabolic network model of *S. cerevisiae* S288C. It was constructed to connect the extracellular metabolomic measurements with intracellular fluxes of cell (Mo et al., 2009). It was constructed from the genome scale network, iND750. The The predictions from the model, iMM904 was validated from the published literature. iMM904 model consists of total of 1557 reactions, 1225 different metabolites and 905 genes.

Constraint-based Flux Balance Analysis (FBA) was performed using the manually curated metabolic model of *S. cerevisiae,* iMM904 (Pereira et al., 2016). The curated model iMM904 is constrained for reversibility of some reactions, inactivation of some reactions and addition of transport reactions for cofactor utilization. The total reactions in this manually curated model is 1581. The model was imported into COBRAPy environment (Ebrahim et al., 2013; Edwards et al., 2001) and optimized using the built-in linear programming solver (Edwards et al., 2001). For

each strain (wild type, mutant), we constrained uptake and secretion rates of the glucose, ethanol, acetate and glycerol metabolites using experimental measurements and optimized the model by maximizing the biomass as the objective function and validated the predicted growth rates with experimentally measured values. The flux in transaldolase reaction (TALA) is set to lower bound to 11 units normalized to 100 units of glucose (Pereira et al., 2016). The flux in the isoprenoid pathway (HMGCOAR) was set to 1.5 units normalized to 100 units of glucose. For flux balance distribution of the mutant strain with additional transcriptomic constraints, the constraints were calculated based on flux values of wild type strain. The flux values shown in figures were normalized to 100 units of glucose.

2.29 Whole genome sequencing analysis

To identify the precise mutations in the genome of EMS mutagenized samples, whole genome sequencing was carried out from Genotypic *Co*, Bangalore. Library preparation was performed at Genotypic Technology's Genomics facility following NEXTFlex DNA library protocol outlined in "NEXTFlex DNA sample preparation guide (Cat # 5140-02). In brief, genomic DNA was sheared to generate fragments of approximately 200-400bp in a Covaris microTube with the S220 system (Covaris, Inc., Woburn, MA, USA). The fragment size distribution was checked using Agilent TapeStation with D1000 DNA Kit (Agilent Technologies) according to the manufacturer's instructions. These fragments were subjected to end-repair, A-tailing, and ligation of the Illumina multiplexing adaptors using the NEXTFlex DNA Sequencing kit as per the manufacturer's instruction. The resulting ligated DNA was cleaned up using HighPrep beads (MagBio Genomics, Inc, Gaithersburg, Maryland). The cleaned product was subjected to 10 rounds of PCR (denaturation at 98˚C for 2 min, cycling (98˚C for 30sec, 65˚C for 30sec and 72˚C for 60s) and final extension at 72˚C for 4 min) using primers provided in the NEXTFlex DNA Sequencing kit. The PCR product was purified using HighPrep beads. Quantification and size distribution of the prepared library were determined using Qubit flourometer and the Agilent D1000 Tape ~Agilent Technologies respectively according to the manufacturer's instructions. The obtained sequencing data was analyzed by Genotypic *Co*, Bangalore.

CHAPTER 3:

To develop and validate a carotenoid based visual genetic assay for increasing the metabolic flux in the isoprenoid pathway of Saccharomyces cerevisiae

3.1 Introduction

Carotenoids are members of the isoprenoid/terpenoid class of compounds and are tetra terpenoids. They have been exploited in the past for increasing the production of building blocks e.g. geranylgeranyl diphosphate and to increase the activity of carotenogenic enzymes and production of novel carotenoids and in substrate consumption assay for improving the activity of taxadiene synthase (Furubayashi et al., 2014; Mitchell et al., 2015; Ohnuma et al., 1994; Schmidt-Dannert et al., 2000; Umeno et al., 2002; Wang et al., 2015; Xie et al., 2014). As carotenoids are colored compounds, their production in the cell has the potential to provide a good visual phenotype for fast and easy assessment of altered fluxes in the isoprenoid biosynthetic pathway.

Several groups have attempted to increase the metabolic flux in the isoprenoid pathway using the carotenoid based visual screen using the carotenogenic enzymes from *Xanthophyllomyces dendrorhous* (Ozaydin et al., 2013; Verwaal et al., 2007a; Yuan and Ching, 2014). However these studies have met with limited success. It was observed that upon increasing the flux in this pathway through known flux increaser such as *tHMG1*, a decrease rather than an increase in pigmentation was observed (Verwaal et al., 2007a; Yuan and Ching, 2014). Estimation of carotenoids revealed that the decrease was most likely due to accumulation of the colorless intermediate, phytoene which masked increase in color due to higher β-carotene (Verwaal et al., 2007a). A visual carotenoid based screen has also been employed to screen the yeast deletion collection to identify gene deletions that could improve isoprenoid production (Ozaydin et al., 2013). Although the study succeeded in obtaining deletion mutants with more β-carotene, it did not appear to be a validated screen for isoprenoids since the deletion mutants with higher pigmentation did not yield increased levels of an alternate isoprenoid, bisabolene. Thus, surprisingly, despite the extensive use of carotenoids in a variety of different screens and assays, their development as a measure of isoprenoid flux has remained unsuccessful so far, owing to absence of correlation between the color and the isoprenoid flux.

Therefore, in this chapter, I have reinvestigated the problems of using carotenoids as a marker for the isoprenoid pathway flux and attempted to overcome the obstacles encountered in the previous carotenoid-based screens. Beginning with the sourcing of the carotenogenic enzymes from the high β-carotene producing yeast *Rhodosporidium toruloides*, I have employed

different metabolic engineering strategies for the successful development of a carotenoid-based screen for isoprenoid flux.

3.2 Results

3.2.1 Reconstruction of carotenoid biosynthetic pathway in *Saccharomyces cerevisiae* using enzymes from *Rhodosporidium toruloides* reveals β-carotene as the majorly produced carotenoid

Instead of using the carotenogenic enzymes from the *X. dendrorhous*, I opted to work with the enzymes from *Rhodosporidium toruloides* as this red yeast has been reported to be the highest producer of β-carotene (Mata-Gomez et al., 2014). Thus, enzymes from this yeast might be better evolved for handling higher flux in the isoprenoid and carotenoid pathways. I therefore sought to first identify and then reconstruct the carotenoid pathway from *R. toruloides* in *S. cerevisiae*. The genome sequence of *R. toruloides* was published by our group along with others (Kumar et al., 2012; Zhu et al., 2012). From the published genome sequence of *R. toruloides* NP11 strain, putative carotenoid biosynthesis genes coding for geranylgeranyl diphosphate synthase (GGPP synthase *Rt*GGPPS), phytoene synthase (*Rt*PSY1) and phytoene dehydrogenase (*Rt*CRTI) were identified from the database available at NCBI on the basis of the sequence similarity with other carotenoid producing organisms (*Xanthophyllomyces dendrorhous*, *Neurospora crassa*) as shown in table 3.1. Among these proteins, an apparent mis-annotation was detected with the predicted phytoene dehydrogenase of *R. toruloides*.

The predicted phytoene dehydrogenase of *R. toruloides* (*Rt*CRTI) was 610 aa in length. It had an extra 56 amino acids at the N-terminal region. Multiple sequence alignment suggested that this may be a consequence of mis-annotation of the start site. Therefore, I considered only the region that fully aligned with the other homologues. This corresponded to the remaining 554 aa which had 68% similarity (E-value $2e^{-176}$) to the phytoene dehydrogenase from *X. dendrorhous* (Figure 3.1A).

Owing to high GC content (62%) and intronic nature of the *R. toruloides* genes, the three putative carotenogenic genes mentioned in table 3-1A were codon optimized for expression in *S. cerevisiae* using online software at EnCor Biotechnology Inc. (http://www.encorbio.com/protocols/Codon.htm) and then custom synthesized by GenScript USA Inc. These were sub-

cloned into the yeast single copy centromeric expression vectors under the TEF promoter (as described in materials and methods Table 2.3) and expressed in *S. cerevisiae* ABC 276 strain. *S. cerevisiae* ABC 276 strain is a derivative of S288c strain which was derived from tetrad analysis of diploids made between BJ5418 and BJ5458 strains which were obtained from Beth Jones laboratory. I observed that expression of these genes in *S. cerevisiae* produces deep orange colored yeast colonies (Figure 3.1B). To analyze the composition of these carotenoids, extraction and analysis of carotenoids accumulated in these cells were carried out. I could detect the carotenoid precursor, the colorless phytoene, and the carotenoids β-carotene, γ-carotene and negligible amount of lycopene based on comparison with retention time of available authentic carotenoid standards in HPLC (Figure 3.1C).

From the figure 3.1B, it was observed that by over expressing *R. toruloides* genes in *S. cerevisiae*, one could obtain β-carotene as the major fraction of total carotenoids along with lower amount of phytoene and negligible amount of lycopene. This was in contrast to the carotenoid profile seen when *X. dendrorhous* enzymes were expressed in *S. cerevisiae*. In this study it was observed that phytoene accumulation was at high levels. This preliminary analysis suggested that opting for genes from *R. toruloides* was probably a good choice since it led to low levels of intermediates (i.e. phytoene and lycopene), relative to β-carotene as compared to previous study of using carotenogenic genes from *X. dendrorhous* (Verwaal et al., 2007a).

Genes/ Enzymes	**ORF no.**	**Length (aa)**	**No. of introns**	**BLASTP with *X. dendrorhous* E-value Similarity**	BLASTP with *N. crassa* E-value Similarity
GGPP synthase (*Rt*GGPPS)	RHTO_02504	359	07	$2e^{-112}$ 63%	$2e^{-116}$ 73%
Phytoene Synthase (*Rt*PSY1)	RHTO_04605	612	07	$1e^{-77}$ 46%	$2e^{-110}$ 54%
Phytoene dehydrogenase (*Rt*CrtI)*	RHTO_04602	610	09	$5e^{-178}$ 67%	0 69%
Phytoene dehydrogenase (*Rt*CrtI)	RHTO_04602	554	09	$1e^{-178}$ 67%	0 69%

Table 3.1 Bioinformatic analysis of putative carotenogenic genes of *R. toruloides*.

*- Full length protein sequence reported in *R. toruloides* database.

```
Rhod_toru  1    MRPLAREEELRCDAEQRKVKVIASGNSSARSPMPGGAVRCLTGLLLSCHQLVSTARMAAA  60
                M    +E++
Xant_dend  1    M---GKEQD-----------------------------------------------------  6

Rhod_toru  61   NGHGKGKPSVLIVGAGVGGTASAARLAQSGFDVTVLEKNDFAGGRCSLFTDPTKSFRFDQ  120
                    + KP+ +IVG G+GG A+AARLA+ GF VTV EKND++GGRCSL       +RFDQ
Xant_dend   7   ----QDKPTAIIVGCGIGGIATAARLAKEGFQVTVFEKNDYSGGRCSLIE--RDGYRFDQ  60

Rhod_toru  121  GPSLFLIPRLFDETFNDLGTSLENEGIKLVKCEPNYRIVFPDKEVVEMSSDLTRMKKQVE  180
                GPSL L+P LF +TF DLG  +E + + L+KCEPNY   F D+E    S+D+  +K++VE
Xant_dend  61    GPSLLLLPDLFKQTFEDLGEKME-DWVDLIKCEPNYVCHFHDEETFTFSTDMALLKREVE  119

Rhod_toru  181  RWEGEKGFEGFLGFLKEGHAHYELSMVHVLHRNFTSLLSMVRPSLIIQLRKLHPFVSVYS  240
                R+EG+ GF+ FL F++E H HYEL++VHVL +NF    + +R   I Q+  LHPF S+++
Xant_dend  120   RFEGKDGFDRFLSFIQEAHRHYELAVVHVLQKNFPGFAAFLRLQFIGQILALHPFESIWT  179


Rhod_toru  241  RATKYFKTDRMRRAFTFASMYLGMSPFDALGAYNLLQYTEHCEGILYPLGGFGRIPQTLQ  300
                R  +YFKTDR+RR F+FA MY+G SP+ A G Y+LLQYTE  EGI YP GGF ++P TL
Xant_dend  180   RVCRYFKTDRLRRVFSFAVMYMGQSPYSAPGTYSLLQYTELTEGIWYPRGGFWQVPNTLL  239

Rhod_toru  301  QLAEKSG--AKFRFNSPVKRVTVE--NGTAKGVELESGEKLTADIVLVNADLVWSMAHLY  356
                Q+ +++   AKF FN+PV +V +      A GV LESGE+  AD+V+VNADLV++  HL
Xant_dend  240   QIVKRNNPSAKFNFNAPVSQVLLSPAKDRATGVRLESGEEHHADVVIVNADLVYASEHLI  299

Rhod_toru  357  EETSYSKRLEERPV----------------SCSSISLYWSMNRKIPQLDSHTIFLAEEYR  400
                 + + +K  +   V                 SCSS+S YWSM+R +  L  H IFLAE+++
Xant_dend  300   PDDARNKIGQLGEVKRSWWADLVGGKKLKGSCSSLSFYWSMDRIVDGLGGHNIFLAEDFK  359

Rhod_toru  401  ESFDSIFREHRIPHEPSFYVNVPSRHDPSAAPADKDAVIVLVPVGHISAALPSSSDWDKV  460
                 SFD+IF E  +P +PSFYVNVPSR DPSAAP  KDA+++LVP GHI A+ P   D++K+
Xant_dend  360   GSFDTIFEELGLPADPSFYVNVPSRIDPSAAPEGKDAIVILVPCGHIDASNPQ--DYNKL  417

Rhod_toru  461  VEETRNKIIGEIERRLDIEDLRSCIEHETINTPITWGEKFNLHRGSILGLSHDFFNVLSF  520
                V   R  +I  +  +L + D    I  E ++   +W ++FNL  GSILGL+H+F  VL F
Xant_dend  418   VARARKFVIQTLSAKLGLPDFEKMIVAEKVHDAPSWEKEFNLKDGSILGLAHNFMQVLGF  477

Rhod_toru  521  RPKTRHPSVKNAYFVGASAHPGTGVPIVLAGARLVATQILND----------LGMPI-  567
                RP TRHP     +FVGAS HPGTGVPIVLAGA+L A Q+L              L +P
Xant_dend  478   RPSTRHPKYDKLFFVGASTHPGTGVPIVLAGAKLTANQVLESFDRSPAPDPNMSLSVPYG  537
```

Figure 3.1A Global sequence alignment of phytoene dehydrogenase (accession no. XP_016275543) from *R. toruloides* with phytoene dehydrogenase (accession no. CAA75240) from *X. dendrorhous* using Needleman and Wunsch algorithm through BLAST server.

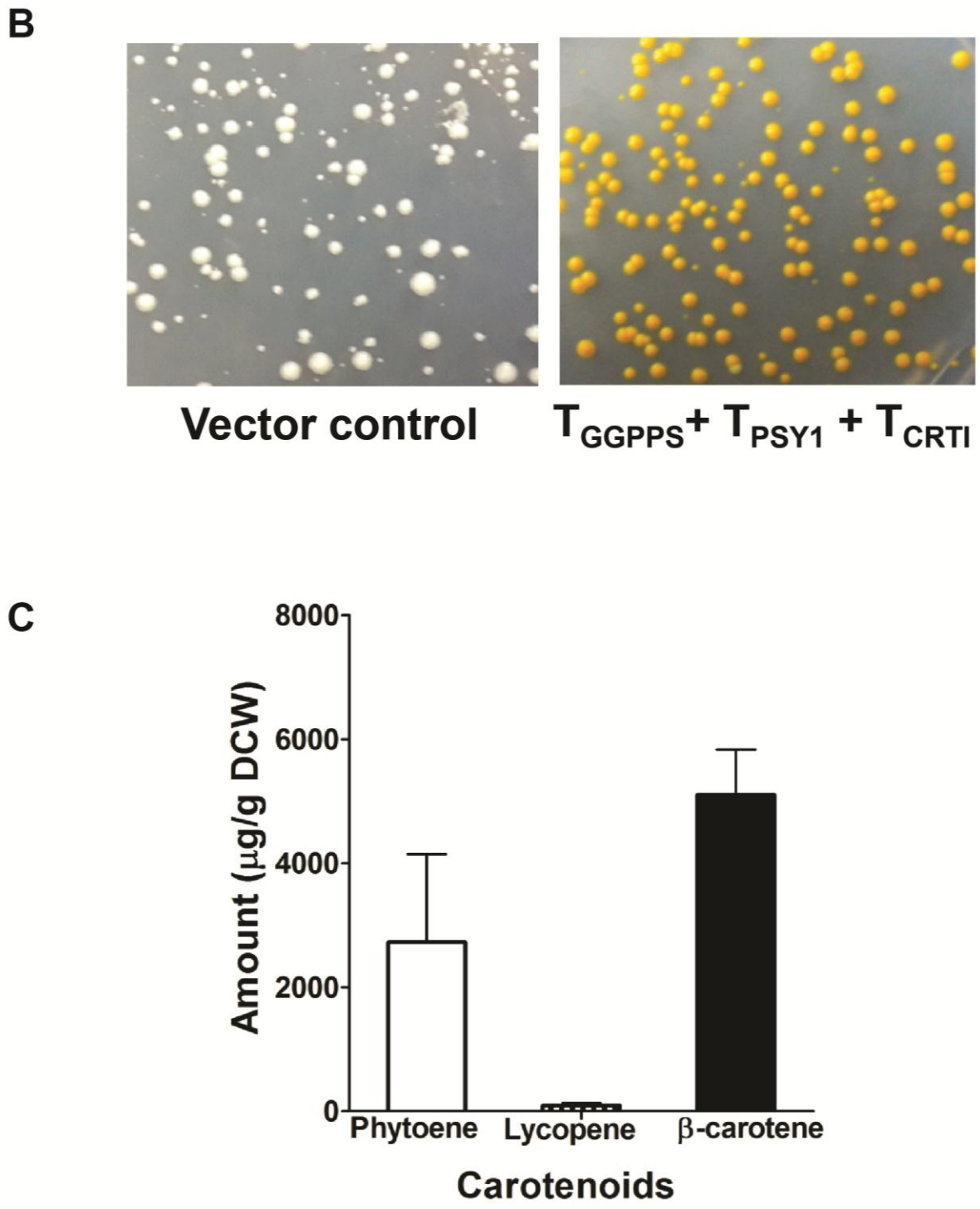

Figure 3.1 (B) Functional expression of core carotenogenic genes from *R. toruloides* in *S. cerevisiae* (C) Amount of key carotenoids produced

T-TEF promoter, GGPPS- GGPP synthase, PSY1- Phytoene synthase, CRTI- Phytoene dehydrogenase

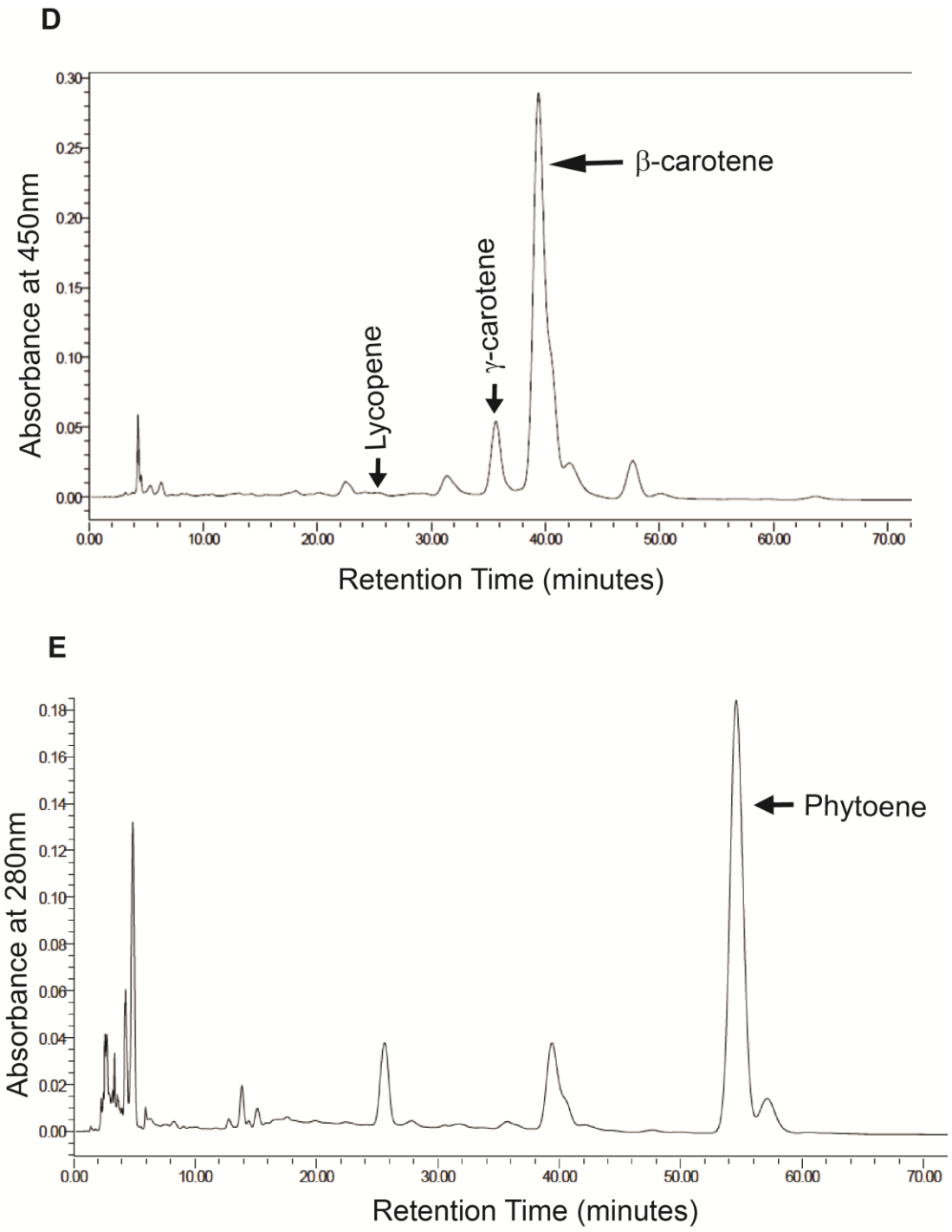

Figure 3.1 HPLC chromatogram of *S. cerevisiae* strain expressing core carotenogenic genes of *R. toruloides*. (D) Different carotenoid peaks (β-carotene, Lycoene, γ-carotene) **(E)** Phytoene based on their standard retention time are now shown

F

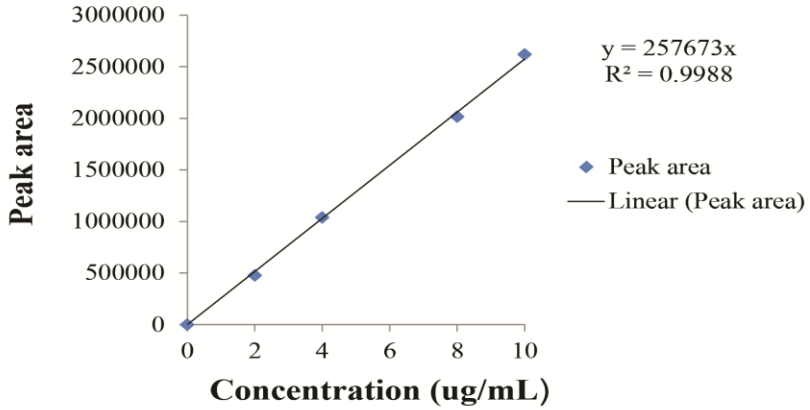

G

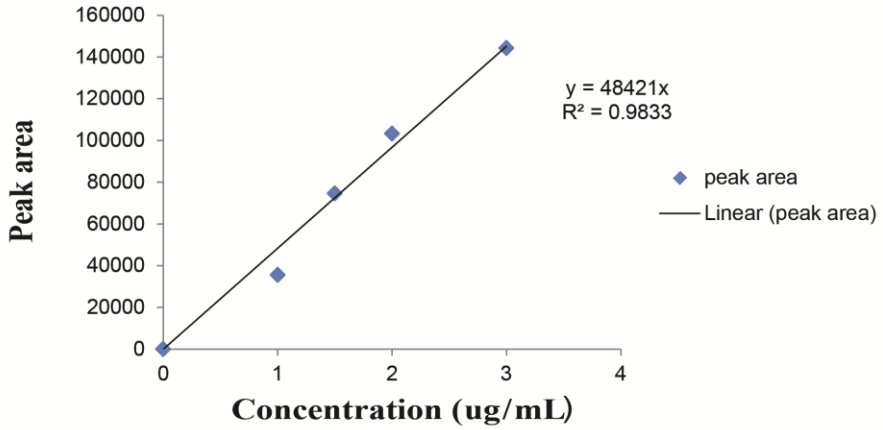

H

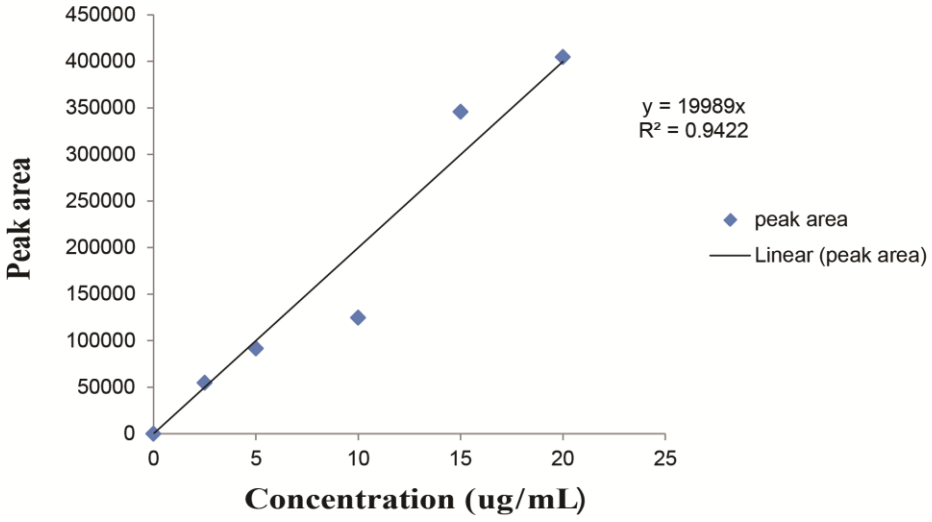

Figure 3.1 Standard calibration curve of (F) β-carotene (G) Lycopene (H) Phytoene

3.2.2 Combinatorial approach of strong and weak promoters for obtaining a low-color strain compatible for screening isoprenoid flux

In an initial experiment, I had expressed all three carotenogenic enzymes from *R. toruloides* under a strong promoter (TEF) which give a deep orange color. However, for the development of a screening strain for carotenoid flux, I needed a low color producing strain that upon increasing the flux would produce more color.

Therefore, I cloned and expressed all the three *R. toruloides* carotenogenic genes under both weak and strong constitutive promoters (CYC and TEF respectively). A *S. cerevisiae* strain was separately transformed with different TEF and CYC promoter combinations of *Rt*GGPPS, *Rt*PSY1and *Rt*CRTI gene constructs. The different transformants bearing combination of three plasmids were dilution spotted and their pigmentation intensity was used as the readout for carotenoid yield as shown in figure 3.2A. As shown in the figure 3.2A, there were eight possible combinations of transformants. Four transformant combinations (no. 1, 2, 3 and 6) showed less pigmentation whereas the remaining four transformants (no. 4, 5, 7 and 8) showed high pigmentation.

Interestingly, all the four combinations showing less pigmentation contained phytoene dehydrogenase (*Rt*CRTI) expressed under a weak constitutive promoter (CYC), while the high pigmentation showing combinations expressed phytoene dehydrogenase under a strong constitutive promoter (TEF). It was observed that the low pigmentation producing transformants can be converted to high pigmentation transformants and vice-versa by changing promoter of only phytoene dehydrogenase (*Rt*CRTI). This observation suggested that phytoene dehydrogenase (*Rt*CRTI) might be rate-limiting. This was confirmed by extraction of carotenoids and HPLC analysis from high and low pigmentation transformants (no. 5 and 6 respectively) (Figure 3.2B). This confirmed that the accumulation of phytoene in low pigmentation transformants no. 6 was due to the rate limiting nature of phytoene dehydrogenase (*Rt*CRTI). Thus, although I obtained the desired ‘low-color’ producing strain, their usefulness as a screen needed to be evaluated carefully since phytoene was significantly accumulating in these strains.

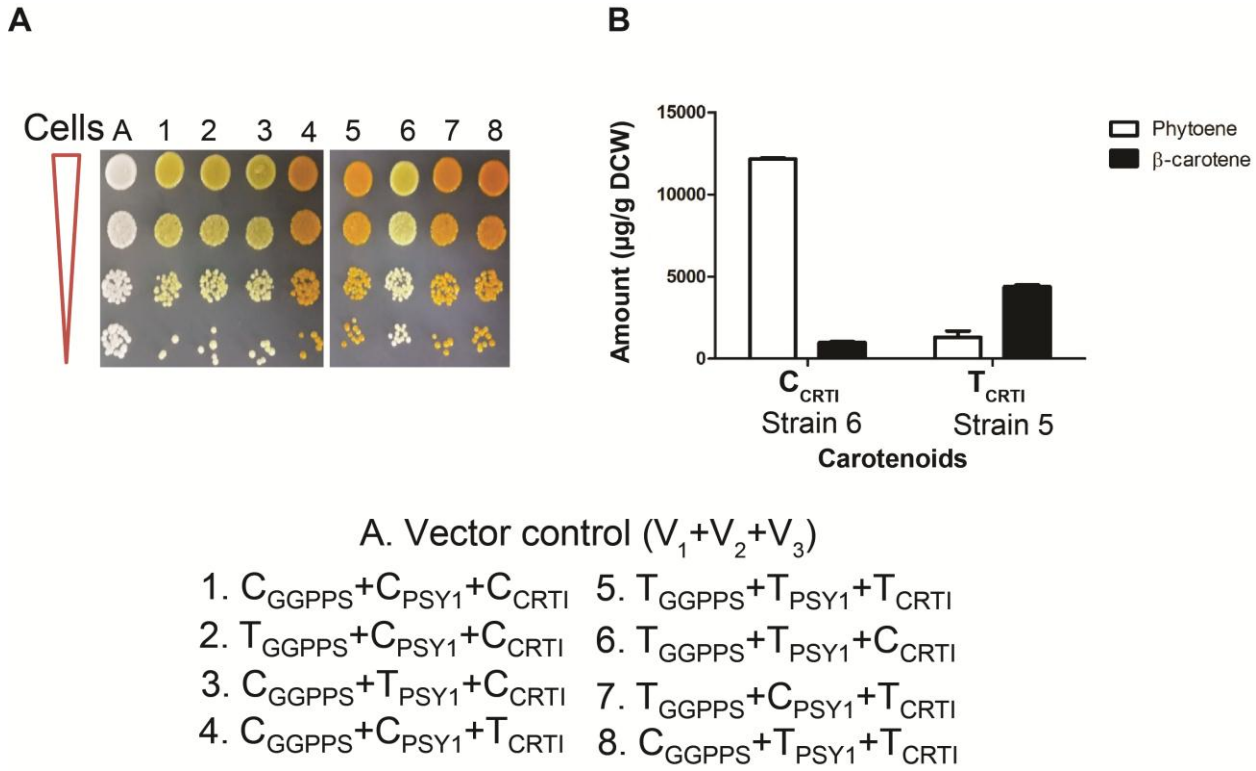

Figure 3.2 Evaluation of isoprenoid flux
(A) On the pigmentation level of different promoter combination strains (dilution spot carrying, $4X10^4$, $4X10^3$, $4X10^2$, $4X10^1$ cells) (B) Amount of key carotenoids in high pigmentation strain (strain 5) and low pigmentation strain (strain 6).

T-TEF promoter, C-CYC promoter, GGPPS- GGPP synthase, PSY1- Phytoene synthase, CRTI- Phytoene dehydrogenase

3.2.3 Rate limiting phytoene dehydrogenase (*Rt*CRTI) hinders the successful development of carotenoid based genetic screen:

Due to the accumulation of phytoene in the low color strains, I suspected that phytoene dehydrogenase (*Rt*CRTI) might be a bottleneck for the development of a carotenoid based visual genetic screen for isoprenoid flux due to the non-linear flux and pigmentation relationship. To examine this issue, I over-expressed the truncated catalytic domain of *HMG1* (*tHMG1*) which is known to increase the flux in the pathway in the different promoter combination strains (mentioned in previous section 3.2.2) and transformants were dilution spotted as shown in figure 3.3A.

It was observed that with overexpression of *tHMG1* in these different transformants, there was no increase in pigmentation despite the expected increase in flux in the isoprenoid pathway. Indeed, transformants with higher pigmentation (no. 5) instead showed a decrease in pigmentation after over expression of *tHMG1*. Chemical analysis of the transformants no. 5 also revealed that there is 2.8 fold increase in levels of phytoene, but only 1.8 fold increase in the levels of β-carotene with over expression of *tHMG1* as shown in figure 3.3B. This confirmed that there was phytoene (metabolite) accumulation at the phytoene dehydrogenase step and accumulation of phytoene in the cell might explain the masking effect on pigmentation of the transformants.

3.2.4 Addressing the metabolic bottleneck phytoene dehydrogenase (*Rt*CRTI) by directed evolution strategy yields catalytically more efficient mutants of enzyme:

For the successful development of a carotenoid-based visual screen where isoprenoid flux correlates with pigmentation, there was a need to overcome the metabolic block at the phytoene dehydrogenase step. Therefore, to reduce the accumulation of phytoene in the cell, the first strategy was to increase the activity of phytoene dehydrogenase (*Rt*CRTI). This could be done either by (a) its expression under strong promoter or (b) increasing copy number of plasmid or (c) isolation of catalytically efficient mutants of enzyme. Expression under the strong promoter did not seem adequate to relieve the block as seen with the use of strong (TEF) and weak (CYC) promoters. Increasing the copy number of plasmid encoding for phytoene dehydrogenase was an approach already unsuccessfully explored previously (Verwaal et al., 2007a).

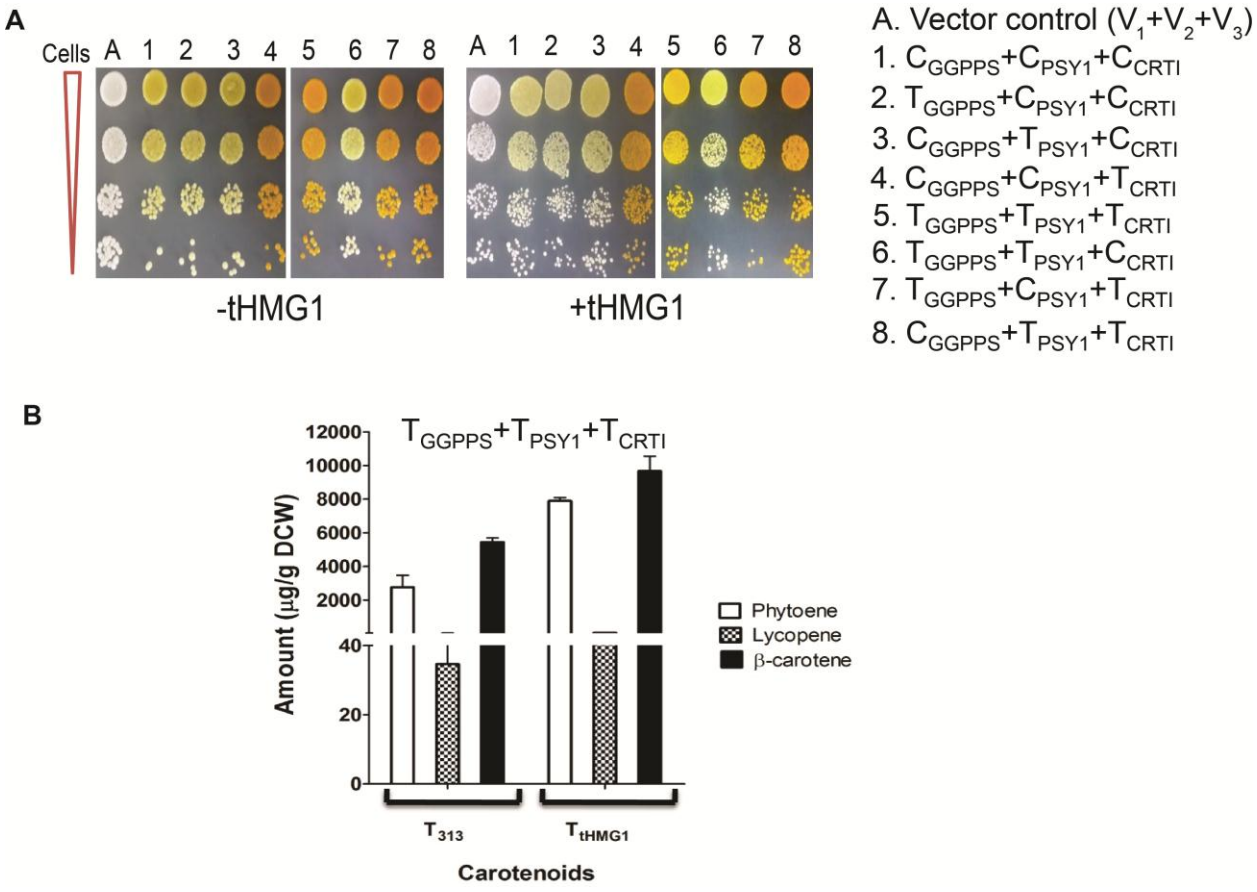

Figure 3.3 Evaluation of isoprenoid flux

(A) On the pigmentation level of different promoter combination strains with and without *tHMG1* (dilution spots carrying, $4X10^4$, $4X10^3$, $4X10^2$, $4X10^1$ cells) (B) Amount of key carotenoids with and without *tHMG1* (under TEF promoter) in strain no. 5

T-TEF promoter, C-CYC promoter, GGPPS- GGPP synthase, PSY1- Phytoene synthase, CRTI- Phytoene dehydrogenase

Furthermore, this strategy would also result in a metabolic burden to the cell resources; hence I did not adopt this strategy. Instead I attempted a directed evolution strategy using random mutagenesis to isolate catalytically more active mutants of phytoene dehydrogenase (*Rt*CRTI) by exploiting the pigmentation phenotype. I performed the directed evolution of *Rt*CRTI through hydroxylamine based *in vitro* random mutagenesis (as described in materials and methods Section 2.11). I first created a mutant library of plasmid containing *Rt*CRTI (where *Rt*CRTI was under the weak CYC promoter). This was a low color producer that was essential for such a color based screen, since higher color led to a saturation in such visual screens (Wang et al., 2000).

This mutant library was transformed into a *S. cerevisiae* strain containing the GGPP synthase (*Rt*GGPPS) and phytoene synthase (*Rt*PSY1), both under the strong constitutive TEF promoter. Transformants were screened on the basis of increased pigmentation as compared to the control parent strain. After screening and selecting the six mutant yeast strains, plasmids were isolated and amplified through *E. coli* and the *Rt*CRTI coding region was sub-cloned into a fresh parent vector background. These sub-cloned *Rt*CRTI mutant plasmids were then retransformed into the parent strain for confirmation of increased pigmentation. Three mutants were confirmed for the desired phenotype and were sequenced. Among the three mutants, two mutants were found to have an Ala393Thr mutation in the coding sequence, while the other mutant was found to have an Ala394Gly mutation. These mutants were further confirmed for their increased activity by HPLC analysis. The *Rt*CRTI_A393T (mutant) enzyme showing enhanced pigmentation and increased β-carotene levels as compared to the *Rt*CRTI (WT) enzyme is shown in figure 3.4A and 3.4B. There was a 2-fold decrease in levels of phytoene and 3.4-fold increase in β-carotene levels with the *Rt*CRTI_A393T (mutant) enzyme as compared to the *Rt*CRTI (WT) enzyme (Figure 3.4B). Hence, I chose *Rt*CRTI_A393T for further experiments.

I was interested to know how these mutants were showing increased activity. I initially examined the conservation pattern of these residues in carotenoid producing fungi and bacteria. Multiple sequence alignment of phytoene dehydrogenase revealed that these residues were not conserved in bacterial or fungal enzymes (Figure 3.4B and 3.4C). Interestingly, *X. dendrorhous* (red yeast used for carotenoid production) has an alanine at 393 position similar to *R. toruloides* genes, while the carotenoid producing bacteria, *Pantoea ananatis* has threonine at 393 position similar

to mutant *R. toruloides* gene. I also performed modelling of *Rt*CRTI using the structure of the enzyme from *Pantoea ananatis* (PDB ID 4DGK) (Schaub et al., 2012) as a template and observed that these residues (A393 and A394) were not present in the active site. The actual reason behind the increased pigmentation seen in these mutants is not known. However as this was not critical to our goal, it was not pursued further.

3.2.5 The catalytically efficient mutant of *Rt*CRTI (*Rt*CRTI_A393T) also fails to yield the desired carotenoid based visual screen :

I was interested to know whether employing this catalytically more efficient mutant of phytoene dehydrogenase (*Rt*CRTI_A393T) would aid in developing correlation between pigmentation and isoprenoid pathway flux. Therefore, to examine this, I over expressed *tHMG1* in strains containing *Rt*GGPPS and *Rt*PSY1 under the strong constitutive promoter (TEF) along with *Rt*CRTI_A393T cloned under either a weak constitutive promoter (CYC) (Figure 3.5A), a strong constitutive promoter (TEF) (Figure 3.5B) and or an even more stronger constitutive promoter (GPD) (Figure 3.5C). Surprisingly, I did not observe any increase in pigmentation with the introduction of *tHMG1* in any of the transformants (Figure 3.5A, 3.5B and 3.5C). The chemical analysis of the strain containing *Rt*GGPPS, *Rt*PSY1and *Rt*CRTI_A393T (all under TEF promoter) along with over-expression of *tHMG1* showed that there was a 2-fold increase in levels of phytoene, with a 1.5-fold decrease in β-carotene levels (Figure 3.5D). This suggested that phytoene was still accumulating to a high level in the cell despite the use of strong promoter and an active mutant of phytoene dehydrogenase (*Rt*CRTI_A393T). The decrease in the β-carotene levels in HPLC chromatogram was surprising. A possible explanation for this is that *Rt*CRTI_A393T pushes flux more towards torulene rather than β-carotene, but this need to be investigated.

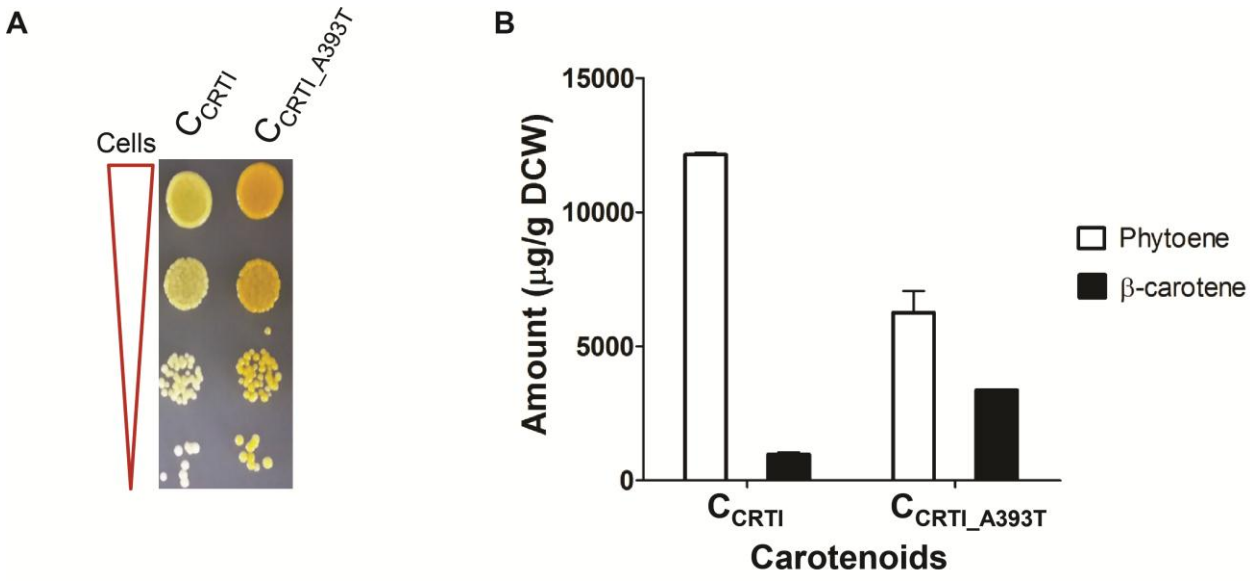

Figure 3.4A Effect of phytoene dehydrogenase mutant *Rt*CRTI_A393T on isoprenoid flux (A) On the pigmentation intensity of strain with and without *CRTI* mutant (dilution spots carrying $4X10^4$, $4X10^3$, $4X10^2$, $4X10^1$ cells) (B) Amount of key carotenoids in strain expressing *GGPPS*, *PSY1* under TEF promoter along with either *CRTI* or *CRTI*_A393T under weak CYC promoter.

C-CYC promoter, CRTI- Phytoene dehydrogenase

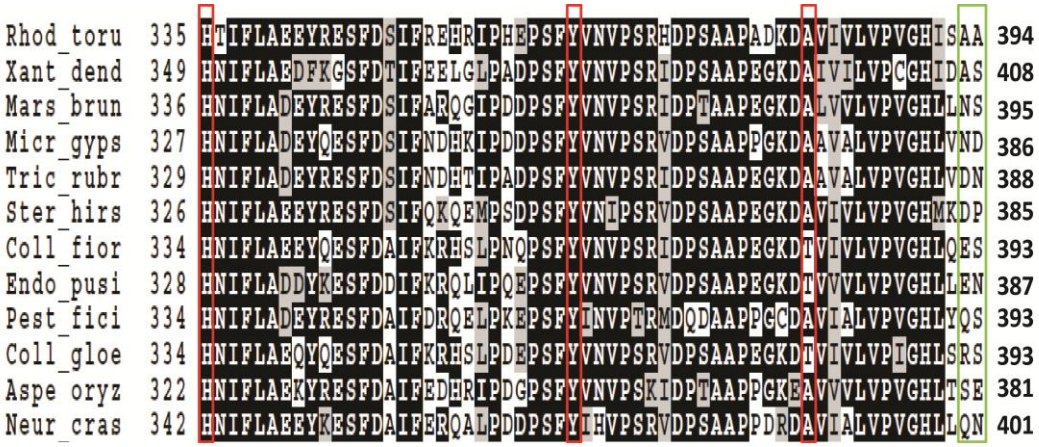

Figure 3.4B Multiple sequence alignment of phytoene dehydrogenase from different fungi. A393 and A394 residue of *R. toruloides* is highlighted by green bar and are not conserved across species. Active site residues are highlighted by red bar. Rhod_toru- *Rhodopsporidium toruloides*, Xant_dend- *Xanthophyllomyces dendrorhous*, Mars_brun- *Marssonina brunnea*, Micr_gyps- *Microsporum gypseum CBS118893*, Tric_rubr- *Trichophyton rubrum CBS118892*, Ster_hirs- *Stereum hirsutum FP_91666SS1*, Coll_fior- *Colletotrichum fiorniae PJ7*, Endo_pusi- *Endocarpon pusillum Z07020*, Pest_fici- *Pestalotiopsis fici W106_1*, Coll_gloe- *Colletotrichum gloeosporioides Nara gc5*, Aspe_oryz- *Aspergillus oryzae RIB40*, Neur_cras- *Neurospora crassa OR74A*

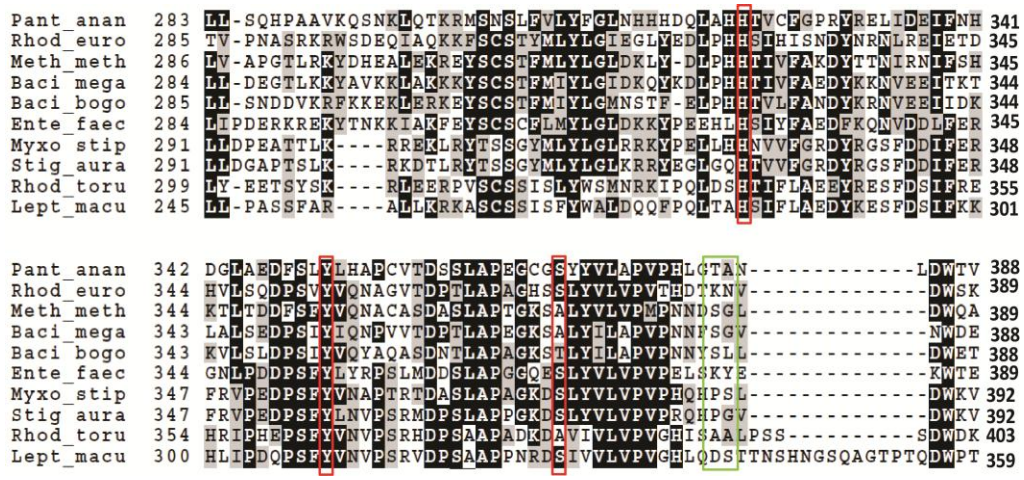

Figure 3.4C Multiple sequence alignment of phytoene dehydrogenase from different bacteria. A393 and A394 residue of *R. toruloides* are highlighted by green bar and are not conserved across species. Active site residues are shown by red bar. Pant_anan- *Pantoea ananatis*, Rhod_euro- *Rhodopirellula europaea*, Meth_meth- *Methylomonas methanica MC09*, Baci_mega- *Bacillus megaterium*, Baci_bogo- *Bacillus bogoriensis*, Ente_faec- *Enterococcus faecium*, Myxo_stip- *Myxococcus stipitatus DSM14675*, Stig_aura- *Stigmatella aurantiaca*, Rhod_toru- *Rhodosporidium toruloides*, Lept_macu- *Leptosphaeria maculans JN3*.

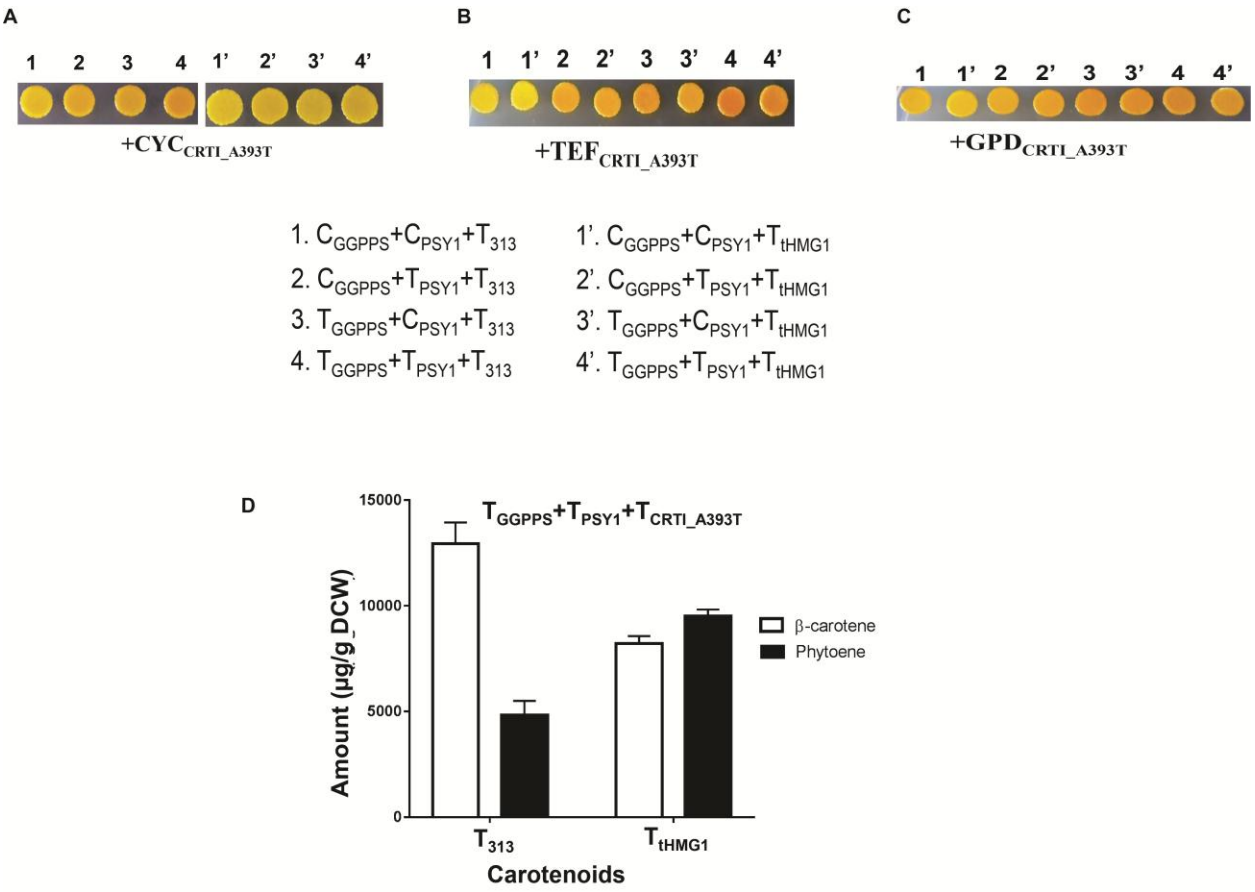

Figure 3.5 Effect of promoter strength of *Rt*CRTI_A393T.
on the pigmentation intensity of strain expressing CRTI_A393T under CYC promoter (A), under TEF promoter (B) and under GPD promoter (C) (dilution spot carries $4X10^4$ cells) (D) Amount of key carotenoids with and without *tHMG1* when the carotenogenic genes (*GGPPS*, *PSY1*, *CRTI*_A393T) were expressed under TEF promoter.

T-TEF promoter, C-CYC promoter, GPD- GPD promoter, GGPPS- GGPP synthase, PSY1- Phytoene synthase, CRTI- Phytoene dehydrogenase, tHMG1- truncated 3-hydroxyl-3-methylglutaryl Coenzyme A reductase

3.2.6 Decreasing the levels of geranyl geranyl diphosphate (GGPP), the metabolic precursor to phytoene yields successful development of a colored based visual screen:

In the previous section I observed that even the catalytically efficient mutant of phytoene dehydrogenase, *Rt*CRTI_A393T was inadequate to handle the accumulation of phytoene pools with increase in metabolic flux in the isoprenoid pathway. Therefore, I considered an alternate strategy i.e. to limit the levels of precursor geranylgeranyl pyrophosphate (GGPP), while simultaneously expressing the *Rt*CRTI_A393T under a strong constitutive promoter (GPD). Limiting GGPP pools could be achieved either by decreasing the expression of the upstream gene, GGPP synthase (*Rt*GGPPS) or replacement by a less efficient GGPP synthase.

As *Rt*GGPPS is an efficient enzyme, I opted to replace *Rt*GGPPS with the less efficient GGPP synthase (*BTS1*) from *S. cerevisiae*, the host. *BTS1* of *S. cerevisiae* encodes GGPP synthase and is reported to be less efficient (Jiang et al., 1995). *BTS1* under the strong constitutive promoter (TEF) did not succeed in increasing the pigmentation with over expression of *tHMG1* (data not shown). Therefore, I attempted to further decrease the phytoene levels by either expressing *BTS1* under a weak promoter CYC or its native promoter. The strain combination expressing *BTS1* under its native promoter along with *Rt*$CRTI_{A393T}$ under the stronger GPD promoter and *Rt*PSY1 under strong TEF promoter, finally led to the desired increase in pigmentation with over expression of *tHMG1* (Figure 3.6A). Further, the chemical analysis of this strain combination along with the overexpression of *tHMG1* showed 31-fold increase in β-carotene and increase in phytoene as compared to strain without overexpression of *tHMG1* (Figure 3.6B). As the levels of β-carotene were significantly higher as compared to phytoene, this was reflected in an increased pigmentation. Therefore, this combination of genes and promoters seemed a suitable visual genetic screen for monitoring the increase in metabolic flux in the isoprenoid pathway.

I also intended to see whether this combination of plasmids will work only in the designed strain background (ABC 276 S288c derivative) or it can also be used in other *S. cerevisiae* strain backgrounds. To examine this, I evaluated the widely used industrially important strain of *S. cerevisiae*, CEN.PK-1C. I observed a similar increase in pigmentation with over expression of *tHMG1* as shown in figure 3.6C, which suggested that the screen combination can be generalized for other *S. cerevisiae* strain backgrounds.

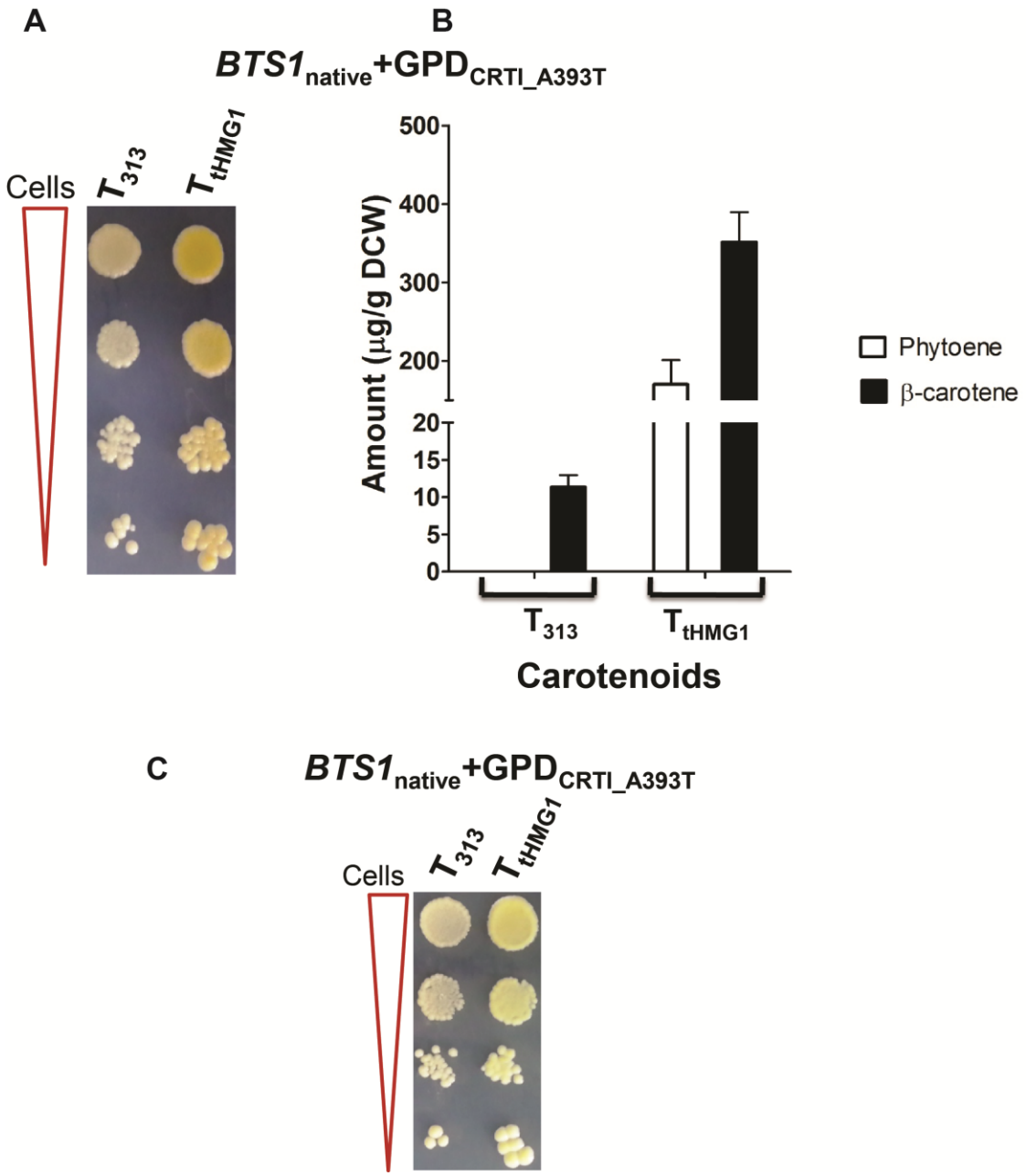

Figure 3.6 Effect of *tHMG1* over expression in the BY4741 strain containing *Rt*CRTI_A393T under GPD promoter and native *BTS1* of *S. cerevisiae* (A) on the pigmentation (B) Amount of key carotenoids (C) on the pigmentation in *CEN. PK-1C* strain containing *Rt*CRTI_A393T under GPD promoter and native *BTS1* (dilution spots carrying, $4X10^4$, $4X10^3$, $4X10^2$, $4X10^1$ cells).

T-TEF promoter, GPD- GPD promoter, BTS1- GGPP synthase, PSY1- Phytoene synthase, CRTI- Phytoene dehydrogenase, tHMG1- truncated 3-hydroxyl-3-methylglutaryl Coenzyme A reductase

3.3 Discussion

In this chapter, I have described the successful development of a carotenoid-based screen that can be used to isolate new genes or mutants that might have an influence in increasing the metabolic flux through the isoprenoid pathway. Although, there are previous reports in the literature (Ozaydin et al., 2013; Verwaal et al., 2007a; Yuan and Ching, 2014) to use carotenoids as a colored visual screen, they were met with limited success, due to lack of correlation between the color of carotenoids and the flux of isoprenoid pathway. In this study, I had addressed this issue by taking various approaches and strategies. First, I selected red yeast (*Rhodosporidium toruloides*) which has been reported to produce more β-carotene and identified, custom synthesized and reconstituted the carotenoid pathway in *S. cerevisiae* with *Rhodosporidium* (*Rt)* genes. I observed higher yields of β-carotene and lower levels of phytoene and lycopene relative to earlier reports (Verwaal et al., 2007a) with these carotenogenic genes, suggesting these enzymes from *R. toruloides* should be preferred in future studies dealing with carotenoids as screens or products in yeasts.

Second, I observed, as had been previously reported, that the rate limiting step of the heterologously expressed carotenoid pathway in *S. cerevisiae* was phytoene dehydrogenase, which led to the accumulation of phytoene. Further, the accumulation of phytoene was preventing the use of the carotenoids as a visual marker for isoprenoid flux. I took a directed evolution strategy to isolate catalytically more efficient mutants of phytoene dehydrogenase (*Rt*CRTI). Several mutants could be isolated. However, the exact mechanism by which the *Rt*CRTI mutants led to increased product conversion was not investigated. Interestingly, the previous efforts to isolate such mutants with *X. dendrorhous* enzyme were not successful (Xie et al., 2015). Although I was able to get catalytically more efficient mutants, the use of these mutants did not completely alleviate the problem of phytoene accumulation.

I therefore employed a third strategy. This was to reduce the accumulation of phytoene by limiting pools of its precursor molecule, geranylgeranyl diphophate (GGPP). This was done by employing a less efficient GGPP synthase, *BTS1* which was native to *S. cerevisiae.* By employing these strategies, I finally succeeded in developing the strain that responded to increased isoprenoid flux with increased pigmentation. This strain also showed a mild growth

defect. As GGPP pools of *S. cerevisiae* are essential for geranylgeranylation of proteins (Jiang et al., 1995), lower pools might be resulting in slow growth.

In conclusion, this study has yielded for the first time a carotenoid based visual screen that showed increase in color with increased isoprenoid flux.

CHAPTER 4:

To isolate mutants for increasing flux in the isoprenoid pathway by using carotenoid based genetic screen

4.1 Introduction

In the previous chapter, I described the development of a carotenoid-based visual assay for isoprenoid flux. In this chapter, I describe our attempts to use this visual assay strain for the isolation of novel mutants with increased isoprenoid pathway flux. Previously strategies for increasing the flux in the isoprenoid pathway in *S. cerevisiae* have focused largely on mevalonate pathway (MVA) or on the pathway feeding cofactors or precursors pools. All of these strategies have been demonstrated to increase the yield of terpenoids in *S. cerevisiae* and has been described in the general introduction.

However in the cell, metabolic pathways are interconnected and tightly regulated (Szappanos et al., 2011), and therefore the possibility exists that besides the mevalonate pathway genes, there might be other genes which may directly or indirectly affect the yield of carotenoids or other terpenoids produced in yeast. Therefore, I was interested in identifying through an unbiased approach, the novel genes/mutants which directly or indirectly affect the isoprenoid pathway flux. In contrast since the screen developed by me was validated with a known flux increaser *tHMG1*, I attempted to isolate new genes/mutants with increased isoprenoid flux using this validated assay. I chose to proceed with two strategies: (a) *SPT15* mutagenesis in which a candidate gene, *SPT15,* known to affect the global gene expression pattern, was chosen for mutagenesis (b) Mutagenesis of yeast and selection of increased isoprenoid pathway flux generating mutants.

4.2 Results

4.2.1 *SPT15* mutagenesis and selection for mutants using the phenotypic pigmentation screen: Identification of *spt15_R98H, spt15_A100T, spt15_A101T*

SPT15 is a global TATA binding protein (TBP) and involved in regulating the expression of many genes and thus involved in multiple pathways and networks (Alper et al., 2006a). It is of 240 amino acids in length. N-terminal (1-60 aa) is variable and C-terminal (61-240 aa) is conserved across all the species. Different *spt15* mutants have been isolated for improving glucose uptake, ethanol tolerance, xylose uptake and utilization. It was reported in the literature that *spt15* mutants cause pleiotropic changes in gene transcription; therefore it is a potential target to reprogramme cell's transcription for improving phenotype, an approach called gTME

(global transcriptional machinery engineering). However, *SPT15* has not been reported to be linked to the isoprenoid pathway in the literature. Therefore, it appeared to be a good target for mutagenesis and selection of mutants with higher pigmentation using the screen.

To carry out *in vitro* mutagenesis, *SPT15* gene was cloned in the yeast centromeric vector under the constitutive promoter (TEF) and random mutagenesis was carried out using hydroxylamine as described in materials and methods (Section 2.11). The *SPT15* mutant library was transformed into the assay strain described in the previous chapter. A total of six colonies were initially selected on the basis of enhanced color as compared to control parent background strain. Plasmids were isolated from these strains, purified, sub-cloned in fresh vector backbone and then amplified through *E. coli* and retransformed into the yeast strain. After retransformation, the transformants were serially diluted on minimal plates to confirm the pigmentation phenotype. Out of six mutants, only three of the mutants from independent mutant stocks were found to display increased pigmentation. The other three colonies failed to show increase in color after sub cloning to fresh vector background suggesting that these colonies may be carrying mutations in regions other than the coding region (vector backbone, promoter sequence). The three mutants which were consistently showing increased pigmentation were sequenced. Sequencing revealed that these mutants were carrying mutations *Arg98His*, *Ala100Val* and *Ala101Thr* respectively (Figure 4.1A). Multiple sequence alignment of *SPT15* from different species as shown in figure 4.1C showed that *spt15* mutant residues were conserved across species and present in the C-terminal stirrup region of *SPT15* (Chasman et al., 1993).

These three mutants were also chemically analyzed to determine β-carotene levels. I observed that while all three mutants showed increased β-carotene levels, the mutant *Ala101Thr* strain showed highest enhancement in amount of β-carotene levels as compared to *SPT15*WT strain and *Arg98His*, *Ala100Val* mutants (Figure 4.1B).

I also wanted to investigate the additive effect of the *spt15* mutants and *tHMG1* on the isoprenoid pathway flux and pigmentation. Therefore, I overexpressed both the *tHMG1* and *spt15* mutants in the developed screen and transformants were dilution spotted and analyzed chemically. However, I could not observe any further increase in pigmentation as seen visually (Figure 4.1D) and also after chemical estimation of the carotenoids (Figure 4.1E).

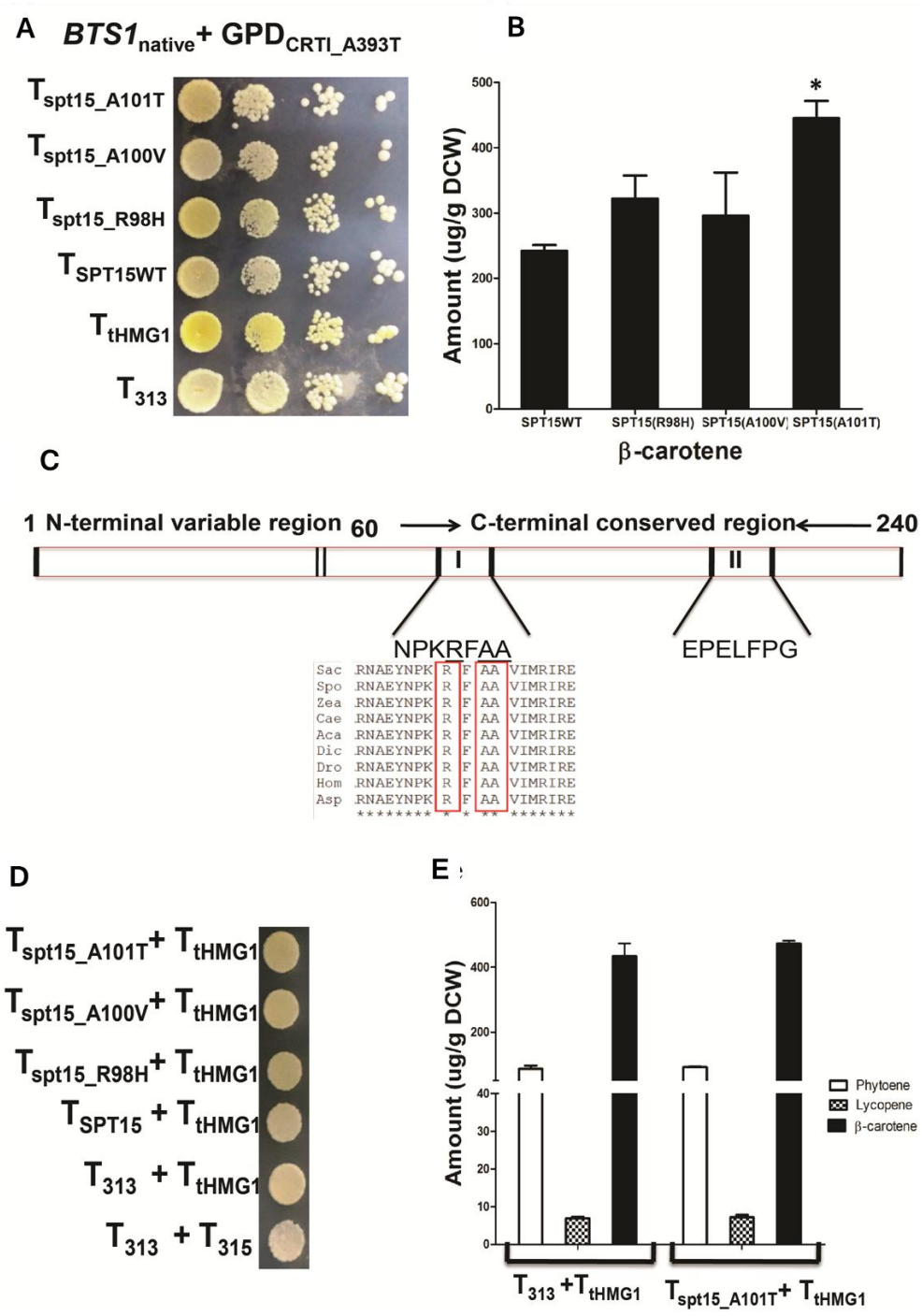

Figure 4.1 Effect of *spt15* mutants
a) on the pigmentation (dilution spot carrying $4X10^4$, $4X10^3$, $4X10^2$, $4X10^1$ cells) b) on the amount of β-carotene c) Structure of *spt15* gene and localization of *spt15* mutants d) effect of *spt15* mutants and *tHMG1* over expression on pigmentation (dilution spot carrying $4X10^4$ cells) e) effect of *spt15* mutants and *tHMG1* overexpression on amount of carotenoids.

4.2.2 The isolated *spt15* mutants increase the overall general isoprenoid pathway flux

After isolating the novel isoprenoid pathway flux increasing mutants, I was keen to investigate whether the isolated *spt15* mutants were increasing the yield of only carotenoids or increasing the overall flux in the isoprenoid pathway in *S. cerevisiae.* Therefore to examine this, I chose heterologous production of an alternative isoprenoid, α-Farnesene that forms from the precursor farnesyl pyrophosphate (FPP) in the isoprenoid pathway of *S. cerevisiae*. I obtained the *Arabidopsis thaliana* α-farnesene synthase gene (ORF no. AT4G16740) from The Arabidopsis information resource (TAIR) database. This was used as a template for PCR cloning. I expressed the α-Farnesene synthase gene of *A. thaliana* under the TEF promoter in *S. cerevisiae* and quantified the production of α-Farnesene as described in materials and methods (Section 2.26).

I observed small amounts of α-Farnesene (0.29 μg/L/OD_{600}) upon overexpression of the α-Farnesene synthase gene of *A. thaliana* but the levels were adequate to test the effects of the *spt15* mutants. Therefore, I over-expressed either *tHMG1* or any of the different *spt15* mutants, along with α-Farnesene synthase gene (*At*FS). Interestingly, I observed that over-expression of *tHMG1* as well as *spt15* mutants individually increased the yield of α-Farnesene upto 1.5 fold.

The maximum increase in α-Farnesene was observed in *spt15_A101T* strain (0.44 μg/L/OD_{600}) (Figure 4.2). Importantly, the increase in the levels of α-Farnesene with *spt15* mutants suggests that they are increasing the overall flux in the isoprenoid pathway and their effects are not exclusive to the carotenoid pathway.

4.2.3 Mutagenesis of *S. cerevisiae* using Ethylmethane sulfate (EMS) for isolating mutant strains with increased isoprenoid pathway flux:

To isolate mutants in the yeast genome, I subjected an assay strain to Ethylmethane sulfate (EMS) mutagenesis. The assay strain that I used for these experiments was a slight variant from what was described in the earlier chapter. This assay strain was developed to produce only one colored carotenoid, Lycopene, so as to avoid the production of mixture of differentially colored carotenoids (Lycopene, γ-carotene, β-carotene, Torulene) (Lourembam, 2015). The assay strain that I had developed in the previous chapter was producing differentially colored carotenoids. The advantage of assay strain with only one colored carotenoid is the linear relationship between

pigmentation and the isoprenoid pathway flux, which was further validated (Lourembam, 2015) by *tHMG1*.

S. cerevisiae strain BY4741 was thus transformed with carotenogenic plasmids phytoene synthase from *A. thaliana* (*At*PS), geranylgeranyl diphosphate synthase (*Rt*GGPPS) and phytoene dehydrogenase (*Rt*CRTI) from *R. toruloides*. Transformants were then mutagenized with EMS as described in materials and methods (Section 2.12). Total six strains were selected on the basis of increased pigmentation. The mutated strains showing increased pigmentation were cured of the carotenogenic plasmids by growing the strains on rich media (YPD) and confirmed by streaking on minimal selection plates. These cured strains were retransformed with carotenogenic plasmids and spotted on minimal plates (Figure 4.3). Only two mutants (M1 and M2) out of six mutants consistently showed the increased pigmentation, suggesting that these two mutants were bearing mutations in the genomic DNA. It is likely that the remaining four strains probably bear mutations in the plasmids, but not in the genome and hence were not pursued. The two mutant strains (M1 and M2) were selected for further analysis. To identify the nature of the mutations in these strains, the strains were diploidized by mating with BY4742 strain of *S. cerevisiae* and selected for growth on minimal media plates with appropriate amino acids. Loss of pigmentation was observed in diploid strains suggesting mutations were recessive.
To identify the precise mutations present in the genome of the mutated strains, whole genome sequencing of the mutated strains (M1 and M2) and comparison with wild type reference strain was carried out from Genotypic Technology Pvt. Limited, Bengaluru. The reference was wild type BY4741 strain as described in materials and methods (Table 2.1). The different SNPs reported in the strains M1 and M2 mutated strains were listed in table 4.1 and table 4.2 respectively. Table 4.1 showed that in M1 mutated strain, there were eight mutations and present in seven different genes. Surprisingly, these genes were not directly from the isoprenoid pathway. In M2 strain, I reported that there were eight different mutations present in six different genes (Table 4.2). These mutations were different from mutations observed in M1 strain background and were also not present in any of isoprenoid pathway genes. However, I have not ascertained whether the phenotype was from a single mutation or because of multiple mutations.

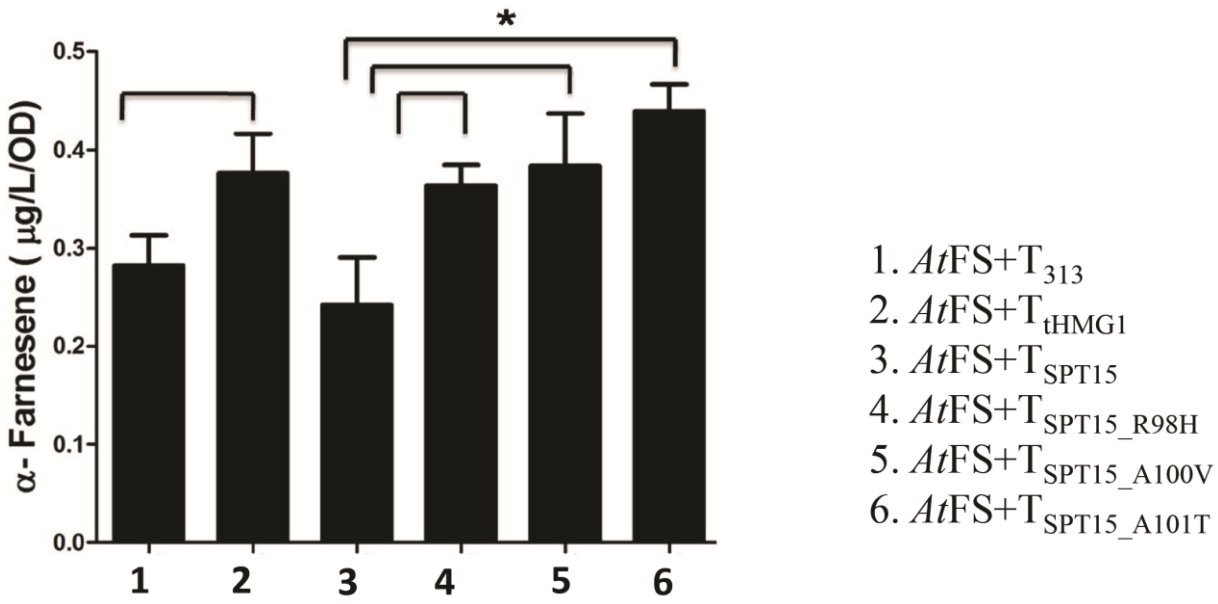

Figure 4.2 Effect of spt15 mutants on the yield of α- Farnesene

*At*FS- Farnesene synthase from *Arabidopsis thaliana*

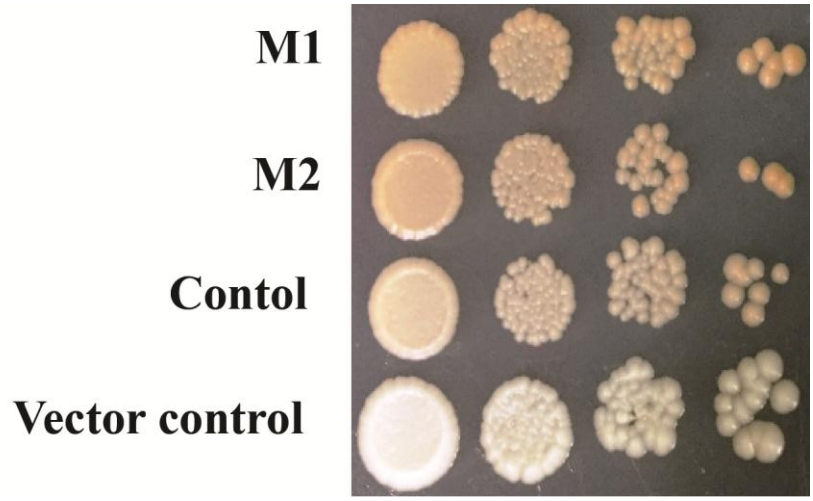

Figure 4.3 Effect of mutations in the mutant strains (M1 and M2) on the pigmentation (Lycopene) (dilution spots carrying $4X10^4$, $4X10^3$, $4X10^2$, $4X10^1$ cells).

Gene ID	Position	SNPs	Gene name	Function
YBL061C	69979	C > T	SKT5	Activator of chitin synthase III
YBL061C	69979	C > G	SKT5	Activator of chitin synthase III
YNR059W	10671	C > T	MNT4	Putative alpha 1,3 mannosyl transferase
YDR285W	40259	A > T	ZIP1	Transverse filament protein of the synaptonemal complex
YNL262W	48607	G > C	POL2	Catalytic subunit of polymerase II
YNL268W	36893	G > T	LYP1	Lysine permease
YPR071W	127498	T > G	YPR071W	Putative membrane protein
YLR310C	63821	G > A	CDC25	Membrane bound Guanine exchange factor/cell division cycle

Table 4.1 List of mutations observed in genome of EMS mutagenized M1 strain through whole genome sequencing (WGS)

Gene ID	Position	SNPs	Gene name	Function
YML099C	12134	G > A	ARG81	Zinc finger transcription factor involved in regulation of arginine responsive genes
YIL135C	73451	G > A	VHS2	Regulator of septin dynamics
YAL028W	66495	C > T	FRT2	ER membrane protein of unknown function
YAL053W	20824	C > T	FLC2	Putative Calcium channel in ER, required for uptake of FAD into ER
YDL231C	5482	G > A	BRE4	Zinc finger protein
YDL231C	5482	G > T	BRE4	Zinc finger protein
YER123W	26672	C > T	YCK3	Vacuolar yeast casein kinase I isoform
YER123W	26672	C > G	YCK3	Vacuolar yeast casein kinase I isoform

Table 4.2 List of mutations observed in EMS mutagenized M2 strain through whole genome sequencing (WGS)

4.3 Discussion

In this chapter, I have explored the carotenoid screen developed in chapter 3, to isolate novel mutants affecting the isoprenoid flux. I initially targeted *SPT15* and identified the three novel mutants of the global TATA binding protein, SPT15, *spt15* (*R98H*, *A100V* and *A101T*). These mutants were also shown to increase the amount of not only carotenoids but also another sesquiterpenoid, α-Farnesene, demonstrating that these mutants affect the overall isoprenoid pathway flux. These results suggest that the visual carotenoid assay that I have developed is indeed a valid screen that can be further expanded and explored for identifying new mutants or genes and also for optimizing the existing genes.

Multiple sequence alignment and localization of these mutants suggested that these mutants were conserved across all the species and present in the stirrup region I (95-101aa) between S2 and S3 β-sheets (Bleichenbacher et al., 2003). The stirrup region I of *SPT15* docks with the TFIIA β-barrel. This region was important for interactions with TFIIA and in the pre-initiation complex (PIC) assembly at the promoter, and transcription by RNA polymerase II. As these residues were not present in the active site but were very close to the active site residues suggesting that the mutation at these sites is likely to change the confirmation of that region which may alter the docking of TBP with TFIIA, alter its association with other factors, and thereby affect the transcription of several genes. The role of *SPT15* and its ability to affect the transcription of several genes is the subject of investigation of the next chapter.

I also isolated two EMS mutagenized *S. cerevisiae* strains that showed increased pigmentation and the isoprenoid pathway flux. Following studies that included curing the strains of the plasmids and then retransformation suggested that I have in fact identified mutations that were carrying the desired phenotype. The fact that mutations were recessive is surprising as I would now have to further investigate and determine which of the mutation(s) might be causing the phenotype. As sequencing revealed that the mutations were from genes unrelated to mevalonate/isoprenoid pathway, thus again indicates the usefulness of the screen in pulling out novel mutations. The whole genome sequencing data of these mutated strains provided a list of mutations present in the different genes that could affect the isoprenoid pathway flux, but the detailed investigation about the role of individual mutation in the genes in these two (M1 and M2) mutated strains needs to be investigated.

CHAPTER 5:

To investigate the mechanism of increased isopreoid flux in the spt15_A101T mutant that was isolated in the screen

5.1 Introduction

In the previous chapter, I employed a "global transcription machinery engineering (gTME) approach" (Alper et al., 2006a) to isolate novel mutants of a TATA-binding protein (TBP), *SPT15* with increased carotenoid levels using the visual carotenoid screen. These *spt15* mutants *spt15_R98H, spt15_A100V, spt15_A101T* were also shown to increase the overall isoprenoid pathway flux in *S. cerevisiae.* These mutants were different from the previously *spt15* mutants that had been isolated for ethanol tolerance and oxidative stress tolerance (Alper et al., 2006a; Yang et al., 2011). Although it is known that *spt15* mutants cause pleiotropic changes in gene transcription, the mechanism by which these mutants improve these different phenotypes is unclear.

In this chapter, I describe our attempts to understand how one of these mutants, *spt15_A101T* increased the flux in the isoprenoid pathway. To understand the mechanism, I employed a combination of metabolic flux analysis and transcriptomics while validating the observations by phenotypic evaluation.

Metabolic flux analysis (MFA) is an analytical technique to quantify the metabolic fluxes as a consequence of catalytical and transcriptional interactions. Metabolic fluxes help to understand the cellular physiology under particular conditions. One can also predict the metabolic capabilities after genetic and environment perturbations. MFA is based on the stoichiometry of metabolic reactions and mass balances around intracellular metabolites under pseudo-steady state assumptions. There are two methods to study the metabolic fluxes, ^{13}C based flux analysis and constraints based flux analysis. In this chapter, I employed constraint based flux analysis approach to understand the mechanism of increased isoprenoid flux in *spt15_A101T* mutant strain. The details of using this approach are given in materials and methods (Section 2.28).

5.2 Results:

5.2.1 The *spt15_A101T* mutant bearing cells display a decreased growth rate in comparison to the *SPT15* WT strain in minimal medium

The *spt15_A101T* mutant was previously shown to result in an approximately 2.25-fold increase in isoprenoid pathway flux in *S. cerevisiae.* I carried out initial growth experiments with *S.*

cerevisiae strains bearing either *SPT15* WT (control) or the *spt15_A101T* (mutant) plasmid. The growth kinetics of these strains is shown in figure 5.1. Interestingly, I observed that the *spt15_A101T* mutant had a slower growth (growth rate 0.19 hr^{-1}) as compared to wild type *SPT15* (growth rate 0.24 hr^{-1}). It was surprising that *spt15_A101T* mutant strain despite being slow growing was increasing the flux in the isoprenoid pathway.

5.2.2 Metabolic flux balance analysis of *SPT15* WT and *spt15_A101T* strains with whole genome scale metabolic model reveals carbon rerouting in *spt15_A101T* strain for increasing the isoprenoid flux:

The flux balance distribution in the central carbon metabolism of *SPT15*WT and *spt15_A101T* strains were determined as described in materials and methods section 2.28 using the constraints given in table 5.1A and shown in figure 5.2. The phenotypic state characterized by the fluxes in the metabolic network was used to postulate mechanisms for increased isoprenoid pathway flux in *spt15_A101T* strain. The metabolic and transport reactions which were up regulated and down regulated in *spt15_A101T* strain might be responsible for the increased isoprenoid flux are given in table 5.2. Since the isoprenoid pathway is connected to the central carbon metabolism via acetyl CoA (precursor), ATP (energy) and NADPH (reducing power) (Vickers et al., 2017), I focused on the effects on the fluxes affecting these metabolites.

Carbon rerouting: The mutant strain demonstrated a 50% lower flux through Pentose phosphate pathway (PPP) which correlated with the observed lower growth rate (Figure 5.1). Most of the pyruvate formed via glycolysis was channeled towards acetaldehyde (via pyruvate decarboxylase, *PDC*) in the cytosol (~89%) and about 7% was transported to mitochondria in *SPT15*WT strain (Figure 5.2A), while these percentages were 94% and 2% in the *spt15_A101T* mutant strain (Figure 5.2B). The excess carbon flux from pyruvate towards acetaldehyde (via *PDC*) in the mutant increased the flux through acetoin and acetate in the cytosol, resulting in 11% lower ethanol formation. It should be noted that in the *SPT15*WT strain, the flux from acetaldehyde was only towards acetoin (Figure 5.2A)

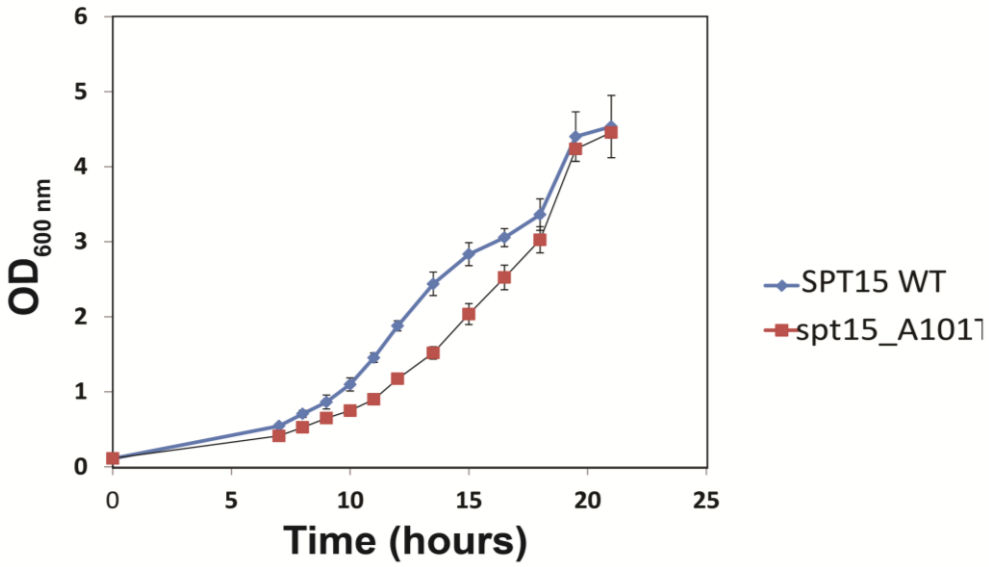

Figure 5.1 Growth curve kinetics of *S. cerevisiae* BY4741 strain carrying either *SPT15*WT or *spt15_A101T* plasmid.

Specific rate in exponential phase	*SPT15*WT	*spt15_A101T*	*spt15_A101T* (at 21 mM Phosphate)
Glucose consumption rate (mmol/gDCW/h)	8.35±0.17	6.65±0.05	7.18±0.07
Ethanol production rate (mmol/gDCW/h)	9.20±0.16	6.52±0.04	7.75±0.03
Glycerol production rate (mmol/gDCW/h)	0.106±0.00	0.08±0.00	0.08±0.00
Acetate production rate (mmol/gDCW/h)	0.00±0.00	0.00±0.00	0.00±0.00

Table 5.1A Parameters for simulations of flux balance distribution

Gene/ID	Flux in *SPT15*WT	Transcriptomic fold change	*spt15_A101T* (Upper Bound)	*spt15_A101T* (Lower Bound)
GLUDC	0	2.15	0.0215	0.0215
PYRDC	12.95	2.1	27.2	15
G3PT	0.106	1.8	0.191	0.191
MCITDm	0.068	0.56	0.068	0.038
IGPDH	0.015	0.42	0.015	0.0063

Table 5.1B Transcriptomic constraints for flux balance distribution of *spt15_A101T*

GLUDC- Glutamate dehydrogenase, PYRDC- pyruvate decarboxylase, G3PT- glycerol-3-phosphatase, MCITDm- methyl citrate dehydratase, IGPDH- imidazole glycerol-3-phosphatase

Gene/ID	Lower bound flux
Actm	4.68
G6PDH2er	0.025
G6Pter	0.025

Table 5.1C Transport/Diffusion constraints

Actm- acetate transport, G6PDH2er- Glucose-6-phosphate dehydrogenase in endoplasmic reticulum, G6Pter- transport of Glucose-6-phosphate to endoplasmic reticulum by diffusion

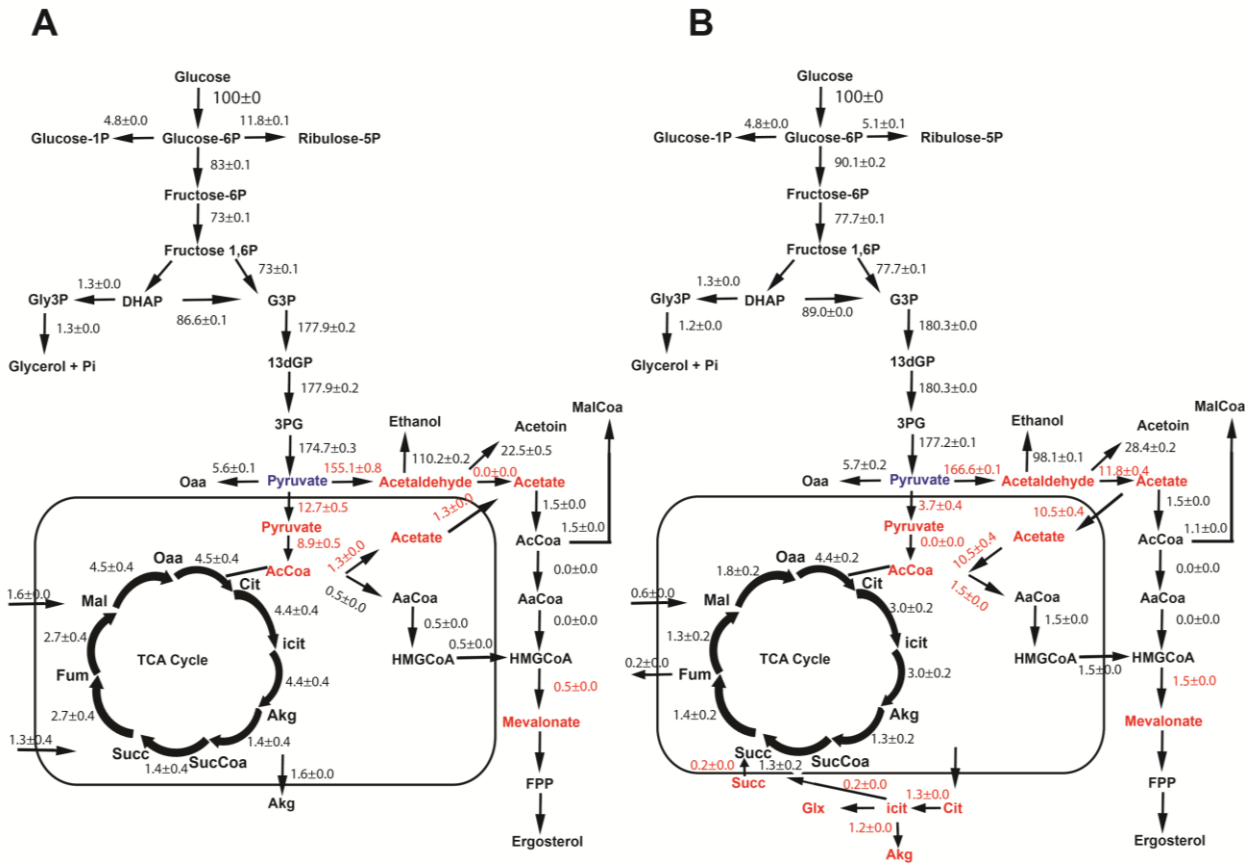

Figure 5.2 Flux distribution in central metabolism of *SPT15*WT and *spt15_A101T* strain without transcriptomic changes. Fluxes are simulated with iMM904 model using experimentally determined constraints for *S. cerevisiae* strain carrying (A) *SPT15*WT plasmid (Control strain) (B) *spt15_A101T* plasmid (mutant strain). The differences in flux distribution between *SPT15*WT and *spt15_A101T* strain are shown in red color.

The excess acetate in the mutant was shunted across the mitochondria towards acetyl-CoA and 3 fold increase of flux towards isoprenoid pathway through HMG-CoA (Figure 5.2B). However, in the *SPT15*WT strain, acetate was formed mainly through pyruvate to acetyl-CoA (via pyruvate dehydrogenase complex (PDHC)) and was channeled towards TCA cycle, thereby reducing the flux in the isoprenoid pathway HMG-CoA.

ATP and Phosphate: The flux balance analysis indicated an increase in mitochondrial ATP (~29%) in the mutant strain (Table 5.3). Increase in the demand of mitochondrial ATP was due to the flux in the reactions catalyzed by acetyl-CoA synthetase and adenylate kinase. Owing to increase in the demand for ATP synthesis by mitochondrial ATP synthase, the cytosolic inorganic phosphate levels were increased as observed in the high flux of inorganic di-phosphatases (Table 5.2). In addition, the transport of phosphate from the cytosol to the mitochondria increased due to increase in flux in the reaction of mitochondrial phosphate transporter by 3% (Table 5.4). This suggested that in spt15_A101T strain, I can postulate that phosphate was imported from cytosol to the mitochondria to increase ATP production.

NADH and NADPH: The total NADPH production in the mutant strain was similar to the wild type strain (Table 5.5). However in the mutant strain, cytosolic NADPH was produced not only through PPP pathway, but also from the cytosolic $NADP^+$ dependent acetaldehyde dehydrogenase and isocitrate dehydrogenase. This is in contrast to the wild type strain, where NADPH was produced majorly through the PPP pathway while cytosolic $NADP^+$ dependent acetaldehyde dehydrogenase and isocitrate dehydrogenase were not contributing for cytosolic NADPH pools (Table 5.5). In case of NADH, the mutant mitochondrial NADH production decreased by 6% due to the absence of flux at the pyruvate dehydrogenase complex (Table 5.6).

Sr. no.	ID	Name	Fold change in flux	Comments
1	PPA	Inorganic diphosphatase (cytoplasm)	>50 fold	No flux in WT strain
2	ALDD2y	Aldehyde dehydrogenase acetaldehyde__NADP	>50 fold	No flux in WT strain

3	ACSm	Acetyl CoA Synthetase (mitochondrial)	>50 fold	No flux in WT strain
4	ADK1m	Adenylate kinase mitochondrial	>50 fold	No flux in WT strain
5	ICDHy	Isocitrate dehydrogenase_ NADP	11.6	No flux in WT strain
6	CITtbm	Citrate transport mitochondrial	7.5	No flux in WT strain
7.	SUCFUMtm	Succinate Fumarate transport mitochondrial	1.5	No flux in WT strain
8.	Actm	Acetate transporter mitochondrial	7.1	
9.	SQLS	Squalene Synthase	3.1	
10.	G6PDH2er	Glucose 6 phosphate dehydrogenase (ER)	3.1	
11.	G6Pter	Glucose 6 phosphate transport (ER)	3.1	
12.	PIt2m	Phosphate transporter mitochondrial	1.2	
13.	NADH2_u6cm	NADH dehydrogenase cytosolic mitochondrial	1.2	
14.	ATPS3m	ATP synthase mitochondrial	1.1	
15.	PYRDC	Pyruvate decarboxylase	1.1	
16.	PYRt2m	Pyruvate transport mitochondrial	0.71	
17.	FUMm	Fumarase mitochondrial	0.5	
18.	PPAm	Inorganic diphosphatase	0.1	
19.	CSm	Citrate synthase	0.1	
20.	AKGMALm	R_alpha_ketoglutarate Citrate_transporter	0	No flux in mutant
21.	ICDHxm	R_Isocitrate_dehydrogenase__NAD_	0	No flux in mutant
22.	PDHm	R_pyruvate_dehydrogenase	0	No flux in mutant

Table 5.2 List of up regulated and down regulated reactions in *spt15_A101T* (without transcriptomic changes) in comparison to *SPT15*WT

ATP production	*SPT15*WT	*spt15_A101T* Without transcriptomic constraints	*spt15_A101T* With transcriptomic constraints	*spt15_A101T* With transcriptomic constraints (at 21 mM Phosphate)
Cytosol	84%	87%	51.3%	51%
Mitochondria	16%	13%	48.7%	49%
Total ATP production (units)	421.3	433.2	794	703
Mitochondrial ATP consumption				
Cytosol	99.3%	71%	63.6%	50%
Mitochondria	0.3%	29.2%	36.4%	50%
Flux in Mitochondrial ATP producing reactions (units)				
ATP synthase	65.5	74	386.5	344
Succinate CoA ligase	1.43	1.28	-	-
Flux in Mitochondrial ATP consuming reactions (units)				
ADP-ATP transporter	66.47	53.23	246.6	174.1
Acetyl CoA synthetase	-	10.52	70.4	85.1
Adenylate kinase	-	10.52	70.4	85.1
Acetylglutmate kinase	0.46	0.93	0.5	0.5

Table 5.3 ATP production and consumption normalized to 100 units of glucose

Phosphate production	***SPT15*WT**	***spt15_A101T* Without transcriptomic constraints**	***spt15_A101T* With transcriptomic constraints**	***spt15_A101T* With transcriptomic constraints (at 21 mM Phosphate)**
Cytosol	90%	91%	39%	51%
Mitochondria	9.6%	9%	61%	49%
Total Pi production (units)	245.5	255.7	584.3	553.5
Consumption of cytosolic phosphate				
Cytoplasm	80.4%	77.5%	86.3%	63.8%
Transport to mitochondria by transporter	19.6%	22.5%	13.8%	36.2%
Consumption of phosphate in mitochondria				
ATP synthase	96%	98%	100%	92.4%
Succinyl CoA ligase	2%	2%	-	-
Succinate transporter	2%	-	-	7.7%

Table 5.4 Phosphate production and consumption normalized to 100 units of glucose

NADPH production	*SPT15*WT	*spt15_A101T* Without transcriptomic constraints	*spt15_A101T* With transcriptomic constraints	*spt15_A101T* With transcriptomic constraints (at 21 mM Phosphate)
Cytosol	90.3%	88.8%	94.4%	82.4%
Mitochondria	9.7%	11.2%	5.6%	17.6%
Total NADPH production (units)	27.1	27	46.6	16.4
Cytosolic NADPH production				
Acetaldehyde dehydrogenase	-	49.4%	91%	89.1
Isocitrate dehydrogenase	-	41.4%	7.3%	-
PPP pathway	87.6%	4.84%	1.7%	2.63%
Cytosolic NADPH consumption				
Glutamate dehydrogenase	58.8%	58.9%	40.6%	-
HMG CoA reductase	4%	12.6%	10.1%	31.8%
Asparatate semialdehyde dehydrogenase	5.2%	5.2%	15.2%	10.1%

Table 5.5 NADPH production and consumption normalized to 100 units of glucose

PPP- Pentose phosphate pathway

NADH production	*SPT15*WT	*spt15_A101T* Without transcriptomic constraints	*spt15_A101T* With transcriptomic constraints	*spt15_A101T* With transcriptomic constraints (at 21 mM Phosphate)
Cytosol	91.3%	97.9%	68.2%	72.4%
Mitochondria	8.7%	2.1%	31.8%	27.6%
Total NADH production (units)	199.9	188.7	404.8	374.9
Cytosolic NADH consumption				
Ethanol production	60.5%	53.1%	35.4%	39.7%
Acetoin production	12.4%	15.3%	0%	0%
Mitochondrial NADH production				
Pyruvate dehydrogenase	51.3%	0%	0%	0%
Malate dehydrogenase	25.9%	46%	92.2%	59%
Isocitrate dehydrogenase	9.9%	0%	0%	0.6%

Table 5.6 NADH production and consumption normalized to 100 units of glucose

5.2.3 Role of Phosphate and NADPH on the isoprenoid flux

The flux balance made it clear that in the mutant cell the demand for inorganic phosphate had increased and cytosolic NADPH was also being produced from new routes (through acetaldehyde dehydrogenase and isocitrate dehydrogenase), therefore suggesting an important role of phosphate and NADPH on the isoprenoid pathway flux.

To investigate the effect of phosphate on growth, *SPT15*WT and *spt15_A101T* strains were grown in minimal media containing varying concentration of phosphate as described in materials and methods (Section 2.7) and growth kinetics were shown in figure 5.3A. Both the strains had an increased growth rate with increasing phosphate concentration and saturating beyond phosphate concentration of 20 mM (Figure 5.3B). However, the mutant strain showed a higher percentage change in growth by ~25% while the wild type showed a meagre 5% increase. A greater increase in the growth rate of mutant strain as compared to wild type strain suggests that the initial slow growth rate of mutant was due to limitation of phosphate and thus addition of 21mM of KH_2PO_4 in the media allowed the growth rate to become similar to that of the wild type strain.

I was also interested to know the effects of increasing NADPH pools on the isoprenoid flux in the cell. To investigate this, I exploited our carotenoid based genetic assay strain (described in chapter 3) for evaluating the isoprenoid flux. In the assay strain, I separately over expressed two NADPH producing enzymes. To increase the cytosolic NADPH, *ZWF1* (glucose-6-phosphate dehydrogenase) was overexpressed and for increasing the mitochondrial NADPH pools, *POS5* (NAD Kinase) was overexpressed. The pigmentation intensity of the colony was used as a visual readout for the flux in the pathway. When these enzymes were individually overexpressed in the carotenoid producing assay strain, I observed that both *ZWF1* and *POS5* could individually lead to an increased carotenoid production (Figure 5.3C). A similar result was also obtained with *PHO13* gene deletion. PHO13 encodes a conserved phosphatase and a *pho13*Δ was known to increase the PPP pathway activity with a consequent increase in NADPH levels in the cells (Kim et al., 2015).The difference in pigmentation of strains with increased NADPH pools was more apparent under low phosphate conditions (Figure 5.3C).

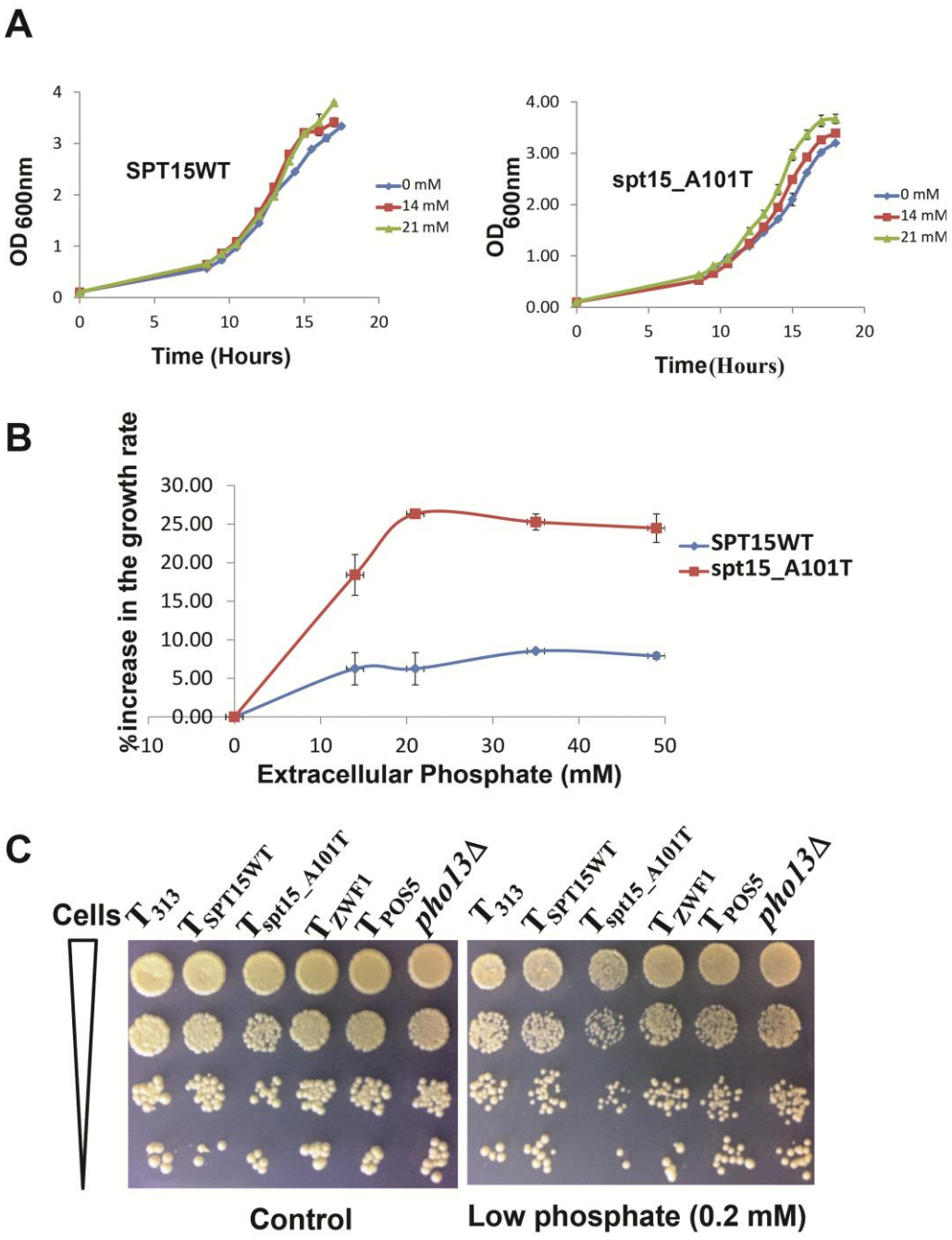

Figure 5.3 Effect of extracellular phosphate and NADPH on the growth rate and isoprenoid pathway flux in *SPT15*WT and *spt15_A101T* strain of *S. cerevisiae*.
Effect of different concentration of extracellular KH_2PO_4 (A) on the growth kinetics (B) percentage increase in the growth rate (C) Effect of over expression of NADPH producing reactions on isoprenoid pathway flux (dilution spot carrying $4X10^4$, $4X10^3$, $4X10^2$, $4X10^1$ cells).

5.2.4 Transcriptome profile analysis of *spt15_A101T* indicates up-regulation of phosphate signaling and response (PHO) pathway and pyruvate decarboxylase

In order to validate the flux balance analysis of *SPT15*WT and *spt15_A101T* strains, I carried out transcriptomic analysis of these strains as described in materials and methods section 2.20. The genes with p-value < 0.05 and fold change equal to or greater than 2, in comparison to wild type strain were clustered and their differential expression pattern was shown in figure 5.4A. The data reflected the global change in the transcription in a cell by *spt15_A101T* mutant. I observed a differential expression of 30 genes, out of which 25 genes were up-regulated while 5 genes were down-regulated in *spt15_A101T* strain, as compared to the wild type *SPT15* strain. Two other metabolic enzymes that could have influence in the pathway, *HOR2* (glycerol-3-phosphatase) and *PDH1* (2-methyl citrate dehydratase) which showed p-value <0.05 and fold change 1.86 and 0.56 were also included in the analysis (Figure 5.4A).

The up-regulated and down-regulated genes were from diverse/ various pathways. Interestingly, out of the 25 up-regulated genes, 11 genes were from phosphate regulation pathway (PHO) pathway (Figure 5.4B). All the PHO pathway genes showed greater than 3-fold up-regulation. The up-regulation of PHO pathway genes in the microarray of *spt15_A101T* strain was also validated by qPCR of three genes, *PHO5*, *PHO84*, *PHO89* (Figure 5.4C). Besides the PHO pathway genes, there was also an up-regulation of glycerol phosphatase (*HOR2*), which hydrolyzes the phosphate ester bond of glycerol phosphate, found in many sugar and lipid metabolites. Further, the analysis determined an up-regulation of pyruvate decarboxylase (*PDC6*) which was also indicated in the flux balance distribution in the *spt15_A101T* strain (Figure 5.2B). Thus, the up-regulation of *PDC6* and phosphate pathway genes in the transcriptomic data correlated well with the metabolic flux balance distribution data. Two metabolic genes (methyl citrate dehydratase (*PDH1*) and imidazole glycerol phosphate dehydratase (*HIS3*)) were also observed to be downregulated. Surprisingly, there were no other metabolic genes up regulated transcriptomically. Therefore, I concluded that the up regulation of acetyl CoA synthetase, $NADP^+$ dependent acetaldehyde dehydrogenase and cytoplasmic $NADP^+$ isocitrate dehydrogenase were being controlled metabolically rather than transcriptomically.

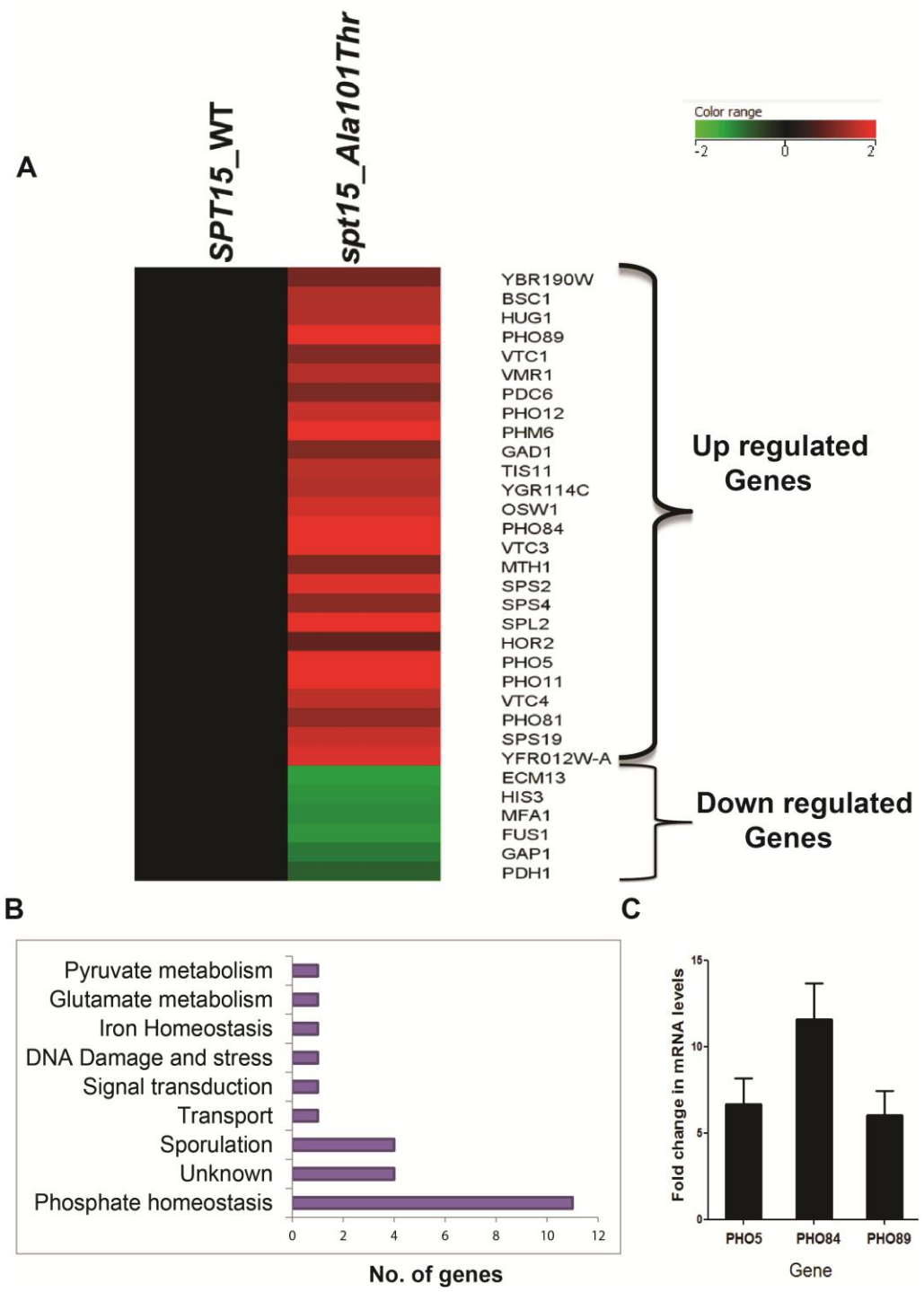

Figure 5.4 Microarray data analysis of *SPT15*WT and *spt15_A101T* strains of *S. cerevisiae* (A) Heat map showing differentially expressed genes in *spt15_A101T* strain (B) Bar chart showing number of genes up regulated in different pathways (C) Validation of top up regulated transcripts, *PHO5*, *PHO84* and *PHO89* of microarray by qPCR. For qPCR, three independent experiments with biological duplicates were performed and data is shown from one independent experiment.

5.2.5 Transcriptomic constraints and other transport/diffusion constraints for simulating the flux balance distribution of *spt15_A101T*

To examine more rigorously the consequence of transcriptomic changes (from microarray data) on flux balance distribution of *spt15_A101T* strain, transcriptomic constraints for three up regulated genes (glutamate decarboxylase (*GAD1*), pyruvate decarboxylase (*PDC6*) and glycerol-3-phosphatase (*HOR2*)) and two down-regulated genes (methyl citrate dehydratase (*PDH1*) and imidazole glycerol phosphate dehydratase (*HIS3*)) from microarray data were calculated based on the simulated flux values from flux balance distribution of *SPT15*WT strain as shown in table 5.1B. These constraints were then applied to simulate the flux balance distribution of *spt15_A101T*. In addition to these transcriptomic constraints, additional transport/ diffusion constraints from flux balance distribution of *spt15_A101T* mutant (having theoretical maximum mevalonate flux) were introduced at given conditions of growth rate and accumulation rates to simulate flux balance distribution. These constraints were mainly on transport of molecules by diffusion which was not possible to detect in the microarray data. These were transport of acetate (Actm), transport of glucose-6-phosphate in endoplasmic reticulum by diffusion (G6Pter) and glucose-6-phosphate dehydrogenase (endoplasmic reticulum) (G6PDH2er) and shown in table 5.1C. These transport/diffusion constraints along with transcriptomic constraints were applied for simulating flux balance distribution of *spt15_A101T* strain.

5.2.6 Flux Balance distribution of *spt15_A101T* strain along with transcriptional and transport/diffusion constraints reveals truncation of the TCA cycle and an increased demand of phosphate in the mitochondria

By applying the constraints mentioned in the previous section 5.2.5, flux through reaction catalyzed by pyruvate decarboxylase (*PDC*) had increased, thereby increasing the flux towards acetaldehyde. The mitochondrial acetate was now mainly forced through transfer of cytosolic acetate synthesized from acetaldehyde in cytoplasm. Thus, the acetate in the mitochondria was channeled to Acetyl-CoA (62/70) and HMG-CoA (2.5/70) pathway thereby increasing the flux through isoprenoid pathway (Figure 5.5). Under these phenotypic conditions, the flux balance predicts a truncated TCA cycle in the mitochondria wherein, the citrate was shunted out to the cytoplasm and reconnects at succinate via the glyoxylate shunt.

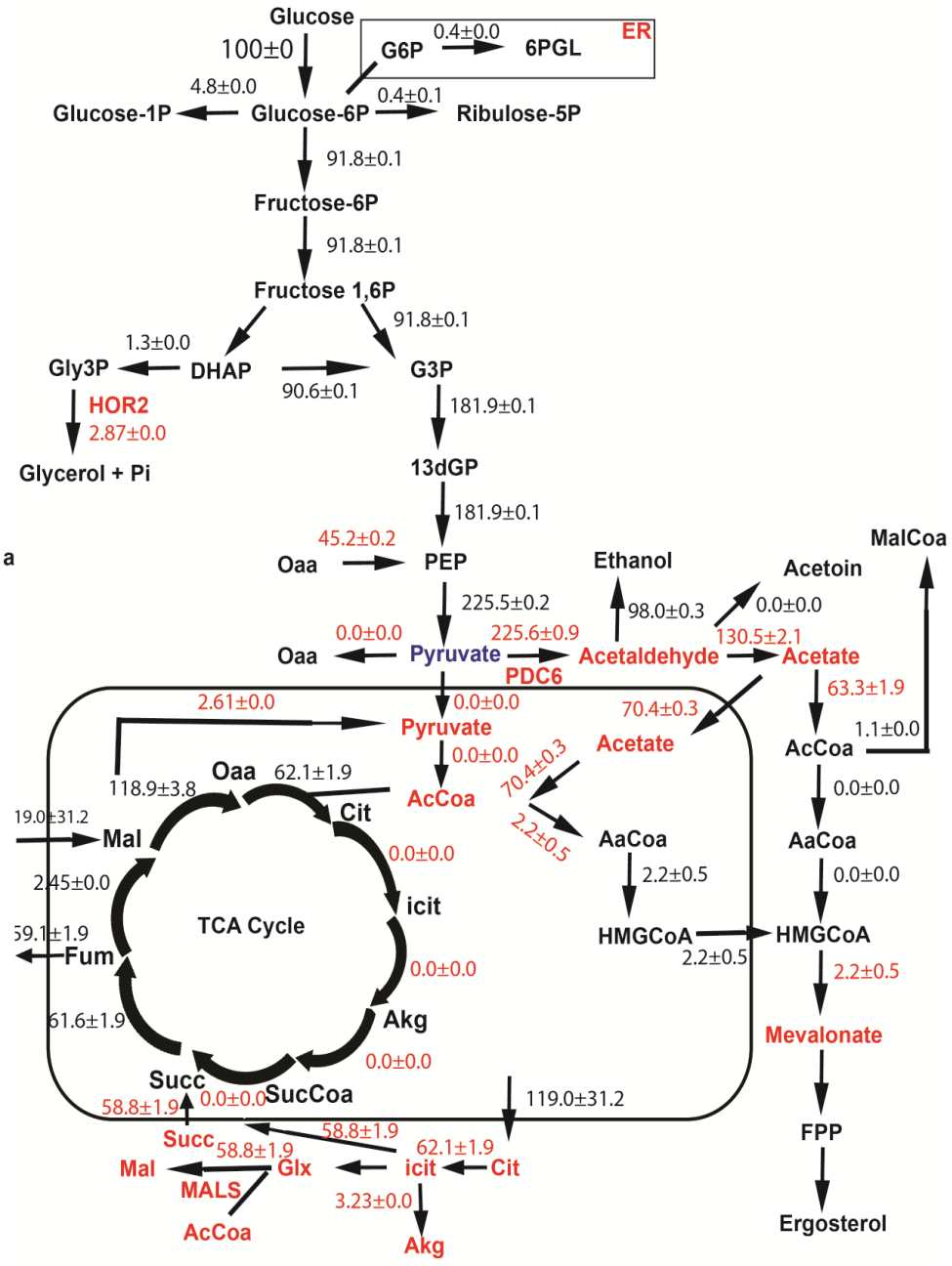

Figure 5.5 Effect of transcriptomic constraints on the flux distribution in central metabolism of spt15_A101T strain. The flux reactions which are affected majorly were shown in red color. Reactions: *PDC6* – pyruvate decarboxylase 6, *HOR2* – glycerol-3-phosphate phosphatase, *MALS*- malate synthase

ATP and Phosphate: The net demand for ATP increased by about two fold thereby limiting phosphate in the cell (Table 5.3). Surprisingly, the transport of phosphate from the cytosol to the mitochondria decreased by 8.8% as shown in table 5.4.This increased demand for mitochondrial phosphate was met from diphosphates through mitochondrial diphosphatases. One can speculate that the mitochondrial production of diphosphates was insufficient to meet the demand of phosphate, and hence the need to import phosphate from cytosol or from extracellular environment. Due to this high demand of phosphate, the mutant strain causes activation of the PHO regulon so as to increase uptake of phosphate from the environment and also the release of phosphate from stored polyphosphates in the vacuole.

NADH and NADPH: The increase in two fold cytosolic NADH pools in mutant strain was due to activation of NAD^+ dependent acetaldehyde dehydrogenase (Table 5.6). Also, mitochondrial NADH pools were increased due to enhanced flux in mitochondrial malate dehydrogenase. The cytosolic NADPH was also increased by 1.8 fold due to the increased flux through HMG-CoA reductase. Interestingly, the enhanced NADPH pools were not only consumed by HMG-CoA reductase due to increased mevalonate flux but also by aspartate semialdehyde dehydrogenase, which utilizes NADPH and produces phosphate in the cytosol (Table 5.5). This flux analysis clearly indicates that the cell was utilizing its best efforts to increase production of phosphate by various ways so as to meet high phosphate demand.

5.2.7 Flux balance distribution of *spt15_A101T* under increased extracellular phosphate pushes the flux to biomass rather than the isoprenoid pathway

To investigate the effect of increased growth rate of the *spt15_A101T* mutant strain observed at 21mM concentration of extracellular phosphate on the flux balance distribution, the *spt15_A101T* mutant strain was grown in minimal media containing 21mM of KH_2PO_4 and the accumulation rates of four extracellular metabolites glucose, glycerol, ethanol and acetate were estimated during the exponential phase of growth curve (Table 5.1A). These accumulation rates were used to predict fluxes along with transcriptomic and transport/diffusion constraints given in table 5.1B and 5.1C.

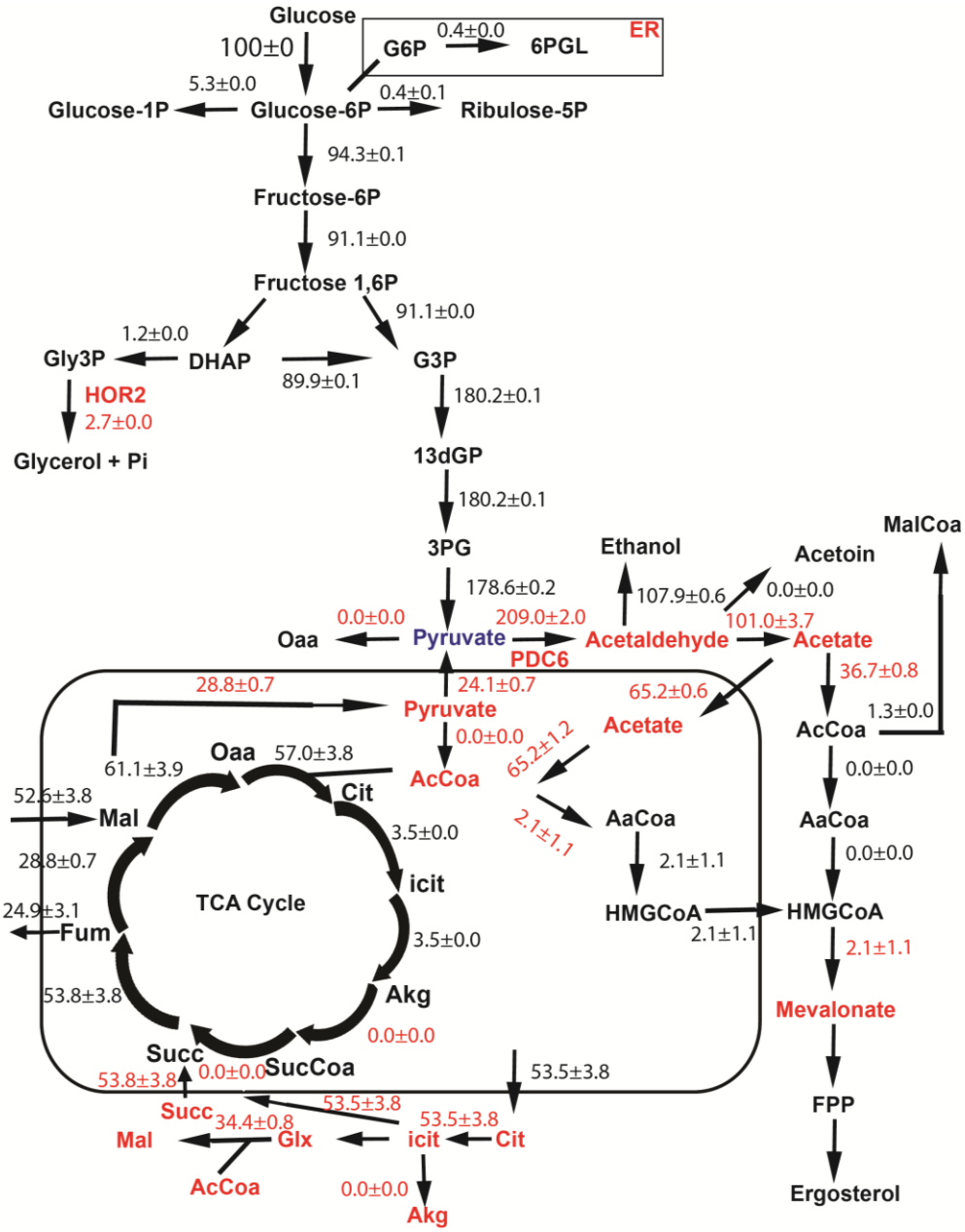

Figure 5.6 Effect of extracellular phosphate (21 mM KH_2PO_4) on the flux distribution in central metabolism of *spt15_A101T* strain with transcriptomic constraints.

From the flux distribution as shown in figure 5.6, it was observed that even with the increased phosphate levels, the TCA cycle was truncated with glyoxylate shunt operational in the cytoplasm. However, the increased phosphate levels allowed about 3.5% increase in flux towards α-ketoglutarate (α-KG) to increase acetyl-CoA pools in the mitochondria. This was accompanied by a 1.4-fold increase in the ethanol formation. The excess pyruvate in mitochondria was transferred to the cytoplasm with a decreased formation of pyruvate through glycolysis (note that the OAA to PEP via phosphoenolpyruvate carboxylase, *ppc* is not operational in high phosphate case). The lowered flux from acetate to acetyl-CoA decreased the requirement of ATP towards acetyl-CoA pool in the mitochondria. This may be correlated to increased growth rate.

The flux balance analysis also revealed that the total ATP production was decreased by 11% (Table 5.3). Due to less ATP production, the demand for phosphate was also reduced. Therefore, the total inorganic phosphate production was decreased by 5.3% (Table 5.4). However, the transport of phosphate from the cytosol to the mitochondria increased by 22% and there was decrease in mitochondrial phosphate production from diphosphates by mitochondrial diphosphatases.

Also, the total NADH levels were decreased by 7.4% (Table 5.6). Interestingly, cytosolic NADH levels increased by 4.2% but there was a decrease in mitochondrial NADH pool due to low flux of malate dehydrogenase. The total NADPH production was decreased by 64.7% (Table 5.5).

5.2.8 Evaluation of the role of pyruvate decarboxylase (*PDC6*) in increasing the isoprenoid pathway flux

Interestingly, I observed an up-regulation of *PDC6* in both the microarray data and the increase in flux of *PDC* in metabolic flux analysis data. It was also noteworthy that in the mutant strain, the flux through *PDC* was increased compared to that in the wild type strain irrespective of whether or not there was excessive phosphate in the media. Therefore, I was keen to investigate the role of *PDC6* in the *spt15_A101T* mutant strain.

To investigate the role of *PDC6*, I over-expressed *SPT15*WT and *spt15_A101T* mutant plasmid in *S. cerevisiae* strains carrying single gene deletions of *pdc1*Δ, *pdc5*Δ and *pdc6*Δ. I did not observe any difference in growth between *SPT15*WT and *spt15_A101T* strains in any of these

strain backgrounds (Figure 5.7A). I also utilized the visual carotenoid screen (described in chapter 3) to investigate the role of *PDCs*. In *S. cerevisiae* BY4741 (control) and *pdc1*Δ, *pdc5*Δ and *pdc6*Δ strains, I over expressed carotenogenic genes along with either *SPT15*WT or the *spt15_A101T* plasmid. These transformants were spotted under low and high phosphate minimal plates as shown in figure 5.7A. The *spt15_A101T* mutant strain showed a slight growth defect in BY4741 strain, which was more severe in the *pdc6*Δ background, but only under low phosphate conditions. No growth defect was observed under high and normal phosphate conditions. This suggests that under low phosphate conditions, *spt15_A101T* mutant needs *PDC6* for growth, but does not require it under high phosphate conditions. To investigate further as to whether the over expression of *PDC6* will also lead to increase in the isoprenoid pathway flux, I over expressed *PDC6* in our visual carotenoid screen alone, and in combination with either *SPT15*WT or *spt15_A101T*. I observed that over- expression of *PDC6* alone is not sufficient to increase the pigmentation and hence the isoprenoid flux, but over expression of *PDC6* in the spt15_A101T mutant strain led to an increased flux in the isoprenoid pathway under low as well as high phosphate conditions (Figure 5.7C). This was also confirmed by chemical analysis under normal phosphate conditions (SD minimal media) (Figure 5.7D). These results suggested that *PDC6* was required for both growth and increase in the isoprenoid flux under low phosphate conditions, but at high phosphate conditions, over expression of *PDC6* in *spt15_A101T* strain led to increased flux in the isoprenoid pathway.

5.3 Discussion

In this chapter, I have examined the metabolic basis for the increased isoprenoid flux observed in a mutant *spt15_A101T*. The mutant strain demonstrated an increased flux in the isoprenoid pathway along with a requirement of additional phosphate. The importance of phosphate demands in mutant strain was interesting in the light of recent observations which have suggested phosphate limitation as being critical for increased flux in both the isoprenoid and lipid pathways (Wu et al., 2010) (Roopnarain et al., 2014).

In the mutant strain, the new route of production of acetyl CoA from acetate results in demand for ATP. The increased pool of acetyl-CoA was channeled to HMG-CoA which increased the flux towards isoprenoid pathway.

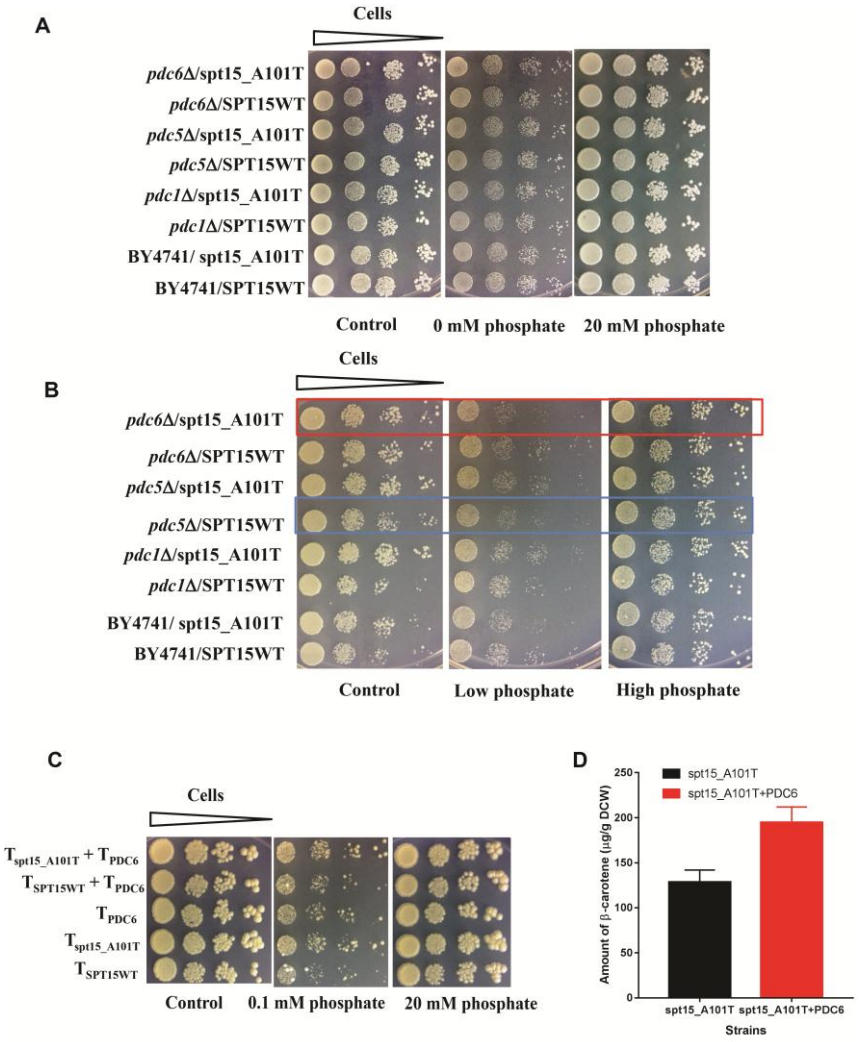

Figure 5.7 Role of Pyruvate decarboxylase (*PDC6*) on pigmentation and growth in *spt15_A101T* mutant strain. (A) Effect of over-expression of *spt15_A101T* on the growth in BY4741 (control) and *pdc1Δ, pdc5Δ* and *pdc6*Δ deletion strains (B) Effect of over-expression of *spt15_A101T* on the growth in BY4741 (control) and *pdc1Δ, pdc5Δ* and *pdc6*Δ deletion strains containing carotenogenic genes (T_{PSY1} and $GPD_{CRTI(A393T)}$) (C) Effect of over-expression of *PDC6* alone and in combination with either *SPT15*WT or *spt15_A101T* on pigmentation of yeast strains (with carotenogenic genes) (D) Amount of carotenoids in the strain overexpressing either *spt15_A101T* alone or in combination with *PDC6.* In 5.7A, 5.7B and 5.7C dilution spots carrying $4X10^4$, $4X10^3$, $4X10^2$, $4X10^1$ cells).

The remaining carbon was routed towards the TCA cycle, albeit a truncated one. The TCA cycle was completed via the glyoxylate shunt as opposed to via succinyl-CoA since this requires additional phosphate for ATP generation. The glyoxylate shunt balances the CoA pool without the need for additional phosphate and hence is the preferred pathway to complete the TCA cycle, especially under phosphate limitation.

The microarray and flux balance analyses also indicated an increased expression of *PDC6* and the corresponding flux from pyruvate to acetaldehyde. The *spt15_A101T* mutant strain essentially requires *PDC6* for growth and increased flux through the isoprenoid pathway under phosphate limitation conditions. This suggested that up-regulation of *PDC6* is exploited by the mutant strain for increased acetaldehyde, acetate and acetyl-CoA pools (both in cytosol and mitochondria) essential for the increased flux through the isoprenoid pathway. In *S. cerevisiae*, there are three genes coding for pyruvate decarboxylase, *PDC1*, *PDC5* and *PDC6*. PDC activity in *S. cerevisiae* is primarily due to expression of *PDC1*. *PDC6* is a minor isoform, where transcription is dependent upon glucose and ethanol and sulfur limited conditions (Boer et al., 2003). The mechanism for the up-regulation of *PDC6* under phosphate limitation conditions is unclear and requires detailed investigation. In any case, the possibility that the *PDC* enzymes could be a route for increasing the isoprenoid pathway flux in *S. cerevisiae* appears to be novel and reviewing the literature seems to indicate that this pathway has not been observed so far.

As shown in figure 5.8, an overall mechanism can be hypothesized as that there is rewiring of carbon metabolism in the *spt15_A101T* mutant strain so as to increase precursor, acetyl CoA and cofactor NADPH for increased isoprenoid pathway flux. This is achieved by up-regulation of *PDC6* which led to increased flux towards acetaldehyde and acetate. Increased pools of acetate were responsible for production of acetyl CoA and hence isoprenoid flux. As a consequence, this route resulted in the increased NADPH pools and increased ATP demand. To increase ATP production in a mutant cell, the cells required phosphate, hence it activated phosphate utilization and the phosphate signaling pathway (PHO) so as to increase the uptake of phosphate from extracellular environment by activation of genes encoding for phosphatases, *PHO5*, *PHO11*, *PHO12* as well as high affinity phosphate transporters- *PHO84*, *PHO89*.

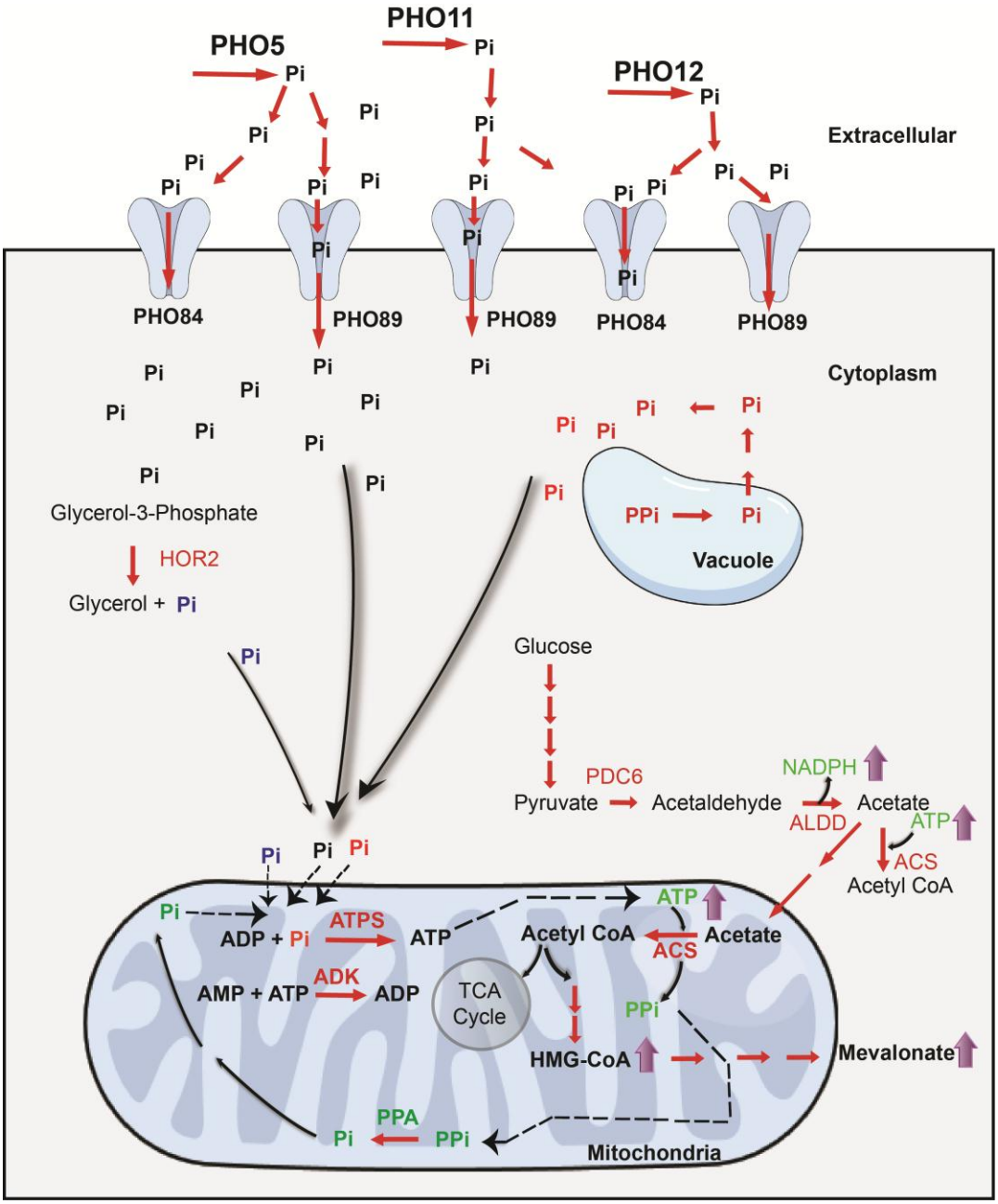

Figure 5.8 Schematic representation for increase in flux of MVA pathway by spt15_A101T mutant strain. *PHO5*- alkaline phosphatase, *PHO11*, *PHO12*- acid phosphatase, *PHO84*, *PHO89*- high affinity phosphate transporters, *PDC6*- pyruvate decarboxylase 6, *HOR2*- glycerol-3-phosphate phosphatase, *ALDD*- acetaldehyde dehydrogenase, *ACS*- acetyl CoA synthetase, *ATPS*- ATP synthase, *ADK*- adenylate kinase

BIBLIOGRAPHY

Bibliography

Ajikumar, P. K., Xiao, W. H., Tyo, K. E., Wang, Y., Simeon, F., Leonard, E., Mucha, O., Phon, T. H., Pfeifer, B., Stephanopoulos, G., 2010. Isoprenoid pathway optimization for Taxol precursor overproduction in Escherichia coli. Science. 330**,** 70-4.

Albertsen, L., Chen, Y., Bach, L. S., Rattleff, S., Maury, J., Brix, S., Nielsen, J., Mortensen, U. H., 2011. Diversion of flux toward sesquiterpene production in Saccharomyces cerevisiae by fusion of host and heterologous enzymes. Appl Environ Microbiol. 77**,** 1033-40.

Alper, H., Moxley, J., Nevoigt, E., Fink, G. R., Stephanopoulos, G., 2006a. Engineering yeast transcription machinery for improved ethanol tolerance and production. Science. 314**,** 1565-8.

Alper, H., Moxley, J., Nevoigt, E., Fink, G. R., Stephanopoulos, G., 2006b. Engineering yeast transcription machinery for improved ethanol tolerance and production. Science (New York, N.Y.). 314**,** 1565-1568.

Asadollahi, M. A., Maury, J., Moller, K., Nielsen, K. F., Schalk, M., Clark, A., Nielsen, J., 2008. Production of plant sesquiterpenes in Saccharomyces cerevisiae: effect of ERG9 repression on sesquiterpene biosynthesis. Biotechnol Bioeng. 99**,** 666-77.

Asadollahi, M. A., Maury, J. r. m., Schalk, M., Clark, A., Nielsen, J., 2010. Enhancement of farnesyl diphosphate pool as direct precursor of sesquiterpenes through metabolic engineering of the mevalonate pathway in Saccharomyces cerevisiae. Biotechnology and bioengineering. 106**,** 86-96.

Babiskin, A. H., Smolke, C. D. C., 2011. A synthetic library of RNA control modules for predictable tuning of gene expression in yeast. Molecular systems biology. 7**,** 471.

Begum, H., Yusoff, F. M., Banerjee, S., Khatoon, H., Shariff, M., 2016. Availability and Utilization of Pigments from Microalgae. Crit Rev Food Sci Nutr. 56**,** 2209-22.

Behrendorff, J. B., Vickers, C. E., Chrysanthopoulos, P., Nielsen, L. K., 2013. 2,2-Diphenyl-1-picrylhydrazyl as a screening tool for recombinant monoterpene biosynthesis. Microb Cell Fact. 12**,** 76.

Beppu, F., Niwano, Y., Tsukui, T., Hosokawa, M., Miyashita, K., 2009. Single and repeated oral dose toxicity study of fucoxanthin (FX), a marine carotenoid, in mice. J Toxicol Sci. 34**,** 501-10.

Bleichenbacher, M., Tan, S., Richmond, T. J., 2003. Novel Interactions Between the Components of Human and Yeast TFIIA/TBP/DNA Complexes. Journal of Molecular Biology. 332**,** 783793.

Boer, V. M., de Winde, J. H., Pronk, J. T., Piper, M. D., 2003. The genome-wide transcriptional responses of Saccharomyces cerevisiae grown on glucose in aerobic chemostat cultures limited for carbon, nitrogen, phosphorus, or sulfur. J Biol Chem. 278**,** 3265-74.

Boettger, D., Hertweck, C., 2013. Molecular diversity sculpted by fungal PKS-NRPS hybrids. Chembiochem. 14**,** 28-42.

Boucher, Y., Doolittle, W. F., 2000. The role of lateral gene transfer in the evolution of isoprenoid biosynthesis pathways. Mol Microbiol. 37**,** 703-16.

Brehm-Stecher, B. F., Johnson, E. A., 2012. Isolation of carotenoid hyperproducing mutants of Xanthophyllomyces dendrorhous (Phaffia rhodozyma) by flow cytometry and cell sorting. Methods Mol Biol. 898**,** 207-17.

Britton, G., 1995. Structure and properties of carotenoids in relation to function. FASEB J. 9**,** 1551-8.

C, K., 1994. Methods in yeast genetics. Cold Spring Harbor Laboratory Press

Chasman, D. I., Flaherty, K. M., Sharp, P. A., Kornberg, R. D., 1993. Crystal structure of yeast TATA-binding protein and model for interaction with DNA. Proceedings of the National Academy of Sciences. 90**,** 8174-8178.

Chen, Y., Daviet, L., Schalk, M., Siewers, V., Nielsen, J., 2013. Establishing a platform cell factory through engineering of yeast acetyl-CoA metabolism. Metab Eng. 15**,** 48-54.

Chooi, Y. H., Tang, Y., 2012. Navigating the fungal polyketide chemical space: from genes to molecules. J Org Chem. 77**,** 9933-53.

Chuyen, H. V., Eun, J. B., 2017. Marine carotenoids: Bioactivities and potential benefits to human health. Crit Rev Food Sci Nutr. 57**,** 2600-2610.

Clinton, S. K., 1998. Lycopene: chemistry, biology, and implications for human health and disease. Nutr Rev. 56**,** 35-51.

Conrado, R. J., Wu, G. C., Boock, J. T., Xu, H., Chen, S. Y., Lebar, T., Turnsek, J., Tomsic, N., Avbelj, M., Gaber, R., Koprivnjak, T., Mori, J., Glavnik, V., Vovk, I., Bencina, M., Hodnik, V., Anderluh, G., Dueber, J. E., Jerala, R., DeLisa, M. P., 2012. DNA-guided

assembly of biosynthetic pathways promotes improved catalytic efficiency. Nucleic Acids Res. 40**,** 1879-89.

Crowley, J. H., Leak, F. W., Jr., Shianna, K. V., Tove, S., Parks, L. W., 1998. A mutation in a purported regulatory gene affects control of sterol uptake in Saccharomyces cerevisiae. J Bacteriol. 180**,** 4177-83.

Dai, Z., Liu, Y., Zhang, X., Shi, M., Wang, B., Wang, D., Huang, L., Zhang, X., 2013. Metabolic engineering of Saccharomyces cerevisiae for production of ginsenosides. Metab Eng. 20**,** 146-56.

Dairi, T., 2005. Studies on biosynthetic genes and enzymes of isoprenoids produced by actinomycetes. J Antibiot (Tokyo). 58**,** 227-43.

de Jong, B. W., Shi, S., Siewers, V., Nielsen, J., 2014. Improved production of fatty acid ethyl esters in Saccharomyces cerevisiae through up-regulation of the ethanol degradation pathway and expression of the heterologous phosphoketolase pathway. Microb Cell Fact. 13**,** 39.

Delgado-Vargas, F., Jimenez, A. R., Paredes-Lopez, O., 2000. Natural pigments: carotenoids, anthocyanins, and betalains--characteristics, biosynthesis, processing, and stability. Crit Rev Food Sci Nutr. 40**,** 173-289.

Dueber, J. E., Wu, G. C., Malmirchegini, G. R., Moon, T. S., Petzold, C. J., Ullal, A. V., Prather, K. L., Keasling, J. D., 2009. Synthetic protein scaffolds provide modular control over metabolic flux. Nat Biotechnol. 27**,** 753-9.

Ebrahim, A., Lerman, J. A., Palsson, B. O., Hyduke, D. R., 2013. COBRApy: COnstraints-Based Reconstruction and Analysis for Python. BMC Syst Biol. 7**,** 74.

Edwards, J. S., Ibarra, R. U., Palsson, B. O., 2001. In silico predictions of Escherichia coli metabolic capabilities are consistent with experimental data. Nat Biotechnol. 19**,** 125-30.

Emmerstorfer-Augustin, A., Moser, S., Pichler, H., 2016. Screening for improved isoprenoid biosynthesis in microorganisms. J Biotechnol. 235**,** 112-20.

Estevez, J. M., Cantero, A., Reindl, A., Reichler, S., Leon, P., 2001. 1-Deoxy-D-xylulose-5-phosphate synthase, a limiting enzyme for plastidic isoprenoid biosynthesis in plants. J Biol Chem. 276**,** 22901-9.

Evans, B. S., Robinson, S. J., Kelleher, N. L., 2011. Surveys of non-ribosomal peptide and polyketide assembly lines in fungi and prospects for their analysis in vitro and in vivo. Fungal Genet Biol. 48**,** 49-61.

Farhi, M., Marhevka, E., Masci, T., Marcos, E., Eyal, Y., Ovadis, M., Abeliovich, H., Vainstein, A., 2011. Harnessing yeast subcellular compartments for the production of plant terpenoids. Metabolic engineering. 13**,** 474-481.

Faulkner, A., Chen, X., Rush, J., Horazdovsky, B., Waechter, C. J., Carman, G. M., Sternweis, P. C., 1999. The LPP1 and DPP1 gene products account for most of the isoprenoid phosphate phosphatase activities in Saccharomyces cerevisiae. J Biol Chem. 274**,** 14831-7.

Fiedor, J., Burda, K., 2014. Potential role of carotenoids as antioxidants in human health and disease. Nutrients. 6**,** 466-88.

Fischer, M. J., Meyer, S., Claudel, P., Bergdoll, M., Karst, F., 2011. Identification of a lysine residue important for the catalytic activity of yeast farnesyl diphosphate synthase. Protein J. 30**,** 334-9.

Fraser, P. D., Truesdale, M. R., Bird, C. R., Schuch, W., Bramley, P. M., 1994. Carotenoid Biosynthesis during Tomato Fruit Development (Evidence for Tissue-Specific Gene Expression). Plant Physiol. 105**,** 405-413.

Frengova, G. I., Beshkova, D. M., 2009. Carotenoids from Rhodotorula and Phaffia: yeasts of biotechnological importance. J Ind Microbiol Biotechnol. 36**,** 163-80.

Furubayashi, M., Ikezumi, M., Kajiwara, J., Iwasaki, M., Fujii, A., Li, L., Saito, K., Umeno, D., 2014. A high-throughput colorimetric screening assay for terpene synthase activity based on substrate consumption. PLoS One. 9**,** e93317.

Gomez-Garcia Mdel, R., Ochoa-Alejo, N., 2013. Biochemistry and molecular biology of carotenoid biosynthesis in chili peppers (Capsicum spp.). Int J Mol Sci. 14**,** 19025-53.

Goodwin, T. W., 1980. The Biochemistry of Carotenoids.

Grossman, A. R., Lohr, M., Im, C. S., 2004. Chlamydomonas reinhardtii in the landscape of pigments. Annu Rev Genet. 38**,** 119-73.

Guthrie, C., Fink, G. R., 1991. Guide to {Y}east {G}enetics and {M}olecular {B}iology. Academic Press: New York.

Heider, S. A., Peters-Wendisch, P., Wendisch, V. F., 2012. Carotenoid biosynthesis and overproduction in Corynebacterium glutamicum. BMC Microbiol. 12**,** 198.

Heo, S. J., Yoon, W. J., Kim, K. N., Ahn, G. N., Kang, S. M., Kang, D. H., Affan, A., Oh, C., Jung, W. K., Jeon, Y. J., 2010. Evaluation of anti-inflammatory effect of fucoxanthin isolated from brown algae in lipopolysaccharide-stimulated RAW 264.7 macrophages. Food Chem Toxicol. 48**,** 2045-51.

Herrero, O., RamÃ³n, D., Orejas, M., 2008. Engineering the Saccharomyces cerevisiae isoprenoid pathway for de novo production of aromatic monoterpenes in wine. Metabolic engineering. 10**,** 78-86.

Ignea, C., Cvetkovic, I., Loupassaki, S., Kefalas, P., Johnson, C. B., Kampranis, S. C., Makris, A. M., 2011. Improving yeast strains using recyclable integration cassettes, for the production of plant terpenoids. Microb Cell Fact. 10**,** 4.

Ignea, C., Trikka, F. A., Nikolaidis, A. K., Georgantea, P., Ioannou, E., Loupassaki, S., Kefalas, P., Kanellis, A. K., Roussis, V., Makris, A. M., Kampranis, S. C., 2015. Efficient diterpene production in yeast by engineering Erg20p into a geranylgeranyl diphosphate synthase. Metab Eng. 27**,** 65-75.

Inada, M., Pleiss, J. A., 2010. Genome-Wide Approaches to Monitor Pre-mRNA Splicing. vol. 470, pp. 51-75.

Ito, H., Fukuda, Y., Murata, K., Kimura, A., 1983. Transformation of intact yeast cells treated with alkali cations. J Bacteriol. 153**,** 163-8.

Jensen, E. D., Ferreira, R., Jakociunas, T., Arsovska, D., Zhang, J., Ding, L., Smith, J. D., David, F., Nielsen, J., Jensen, M. K., Keasling, J. D., 2017. Transcriptional reprogramming in yeast using dCas9 and combinatorial gRNA strategies. Microb Cell Fact. 16**,** 46.

Jiang, Y., Proteau, P., Poulter, D., Ferro-Novick, S., 1995. BTS1 encodes a geranylgeranyl diphosphate synthase in Saccharomyces cerevisiae. J Biol Chem. 270**,** 21793-9.

Keasling J, N. J., Pitera D, Method for enhancing production of isoprenoid compounds. US, 2010.

Keasling, J. D., 2010. Manufacturing molecules through metabolic engineering. Science (New York, N.Y.). 330**,** 1355-1358.

KH, K., 2010. History and sources of essential oil research. In: K. Husnu Can Baser, G. B., (Ed.), handbook of essential oils: science, technology, and applications pp. 3-38.

Kim, S. R., Xu, H., Lesmana, A., Kuzmanovic, U., Au, M., Florencia, C., Oh, E. J., Zhang, G., Kim, K. H., Jin, Y. S., 2015. Deletion of PHO13, encoding haloacid dehalogenase type IIA phosphatase, results in upregulation of the pentose phosphate pathway in Saccharomyces cerevisiae. Appl Environ Microbiol. 81**,** 1601-9.

Kirby, J., Nishimoto, M., Chow, R. W., Pasumarthi, V. N., Chan, R., Chan, L. J., Petzold, C. J., Keasling, J. D., 2014. Use of nonionic surfactants for improvement of terpene production in Saccharomyces cerevisiae. Appl Environ Microbiol. 80**,** 6685-93.

Kocharin, K., Chen, Y., Siewers, V., Nielsen, J., 2012. Engineering of acetyl-CoA metabolism for the improved production of polyhydroxybutyrate in Saccharomyces cerevisiae. AMB Express. 2**,** 52.

Kocharin, K., Siewers, V., Nielsen, J., 2013. Improved polyhydroxybutyrate production by Saccharomyces cerevisiae through the use of the phosphoketolase pathway. Biotechnol Bioeng. 110**,** 2216-24.

Kozak, B. U., van Rossum, H. M., Benjamin, K. R., Wu, L., Daran, J. M., Pronk, J. T., van Maris, A. J., 2014a. Replacement of the Saccharomyces cerevisiae acetyl-CoA synthetases by alternative pathways for cytosolic acetyl-CoA synthesis. Metab Eng. 21**,** 46-59.

Kozak, B. U., van Rossum, H. M., Luttik, M. A., Akeroyd, M., Benjamin, K. R., Wu, L., de Vries, S., Daran, J. M., Pronk, J. T., van Maris, A. J., 2014b. Engineering acetyl coenzyme A supply: functional expression of a bacterial pyruvate dehydrogenase complex in the cytosol of Saccharomyces cerevisiae. MBio. 5**,** e01696-14.

Kumar, S., Kushwaha, H., Bachhawat, A. K., Raghava, G. P., Ganesan, K., 2012. Genome sequence of the oleaginous red yeast Rhodosporidium toruloides MTCC 457. Eukaryot Cell. 11**,** 1083-4.

L.Frenz, J. U., Methods and compositions for detecting microbial production of water-immiscible compounds 2012.

Lange, B. M., Rujan, T., Martin, W., Croteau, R., 2000. Isoprenoid biosynthesis: the evolution of two ancient and distinct pathways across genomes. Proc Natl Acad Sci U S A. 97**,** 13172-7.

Lauchli, R., Rabe, K. S., Kalbarczyk, K. Z., Tata, A., Heel, T., Kitto, R. Z., Arnold, F. H., 2013. High-throughput screening for terpene-synthase-cyclization activity and directed evolution of a terpene synthase. Angew Chem Int Ed Engl. 52**,** 5571-4.

Lee, P. C., Petri, R., Mijts, B. N., Watts, K. T., Schmidt-Dannert, C., 2005. Directed evolution of Escherichia coli farnesyl diphosphate synthase (IspA) reveals novel structural determinants of chain length specificity. Metab Eng. 7**,** 18-26.

Leonard, E., Ajikumar, P. K., Thayer, K., Xiao, W. H., Mo, J. D., Tidor, B., Stephanopoulos, G., Prather, K. L., 2010. Combining metabolic and protein engineering of a terpenoid biosynthetic pathway for overproduction and selectivity control. Proc Natl Acad Sci U S A. 107**,** 13654-9.

Li, J., Zhu, D., Niu, J., Shen, S., Wang, G., 2011. An economic assessment of astaxanthin production by large scale cultivation of Haematococcus pluvialis. Biotechnol Adv. 29**,** 568-74.

Li, S., Jendresen, C. B., Nielsen, A. T., 2016. Increasing production yield of tyrosine and mevalonate through inhibition of biomass formation. Process Biochemistry. 51**,** 1992-2000.

Lian, J., Si, T., Nair, N. U., Zhao, H., 2014. Design and construction of acetyl-CoA overproducing Saccharomyces cerevisiae strains. Metab Eng. 24**,** 139-49.

Lourembam, T., Identifying genes to increase flux in the isoprenoid pathway in Saccharomyces cerevisiae. Department of Biological Sciences, Vol. BS-MS. Indian Institute of Science Education and Research , Mohali, 2015.

Lv, X., Xie, W., Lu, W., Guo, F., Gu, J., Yu, H., Ye, L., 2014. Enhanced isoprene biosynthesis in Saccharomyces cerevisiae by engineering of the native acetyl-CoA and mevalonic acid pathways with a push-pull-restrain strategy. J Biotechnol. 186**,** 128-36.

Ma, S. M., Garcia, D. E., Redding-Johanson, A. M., Friedland, G. D., Chan, R., Batth, T. S., Haliburton, J. R., Chivian, D., Keasling, J. D., Petzold, C. J., Lee, T. S., Chhabra, S. R., 2011. Optimization of a heterologous mevalonate pathway through the use of variant HMG-CoA reductases. Metab Eng. 13**,** 588-97.

MacPherson, S., Larochelle, M., Turcotte, B., 2006. A fungal family of transcriptional regulators: the zinc cluster proteins. Microbiol Mol Biol Rev. 70**,** 583-604.

Manayi, A., Abdollahi, M., Raman, T., Nabavi, S. F., Habtemariam, S., Daglia, M., Nabavi, S. M., 2016. Lutein and cataract: from bench to bedside. Crit Rev Biotechnol. 36**,** 829-39.

Mata-Gomez, L. C., MontaÃ±ez, J. C., MÃ©ndez-Zavala, A., Aguilar, C. b. N. C., 2014. Biotechnological production of carotenoids by yeasts: an overview. Microbial cell factories. 13**,** 12.

Meadows, A. L., Hawkins, K. M., Tsegaye, Y., Antipov, E., Kim, Y., Raetz, L., Dahl, R. H., Tai, A., Mahatdejkul-Meadows, T., Xu, L., Zhao, L., Dasika, M. S., Murarka, A., Lenihan, J., Eng, D., Leng, J. S., Liu, C. L., Wenger, J. W., Jiang, H., Chao, L., Westfall, P., Lai, J., Ganesan, S., Jackson, P., Mans, R., Platt, D., Reeves, C. D., Saija, P. R., Wichmann, G., Holmes, V. F., Benjamin, K., Hill, P. W., Gardner, T. S., Tsong, A. E., 2016. Rewriting yeast central carbon metabolism for industrial isoprenoid production. Nature. 537**,** 694-697.

Mitchell, L. A., Chuang, J., Agmon, N., Khunsriraksakul, C., Phillips, N. A., Cai, Y., Truong, D. M., Veerakumar, A., Wang, Y., Mayorga, M., Blomquist, P., Sadda, P., Trueheart, J., Boeke, J. D., 2015. Versatile genetic assembly system (VEGAS) to assemble pathways for expression in S. cerevisiae. Nucleic Acids Res. 43**,** 6620-30.

Mo, M. L., Palsson, B. O., Herrgard, M. J., 2009. Connecting extracellular metabolomic measurements to intracellular flux states in yeast. BMC Syst Biol. 3**,** 37.

Moline, M., Libkind, D., van Broock, M., 2012. Production of torularhodin, torulene, and beta-carotene by Rhodotorula yeasts. Methods Mol Biol. 898**,** 275-83.

Mumberg, D., Muller, R., Funk, M., 1995. Yeast vectors for the controlled expression of heterologous proteins in different genetic backgrounds. Gene. 156**,** 119-22.

Nanba, K., Toyooka, S., Soh, J., Tsukuda, K., Yamamoto, H., Sakai, A., Ouchida, M., Kobayashi, N., Matsuo, K., Koide, N., Kusaka, K., Shimizu, K., Date, H., 2008. The allelic distribution of a single nucleotide polymorphism in the PDCD5 gene locus of Japanese non-small cell lung cancer patients. Mol Med Rep. 1**,** 667-71.

Nisar, N., Li, L., Lu, S., Khin, N. C., Pogson, B. J., 2015. Carotenoid metabolism in plants. Mol Plant. 8**,** 68-82.

Nishimura, A., Morita, M., Nishimura, Y., Sugino, Y., 1990. A rapid and highly efficient method for preparation of competent Escherichia coli cells. Nucleic Acids Res. 18**,** 6169.

Ohnuma, S., Suzuki, M., Nishino, T., 1994. Archaebacterial ether-linked lipid biosynthetic gene. Expression cloning, sequencing, and characterization of geranylgeranyl-diphosphate synthase. J Biol Chem. 269**,** 14792-7.

Ozaydin, B., Burd, H., Lee, T. S., Keasling, J. D., 2013. Carotenoid-based phenotypic screen of the yeast deletion collection reveals new genes with roles in isoprenoid production. Metabolic engineering. 15**,** 174-183.

Paddon, C. J., Westfall, P. J., Pitera, D. J., Benjamin, K., Fisher, K., McPhee, D., Leavell, M. D., Tai, A., Main, A., Eng, D., Polichuk, D. R., Teoh, K. H., Reed, D. W., Treynor, T., Lenihan, J., Fleck, M., Bajad, S., Dang, G., Dengrove, D., Diola, D., Dorin, G., Ellens, K. W., Fickes, S., Galazzo, J., Gaucher, S. P., Geistlinger, T., Henry, R., Hepp, M., Horning, T., Iqbal, T., Jiang, H., Kizer, L., Lieu, B., Melis, D., Moss, N., Regentin, R., Secrest, S., Tsuruta, H., Vazquez, R., Westblade, L. F., Xu, L., Yu, M., Zhang, Y., Zhao, L., Lievense, J., Covello, P. S., Keasling, J. D., Reiling, K. K., Renninger, N. S., Newman, J. D., 2013. High-level semi-synthetic production of the potent antimalarial artemisinin. Nature. 496**,** 528-32.

Peng, B., Plan, M. R., Carpenter, A., Nielsen, L. K., Vickers, C. E., 2017a. Coupling gene regulatory patterns to bioprocess conditions to optimize synthetic metabolic modules for improved sesquiterpene production in yeast. Biotechnol Biofuels. 10**,** 43.

Peng, B., Plan, M. R., Chrysanthopoulos, P., Hodson, M. P., Nielsen, L. K., Vickers, C. E., 2017b. A squalene synthase protein degradation method for improved sesquiterpene production in Saccharomyces cerevisiae. Metab Eng. 39**,** 209-219.

Peng, J., Yuan, J. P., Wu, C. F., Wang, J. H., 2011. Fucoxanthin, a marine carotenoid present in brown seaweeds and diatoms: metabolism and bioactivities relevant to human health. Mar Drugs. 9**,** 1806-28.

Peralta-Yahya, P. P., Ouellet, M., Chan, R., Mukhopadhyay, A., Keasling, J. D., Lee, T. S., 2011. Identification and microbial production of a terpene-based advanced biofuel. Nat Commun. 2**,** 483.

Pereira, R., Nielsen, J., Rocha, I., 2016. Improving the flux distributions simulated with genome-scale metabolic models of Saccharomyces cerevisiae. Metabolic Engineering Communications. 3**,** 153-163.

Pfleger, B. F., Pitera, D. J., Smolke, C. D., Keasling, J. D., 2006. Combinatorial engineering of intergenic regions in operons tunes expression of multiple genes. Nat Biotechnol. 24**,** 1027-32.

Polakowski, T., Stahl, U., Lang, C., 1998. Overexpression of a cytosolic hydroxymethylglutaryl-CoA reductase leads to squalene accumulation in yeast. Appl Microbiol Biotechnol. 49**,** 66-71.

Ramel, F., Birtic, S., Ginies, C., Soubigou-Taconnat, L., Triantaphylides, C., Havaux, M., 2012. Carotenoid oxidation products are stress signals that mediate gene responses to singlet oxygen in plants. Proc Natl Acad Sci U S A. 109**,** 5535-40.

Reyes, L. H., Gomez, J. M., Kao, K. C., 2014. Improving carotenoids production in yeast via adaptive laboratory evolution. Metab Eng. 21**,** 26-33.

Ro, D.-K. K., Paradise, E. M., Ouellet, M., Fisher, K. J., Newman, K. L., Ndungu, J. M., Ho, K. A., Eachus, R. A., Ham, T. S., Kirby, J., Chang, M. C., Withers, S. T., Shiba, Y., Sarpong, R., Keasling, J. D., 2006a. Production of the antimalarial drug precursor artemisinic acid in engineered yeast. Nature. 440**,** 940-943.

Ro, D. K., Paradise, E. M., Ouellet, M., Fisher, K. J., Newman, K. L., Ndungu, J. M., Ho, K. A., Eachus, R. A., Ham, T. S., Kirby, J., Chang, M. C., Withers, S. T., Shiba, Y., Sarpong, R., Keasling, J. D., 2006b. Production of the antimalarial drug precursor artemisinic acid in engineered yeast. Nature. 440**,** 940-3.

Rohmer, M., 1999. The discovery of a mevalonate-independent pathway for isoprenoid biosynthesis in bacteria, algae and higher plants. Nat Prod Rep. 16**,** 565-74.

Roopnarain, A., Gray, V. M., Sym, S. D., 2014. Phosphorus limitation and starvation effects on cell growth and lipid accumulation in Isochrysis galbana U4 for biodiesel production. Bioresour Technol. 156**,** 408-11.

Rose, M. D., Fink, G. R., 1987a. KAR1, a gene required for function of both intranuclear and extranuclear microtubules in yeast. Cell. 48**,** 1047-1060.

Rose, M. D., Fink, G. R., 1987b. KAR1, a gene required for function of both intranuclear and extranuclear microtubules in yeast. Cell. 48**,** 1047-60.

Sambrook, J., 1989. Molecular Cloning: A Laboratory Manual. Cold Spring Harbor Laboratory Press.

Sambrook, J., Russell, D., 2001. Molecular Cloning: A Laboratory Manual. Cold Spring Harbor Laboratory Press.

Scalcinati, G., Knuf, C., Partow, S., Chen, Y., Maury, J., Schalk, M., Daviet, L., Nielsen, J., Siewers, V., 2012a. Dynamic control of gene expression in Saccharomyces cerevisiae engineered for the production of plant sesquitepene alpha-santalene in a fed-batch mode. Metab Eng. 14**,** 91-103.

Scalcinati, G., Partow, S., Siewers, V., Schalk, M., Daviet, L., Nielsen, J., 2012b. Combined metabolic engineering of precursor and co-factor supply to increase alpha-santalene production by Saccharomyces cerevisiae. Microb Cell Fact. 11**,** 117.

Schaub, P., Yu, Q., Gemmecker, S., Poussin-Courmontagne, P., Mailliot, J., McEwen, A. G., Ghisla, S., Al-Babili, S., Cavarelli, J., Beyer, P. C., 2012. On the structure and function of the phytoene desaturase CRTI from Pantoea ananatis, a membrane-peripheral and FAD-dependent oxidase/isomerase. PloS one. 7.

Schmidt-Dannert, C., Umeno, D., Arnold, F. H., 2000. Molecular breeding of carotenoid biosynthetic pathways. Nat Biotechnol. 18**,** 750-3.

Shiba, Y., Paradise, E. M., Kirby, J., Ro, D. K., Keasling, J. D., 2007. Engineering of the pyruvate dehydrogenase bypass in Saccharomyces cerevisiae for high-level production of isoprenoids. Metab Eng. 9**,** 160-8.

Simpson, K. L., Nakayama, T. O., Chichester, C. O., 1964. Biosynthesis of Yeast Carotenoids. J Bacteriol. 88**,** 1688-94.

Szappanos, B. z., KovÃ¡cs, K. r., Szamecz, B. l., Honti, F., Costanzo, M., Baryshnikova, A., Gelius-Dietrich, G., Lercher, M. J., Jelasity, M. r., Myers, C. L., Andrews, B. J., Boone, C., Oliver, S. G., PÃ¡l, C., Papp, B. z. C., 2011. An integrated approach to characterize genetic interaction networks in yeast metabolism. Nature genetics. 43**,** 656-662.

Tang, S. Y., Cirino, P. C., 2011. Design and application of a mevalonate-responsive regulatory protein. Angew Chem Int Ed Engl. 50**,** 1084-6.

Thompson, J. D., Gibson, T. J., Plewniak, F., Jeanmougin, F., Higgins, D. G., 1997. The CLUSTAL_X windows interface: flexible strategies for multiple sequence alignment aided by quality analysis tools. Nucleic Acids Res. 25**,** 4876-82.

Trikka, F. A., Nikolaidis, A., Athanasakoglou, A., Andreadelli, A., Ignea, C., Kotta, K., Argiriou, A., Kampranis, S. C., Makris, A. M., 2015. Iterative carotenogenic screens

identify combinations of yeast gene deletions that enhance sclareol production. Microb Cell Fact. 14**,** 60.

Ukibe, K., Hashida, K., Yoshida, N., Takagi, H., 2009. Metabolic engineering of Saccharomyces cerevisiae for astaxanthin production and oxidative stress tolerance. Appl Environ Microbiol. 75**,** 7205-11.

Ukibe, K., Katsuragi, T., Tani, Y., Takagi, H., 2008. Efficient screening for astaxanthin-overproducing mutants of the yeast Xanthophyllomyces dendrorhous by flow cytometry. FEMS Microbiol Lett. 286**,** 241-8.

Umeno, D., Arnold, F. H., 2004. Evolution of a pathway to novel long-chain carotenoids. J Bacteriol. 186**,** 1531-6.

Umeno, D., Tobias, A. V., Arnold, F. H., 2002. Evolution of the C30 carotenoid synthase CrtM for function in a C40 pathway. J Bacteriol. 184**,** 6690-9.

Vardakou, M., Salmon, M., Faraldos, J. A., O'Maille, P. E., 2014. Comparative analysis and validation of the malachite green assay for the high throughput biochemical characterization of terpene synthases. MethodsX. 1**,** 187-96.

Varela, J. C., Pereira, H., Vila, M., Leon, R., 2015. Production of carotenoids by microalgae: achievements and challenges. Photosynth Res. 125**,** 423-36.

Verwaal, R., Wang, J., Meijnen, J.-P. P., Visser, H., Sandmann, G., van den Berg, J. A., van Ooyen, A. J. J. C., 2007a. High-level production of beta-carotene in Saccharomyces cerevisiae by successive transformation with carotenogenic genes from Xanthophyllomyces dendrorhous. Applied and environmental microbiology. 73**,** 4342-4350.

Verwaal, R., Wang, J., Meijnen, J. P., Visser, H., Sandmann, G., van den Berg, J. A., van Ooyen, A. J., 2007b. High-level production of beta-carotene in Saccharomyces cerevisiae by successive transformation with carotenogenic genes from Xanthophyllomyces dendrorhous. Appl Environ Microbiol. 73**,** 4342-50.

Vickers, C. E., Williams, T. C., Peng, B., Cherry, J., 2017. Recent advances in synthetic biology for engineering isoprenoid production in yeast. Curr Opin Chem Biol. 40**,** 47-56.

Wang, C., Oh, M. K., Liao, J. C., 2000. Directed evolution of metabolically engineered Escherichia coli for carotenoid production. Biotechnol Prog. 16**,** 922-6.

Wang, C., Yoon, S.-H. H., Jang, H.-J. J., Chung, Y.-R. R., Kim, J.-Y. Y., Choi, E.-S. S., Kim, S.-W. W., 2011. Metabolic engineering of Escherichia coli for Î±-farnesene production. Metabolic engineering. 13**,** 648-655.

Wang, Q., Feng, L. R., Luo, W., Li, H. G., Zhou, Y., Yu, X. B., 2015. Effect of inoculation process on lycopene production by Blakeslea trispora in a stirred-tank reactor. Appl Biochem Biotechnol. 175**,** 770-9.

Westfall, P. J., Pitera, D. J., Lenihan, J. R., Eng, D., Woolard, F. X., Regentin, R., Horning, T., Tsuruta, H., Melis, D. J., Owens, A., Fickes, S., Diola, D., Benjamin, K. R., Keasling, J. D., Leavell, M. D., McPhee, D. J., Renninger, N. S., Newman, J. D., Paddon, C. J., 2012a. Production of amorphadiene in yeast, and its conversion to dihydroartemisinic acid, precursor to the antimalarial agent artemisinin. Proc Natl Acad Sci U S A. 109**,** E111-8.

Westfall, P. J., Pitera, D. J., Lenihan, J. R., Eng, D., Woolard, F. X., Regentin, R., Horning, T., Tsuruta, H., Melis, D. J., Owens, A., Fickes, S., Diola, D., Benjamin, K. R., Keasling, J. D., Leavell, M. D., McPhee, D. J., Renninger, N. S., Newman, J. D., Paddon, C. J. C., 2012b. Production of amorphadiene in yeast, and its conversion to dihydroartemisinic acid, precursor to the antimalarial agent artemisinin. Proceedings of the National Academy of Sciences of the United States of America. 109**,** 8.

Wu, J., Du, G., Zhou, J., Chen, J., 2013. Metabolic engineering of Escherichia coli for (2S)-pinocembrin production from glucose by a modular metabolic strategy. Metab Eng. 16**,** 48-55.

Wu, S., Hu, C., Jin, G., Zhao, X., Zhao, Z. K., 2010. Phosphate-limitation mediated lipid production by Rhodosporidium toruloides. Bioresour Technol. 101**,** 6124-9.

Xie, W., Liu, M., Lv, X., Lu, W., Gu, J., Yu, H., 2014. Construction of a controllable beta-carotene biosynthetic pathway by decentralized assembly strategy in Saccharomyces cerevisiae. Biotechnol Bioeng. 111**,** 125-33.

Xie, W., Lv, X., Ye, L., Zhou, P., Yu, H., 2015. Construction of lycopene-overproducing Saccharomyces cerevisiae by combining directed evolution and metabolic engineering. Metab Eng. 30**,** 69-78.

Xu, P., Gu, Q., Wang, W., Wong, L., Bower, A. G., Collins, C. H., Koffas, M. A., 2013. Modular optimization of multi-gene pathways for fatty acids production in E. coli. Nat Commun. 4**,** 1409.

Yang, J., Bae, J. Y., Lee, Y. M., Kwon, H., Moon, H. Y., Kang, H. A., Yee, S. B., Kim, W., Choi, W., 2011. Construction of Saccharomyces cerevisiae strains with enhanced ethanol tolerance by mutagenesis of the TATA-binding protein gene and identification of novel genes associated with ethanol tolerance. Biotechnol Bioeng. 108**,** 1776-87.

Ye, Z. W., Jiang, J. G., Wu, G. H., 2008. Biosynthesis and regulation of carotenoids in Dunaliella: progresses and prospects. Biotechnol Adv. 26**,** 352-60.

Yuan, J., Ching, C. B., 2014. Combinatorial engineering of mevalonate pathway for improved amorpha-4,11-diene production in budding yeast. Biotechnology and bioengineering. 111**,** 608-617.

Yuan, J., Ching, C. B., 2015. Dynamic control of ERG9 expression for improved amorpha-4,11-diene production in Saccharomyces cerevisiae. Microb Cell Fact. 14**,** 38.

Zhang, J., Sun, Z., Sun, P., Chen, T., Chen, F., 2014. Microalgal carotenoids: beneficial effects and potential in human health. Food Funct. 5**,** 413-25.

Zhou, K., Zou, R., Zhang, C., Stephanopoulos, G., Too, H. P., 2013. Optimization of amorphadiene synthesis in bacillus subtilis via transcriptional, translational, and media modulation. Biotechnol Bioeng. 110**,** 2556-61.

Zhou, Y. J., Gao, W., Rong, Q., Jin, G., Chu, H., Liu, W., Yang, W., Zhu, Z., Li, G., Zhu, G., Huang, L., Zhao, Z. K., 2012a. Modular pathway engineering of diterpenoid synthases and the mevalonic acid pathway for miltiradiene production. Journal of the American Chemical Society. 134**,** 3234-3241.

Zhou, Y. J., Gao, W., Rong, Q., Jin, G., Chu, H., Liu, W., Yang, W., Zhu, Z., Li, G., Zhu, G., Huang, L., Zhao, Z. K., 2012b. Modular pathway engineering of diterpenoid synthases and the mevalonic acid pathway for miltiradiene production. J Am Chem Soc. 134**,** 3234-41.

Zhu, Z., Zhang, S., Liu, H., Shen, H., Lin, X., Yang, F., Zhou, Y. J., Jin, G., Ye, M., Zou, H., Zou, H., Zhao, Z. K. C., 2012. A multi-omic map of the lipid-producing yeast Rhodosporidium toruloides. Nature communications. 3**,** 1112.

Appendix 1:

Development of tools and techniques for Rhodosporidium toruloides: Attempts to decipher the gene encoding Torularhodin synthase

A1.1 Background

In addition to carrying out the work described in this thesis, efforts were made to develop methods for the red yeast, *Rhodosporidium toruloides*. This yeast has the potential to be a good host for several biotechnological applications. *R. toruloides* is an oleaginous yeast and is a high carotenoid producer. It has several industrially useful features, such as the capacity to grow to high cell density and the ability to utilize a wide range of carbon and nitrogen sources. Thus it has the potential to be exploited for the production of high-value products from low-cost substrates.

One of the products that were of great interest to us was the carotenoid torularhodin which *R. toruloides* produces as a major carotenoid in addition to torulene, β-carotene and γ-carotene. Torularhodin has one β-ionone ring and a longer polyene chain with 13 double bonds which imparts the red color. It is one of the few carotenoids with carboxylic group. Torularhodin has been reported to have very strong antioxidising properties and many reports have indicated potential uses of torularhodin as an antioxidant, (Sakaki et al., 2001), as components of cosmetics and food (Zoz et al., 2015), as ingredients of drugs (Ungureanu et al., 2013), and in some cancer treatments (Du et al., 2017) (Bhosale and Gadre, 2002). In the proposed carotenoid pathway of *Rhodotorula* spp. (shown in figure 7 in introduction), it has been predicted that torularhodin is produced from the precursor torulene. However, the enzyme catalyzing the conversion of torulene to torularhodin is still unknown. While developing the tools for *R.toruloides* I thus focussed on deciphering this pathway.

A1.2 Construction of modified vectors for transformation and disruption in *R. toruloides*

The molecular biology and genetic manipulation tools for *R. toruloides* are still in a developing stage. The most accepted transformation method for this yeast is the *Agrobacterium tumefaciens* mediated transformation (ATMT) since the lithium acetate method has not been successful (Figure A.1A) (Liu et al., 2013). The vectors that were developed for *R. toruloides* based on this ATMT were obtained from Temasek life sciences laboratories, Singapore (Liu et al., 2013). This vector, pRH203-1 (Figure A.1B), is a shuttle vector for bacteria and yeast. The selection marker for both *E. coli, Agrobacterium* is spectinomycin. The selection cassette for transfer to *R. toruloides* is present between the right and left border and this cassette is eventually transferred

from *Agrobacterium* to *Rhodosporidium*. The cassette consists of 1429 bp of the *R. toruloides* GPD promoter, *Rt*GPD1 (Glyceraldehyde-3-phosphate dehydrogenase) promoter which drives the expression of codon optimized enhanced green fluorescent protein gene (*Rt*GFP) (726bp) and 35T terminator. The cassette also contains the *Ustilago maydis* GPD promoter (*Um*GPD) (593 bp) which drives the expression of codon-optimized hygromycin phosphotransferase gene (*hpt-3*) for selection on hygromycin in *R. toruloides* followed by nopaline synthase terminator (nos). Since, the promoter driving the expression of hygromycin resistance (*hpt-3)* gene is from *U. maydis* (*gpd*), expression was not optimal and needed to be replaced by promoter from *R. toruloides* for better transformation efficiency in *R. toruloides*.

Therefore, vectors pMWR101, pMWR102 and pMWR103 were developed from pRH203-1 and their vector maps were shown in figure in A.1C, A.1D and A.1E respectively. The cassette between left border and right border in pMWR101contains *Rt*GPD1 promoter, *hpt-3* gene and nopaline synthase terminator. In pMWR102 vector, the cassette contains *Rt*GPD1 promoter, codon optimized enhanced green fluorescent protein gene (*Rt*GFP) followed by 35 terminator. The vector pMWR103 is similar to vector pRH203-1 except that *gpd* promoter from *U. maydis* is replaced by *Rt*GPD1 promoter from *R. toruloides*.

I then compared the transformation efficiency with the modified vectors. As observed in figure A.1F, the transformation efficiency in *R. toruloides ku70Δe* increased with modified vector pMWR101 as compared to pRH203-1 vector. *R. toruloides* transformants were selected on hygromycin plate and also confirmed by fluorescence microscopy for GFP as shown in figure A.1G and A.1H.

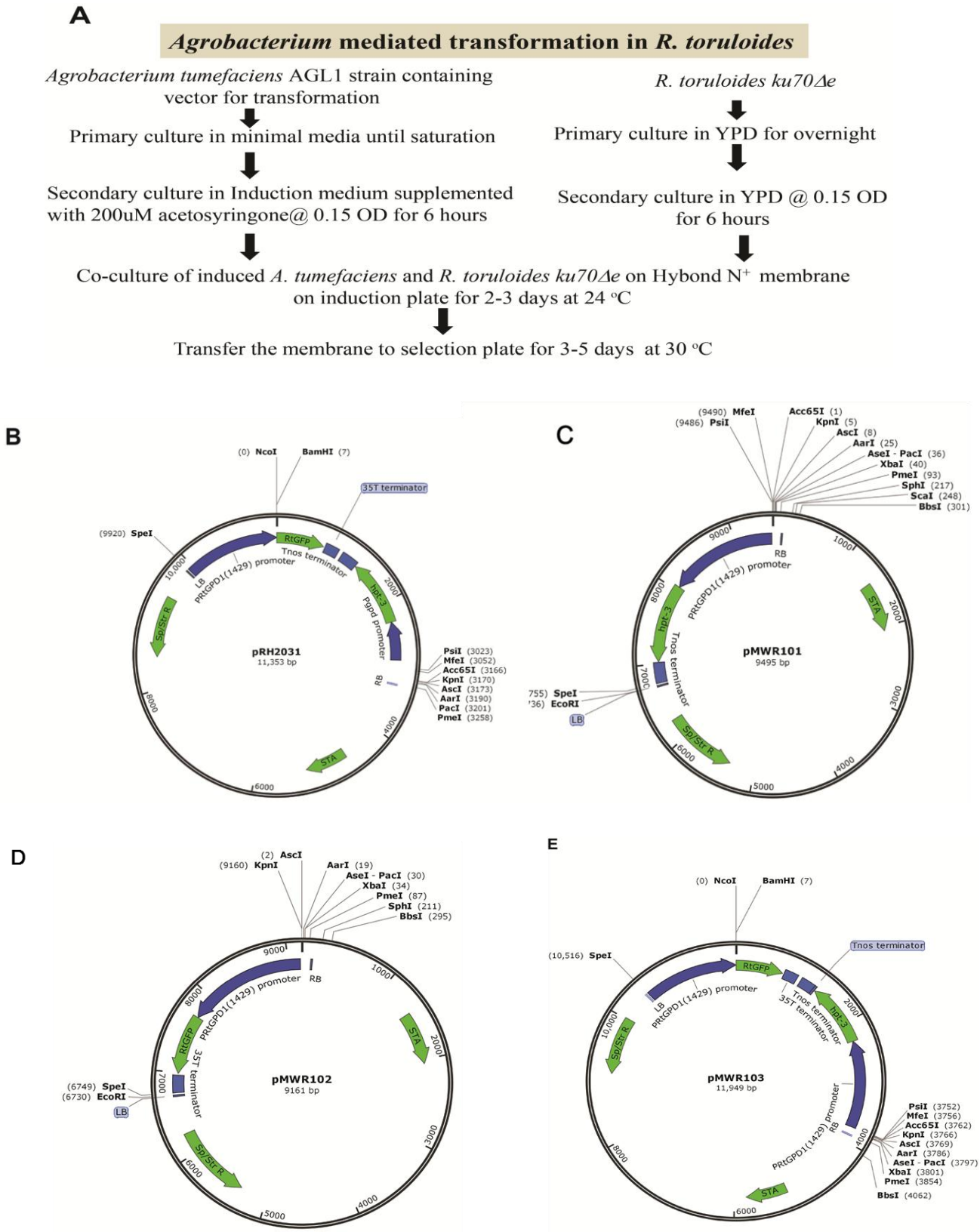
A
Agrobacterium mediated transformation in R. toruloides
Agrobacterium tumefaciens AGL1 strain containing vector for transformation
Primary culture in minimal media until saturation
Secondary culture in Induction medium supplemented with 200uM acetosyringone@ 0.15 OD for 6 hours
R. toruloides ku70Δe
Primary culture in YPD for overnight
Secondary culture in YPD @ 0.15 OD for 6 hours
Co-culture of induced A. tumefaciens and R. toruloides ku70Δe on Hybond N+ membrane on induction plate for 2-3 days at 24 °C
Transfer the membrane to selection plate for 3-5 days at 30 °C
B
pRH2031
11,353 bp
C
pMWR101
9495 bp
D
pMWR102
9161 bp
E
pMWR103
11,949 bp

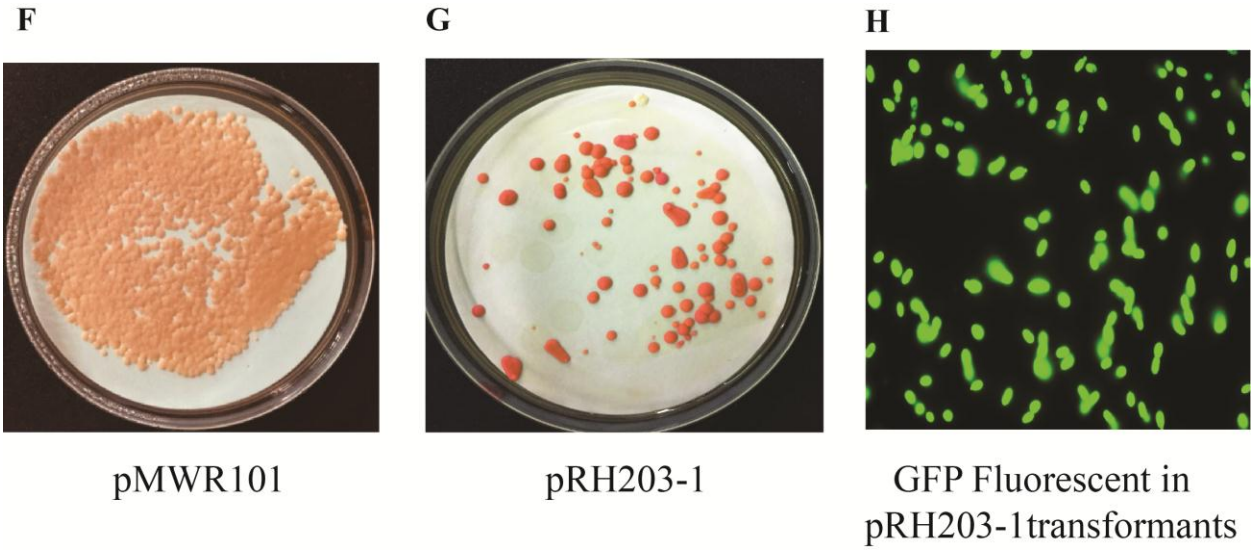

Figure A.1 (A) *Agrobacterium* mediated transformation in *Rhodosporidium* ,Vector maps of pRH203-1 (B), pMWR101 (C), pMWR102(D), pMWR103 (E), transformants with pMWR101 (F), transformants with pRH203-1(G),pRH203-1 transformants under fluorescent microscope (H).

A1.3 Construction of disruption vector for creating a gene deletion of the putative torularhodin synthase (RHTO_06383)

A putative torularhodin synthase gene was first identified using the following logic: In the yeast *Xanthophyllomyces dendrorhous*, the biosynthesis of astaxanthin (carotenoid) from β-carotene was catalyzed by astaxanthin synthase which belongs to cytochrome P450 monooxygenase 3A subfamily (Figure A.2A). The reaction mechanism/steps for the production of astaxanthin from β-carotene involve ketolation and hydroxylation of β-carotene. Similarly, in the plant *Solanum lycopersicum* the biosynthesis of zeinxanthin and α-cryptoxanthin from lutein and biosynthesis of lutein from α-cryptoxanthin involves Cytochrome P450 monoxygenase 97A29, 97C11 and 97C11 respectively (Figure A.2B). Based on the similarity of the reactions in *R. toruloides*, the biosynthesis of torularhodin from torulene which involves oxidation and hydroxylation step is also likely to be catalyzed by one of the cytochorome P450 oxidases (Figure A.2C).

With this logic, a bioinformatics analysis was carried out. *Rhodosporidium toruloides* was found to contain twelve genes encoding for cytochrome P450 oxidases and only one gene encoding for cytochrome P450 reductase (Table A.1). Through BLAST and reverse BLAST analysis with the astaxanthin synthase of *X. dendrorhous* cytochrome P450 monoxygenase 97A29 from *S. lycopersicum*, the ORF RHTO_06383 it appeared, could be the potential torularhodin synthase (Table A.2).

To confirm the prediction of ORF RHTO_06383 as the potential torularhodin synthase a gene deletion was planned. For the deletion of a putative torularhodin synthase (RHTO_06383) in *R. toruloides*, 5' and 3' flanking end of gene (each 1000 bp in length) was cloned in pMWR101 vector at RB and LB using *Xba*I-*Kpn*I and *Spe*I-*Eco*RI enzymes (Figure A.3A and A.3B). As shown in figure A.3C, between the 5'-3' flanking gene sequence, the selection cassette for *R. toruloides* transformats is present. This ORF RHTO_06383 knockout vector constructed in pMWR101vector backbone was transformed in *Agrobacterium tumefaciens AGL1* strain by electroporation and transformants were selected on the spectinomycin plates. Thus *A. tumefaciens AGL1* transformants carrying pMWR101vector (control) and knockout vector (test) were then used for transformation in *R. toruloides ku70Δe* strains through *Agrobacterium* mediated transformation (ATMT). The transformants were selected on the spectinomycin and hygromycin selection plates and shown in figure A.3D (control plate) and A.3E (test plate).

Although colonies were observed in the control vector, I was not able to get any transformants with knockout vector. This could be either due to either the inefficiency of the recombination required for the generation of the disruption or the essentiality of the gene.

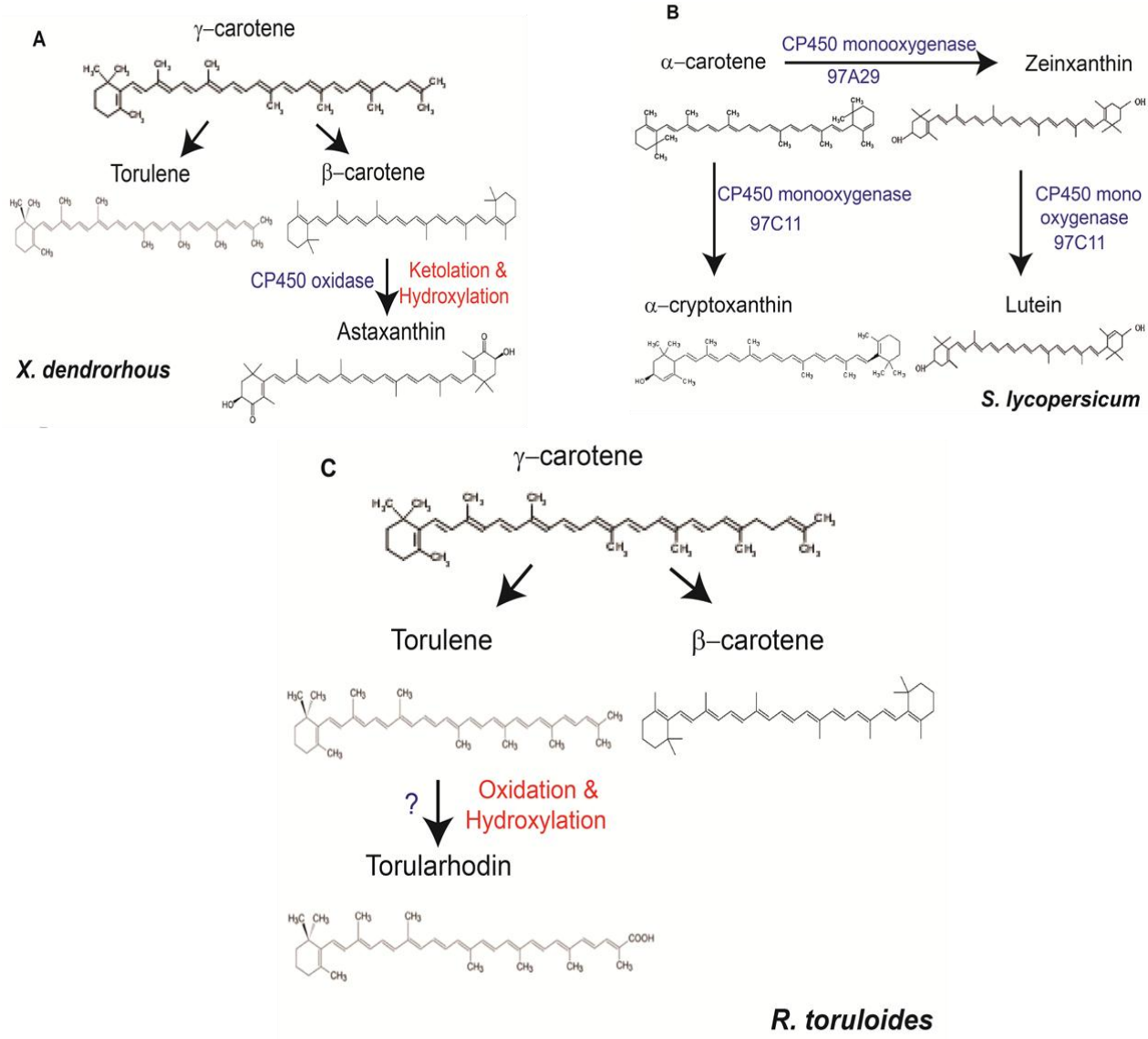

Figure A.2. Role of Cytochrome P450 enzymes in carotenoid biosynthesis pathway in different organisms (A) Biosynthesis of astaxanthin in *Xanthophyllomces dendrorhous* (B) Biosynthesis of zeinxanthin, cryptoxanthin and lutein in *Solanum lycopersicum* (C) Biosynthesis of torularhodin - *Rhodosporidium toruloides* (red yeast) (proposed)

Protein ID	Size (aa)	Characterization/Annotation
RHT0_0164	525	Sterol 12-α-hydroxylase
RHT0_0381	567	Leukotriene B420- monooxygenase
RHT0_02505	549	Not Characterized
RHT0_03865	535	Sterol-14- demethylase
RHT0_04142	537	Family 4, subfamily A
RHT0_04197	530	Family 4, subfamily A
RHT0_04252	540	Family 2, subfamily U
RHT0_04967	536	Steroid 17-α-monooxygenase
RHT0_06312	542	Family 83, subfamily A polypeptide A
RHT0_06383	596	Family 46, subfamily A Cholesterol 24 (S)- hydroxylase
RHT0_06833	540	Family 3, subfamily A
RHTO_07105	526	Not Characterized
RHTO_06309	712	Cytochrome P450 oxidoreductase

Table A.1. List of putative Cytochrome P450 oxidases and oxidoreductase present in *R. toruloides NP11*.

Protein	Astaxanthin synthase (*X. dendrorhous*)	CP450 monooxygenase 97A29 *S. lycoperpersicum*	CP450 monooxygenase 97C11 *S. lycoperpersicum*
RHT0_164	0.007, 43%	3e-05, 37%	2e-05, 41%
RHT0_381	1e-67, 47%	4e-29, 45%	1e-27, 42%
RHT0_2505	1e-18, 41%	9e-16, 39%	5e-18, 37%
RHT0_3865	2e-17, 42%	1e-11, 37%	2e-08, 39%
RHT0_4142	4e-20, 40%	5e-37, 44%	2e-27, 41%
RHT0_4197	4e-15, 40%	1e-26, 43%	4e-22, 44%
RHT0_4252	8e-04, 40%	7e-18, 38%	3e-12, 42%
RHT0_4967	1e-11, 43%	1e-24, 37%	4e-13, 41%
RHT0_6312	2e-08, 42%	2e-19, 40%	3e-12, 44%
RHT0_6383	4e-91, 49%	2e-32, 43%	2e-23, 41%
RHT0_6833	7e-19, 41%	4e-23, 39%	8e-19, 44%
RHTO_7105	4e-19, 39%	3e-15, 40%	4e-16, 37%

Table A.2 Bioinformatic analysis of putative CP450 oxidases of *R. toruloides* against cytochrome P450 oxidases present in *X. dendrorhous* and *S. lycopersicum*.

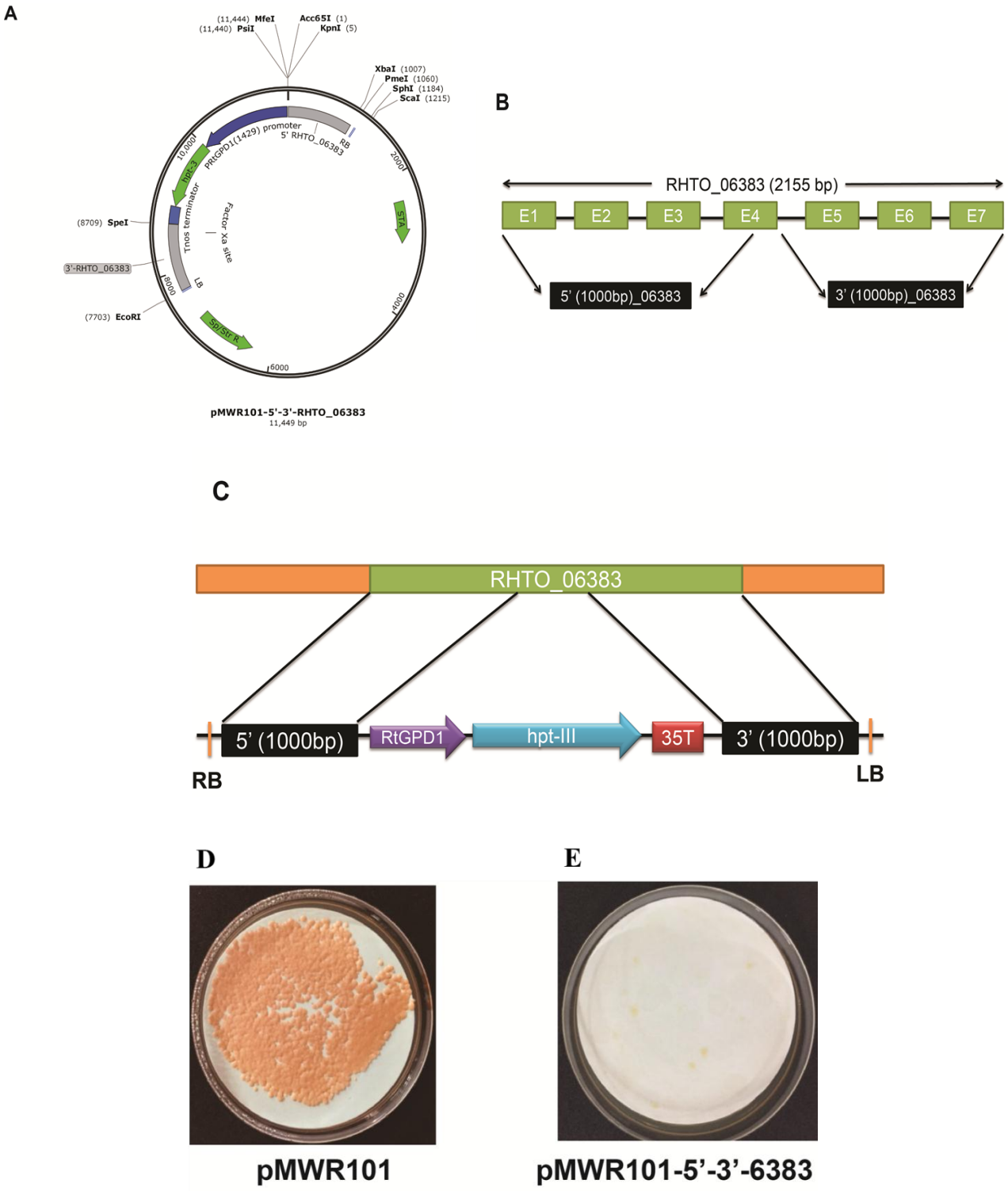

Figure A.3. (A) Vector map of knockout vector in pMWR101 backbone (B) Gene structure of RHTO_06383 (C) structure of cassette for knockout of RHTO_06383 (D) Transformants on control plate (pMWR101) (E) No colonies on test plate (pMWR101-5'-3'-6383)

A1.4 Efforts at cloning and expressing the putative Cytochrome P450 and the reductase in *S. cerevisiae*:

Cytochrome P450 oxidase (RHTO_06383) and cytochrome P450 oxidoreducatse (RHTO_06309) genes were codon optimized and custom synthesized for expression in *S.cerevesiae*. These genes were then cloned in centromeric vectors under TEF promoter pRS314TEF and pRS313TEF respectively. These two genes were expressed along with other three carotenogenic genes (GGPP synthase, phytoene synthase and phytoene dehydrogenase) in *S. cerevisiae* ABC 276 strain and transformants were spotted on minimal plates as shown in figure A.4A. Expression of cytochrome P450 oxidase (RHTO_06383) in yeast strain either alone or in combination with cytochrome P450 oxidoreductase (RHTO_06309) did not result in increase in pigmentation of transformants.

A1.5 Standardization of carotenoid profile of *R. toruloides*

For the chemical analysis of torularhodin in the carotenoid extract from *S. cerevisiae* yeast transformants, first the carotenoid extraction was standardized from torularhodin producing yeast, *R. toruloides ku70Δe* strain using the modified method described in materials and methods (Section 2.24).The torularhodin peak was identified by comparing the peak retention time with authentic standard of torularhodin obtained from CaroteNature GmbH, Switzerland. In HPLC chromatogram, the standard torularhodin (dissolved in ethyl acetate) is giving two peaks- one sharp peak at RT-2.29 at 286nm and another broad peak at RT-4.859 at 495nm. In the carotenoid extract from *R. toruloides*, two peaks corresponding to torulahrodin were identified and other peaks identified as- β-carotene (RT- 4.4), γ-carotene (RT- 4.0) and Lycopene (RT- 3.8) based on retention time of authentic standards. The HPLC chromatogram from *R. toruloides* and standard curve of torularhodin is shown in figure A.4B and A.4C respectively.

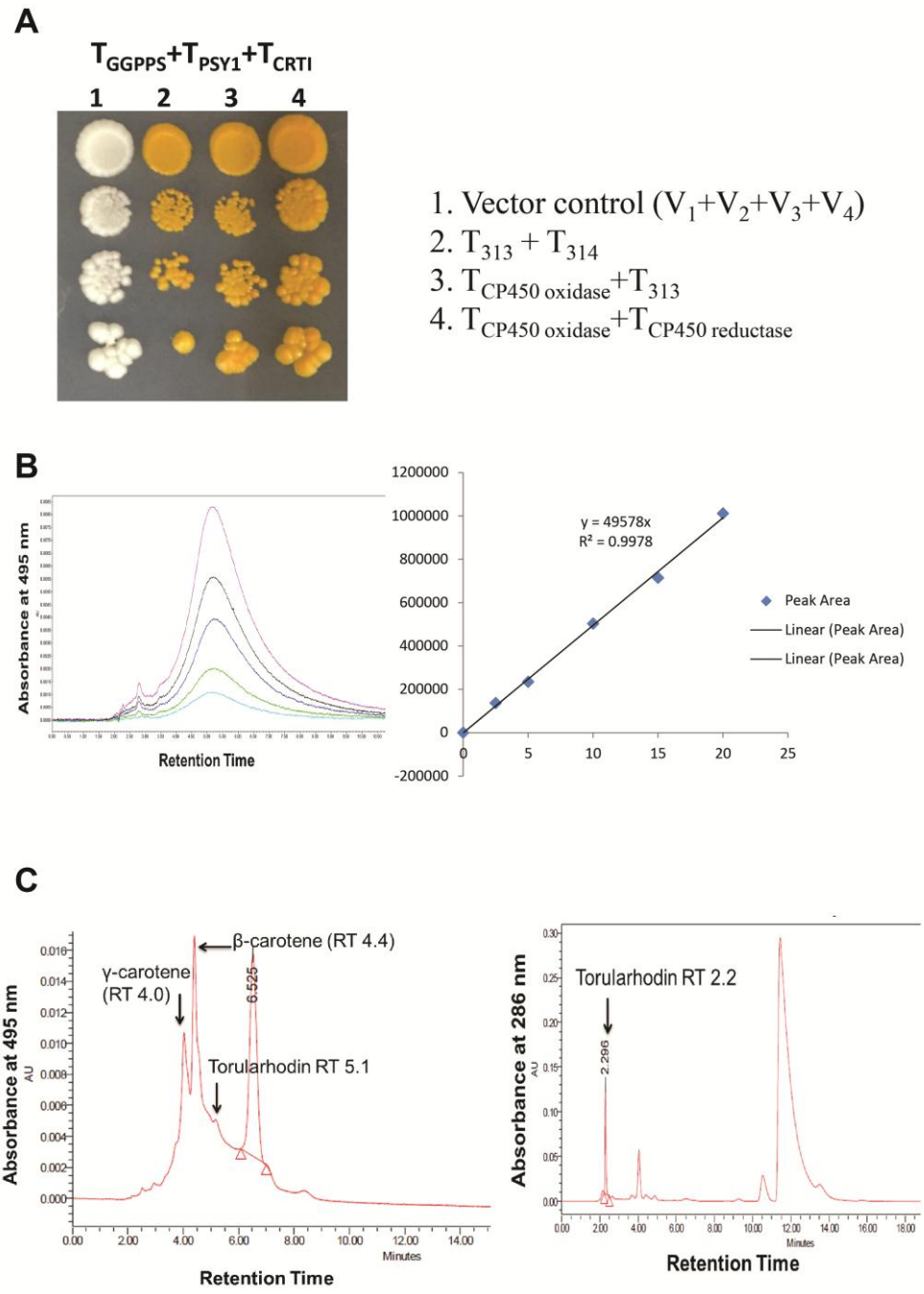

Figure A.4 (A) Dilution spotting of *S. cerevisiae* strain expressing Cytochrome P450 oxidase and /or cytochrome P450 reductase (B) Torularhodin standard curve and torularhodin (different conc.) peak at 495 nm (C) HPLC chromatogram of carotenoids extracted from *R. toruloides ku70Δes*

A1.6 Conclusions:

Rhodoporidium toruloides is an industrial yeast that has a potential for exploitation once tools are developed. Tool development is thus an important aspect of studying such otherwise poorly studied yeasts. With this goal in the mind, new vectors were developed for *R. toruloides* to be eventually used for various purposes including the deciphering of the torularhodin biosynthetic pathway.

A1.7 References:

Bhosale, P., Gadre, R. V., 2002. Manipulation of temperature and illumination conditions for enhanced beta-carotene production by mutant 32 of Rhodotorula glutinis. Lett Appl Microbiol. 34**,** 349-53.

Du, C., Guo, Y., Cheng, Y., Han, M., Zhang, W., Qian, H., 2017. Torulene and torularhodin, protects human prostate stromal cells from hydrogen peroxide-induced oxidative stress damage through the regulation of Bcl-2/Bax mediated apoptosis. Free Radic Res. 51**,** 113-123.

Liu, Y., Koh, C. M., Sun, L., Hlaing, M. M., Du, M., Peng, N., Ji, L., 2013. Characterization of glyceraldehyde-3-phosphate dehydrogenase gene RtGPD1 and development of genetic transformation method by dominant selection in oleaginous yeast Rhodosporidium toruloides. Appl Microbiol Biotechnol. 97**,** 719-29.

Sakaki, H., Nakanishi, T., Tada, A., Miki, W., Komemushi, S., 2001. Activation of torularhodin production by Rhodotorula glutinis using weak white light irradiation. J Biosci Bioeng. 92**,** 294-7.

Ungureanu, C., Marchal, L., Chirvase, A. A., Foucault, A., 2013. Centrifugal partition extraction, a new method for direct metabolites recovery from culture broth: case study of torularhodin recovery from Rhodotorula rubra. Bioresour Technol. 132**,** 406-9.

Zoz, L., Carvalho, J. C. d., Soccol, V. T., Casagrande, T. A. C., Cardoso, L. A. d. C., Torularhodin and Torulene: Bioproduction, Properties and Prospective Applications in Food and Cosmetics - a Review. Braz. arch. biol.technol, 2015.